Supporting Information

Strongly luminescent 5d/4f heterometal-organic macrocycles with open metal sites: post-assembly modification and sensing

Qiang-Yu Zhu,[a,b] Li-Peng Zhou [a] and Qing-Fu Sun*[a]

[a] *State Key Laboratory of Structural Chemistry, Fujian Institute of Research on the Structure of Matter, Chinese Academy of Sciences, Fuzhou 350002, PR China.*
[b] *University of Chinese Academy of Sciences, Beijing 100049, PR China.*

Contents

1. General

Unless otherwise stated, all chemicals and solvents were purchased from commercial companies and used without further purification. Anhydrous solvents were distilled according to standard procedures. Deuterated solvents were purchased from Admas, J&K scientific and Sigma-Aldrich. 1D and 2D-NMR spectra were measured on a Bruker Biospin Avance III (400 MHz) spectrometer. ^{1}H-NMR chemical shifts were determined with respect to residual signals of the deuterated solvents used. Electro-spray-ionization time-of-flight mass-spectroscopy (ESI-TOF-MS) were recorded on an Impact II UHR-TOF mass spectrometry from Bruker, with tuning mix as the internal standard. Data analysis was conducted with the Bruker Data Analysis software (Version 4.3) and simulations were performed with the Bruker Isotope Pattern software. UV-Vis spectra are recorded on UV-2700 UV-Visible spectrophotometer from SHIMADZU. Excitation and emission spectra were recorded on the FS5 spectrofluorometer from Edinburg Photonics. All spectra were corrected for the experimental functions.

2. Synthesis and characterization

2.1 Synthetic procedures

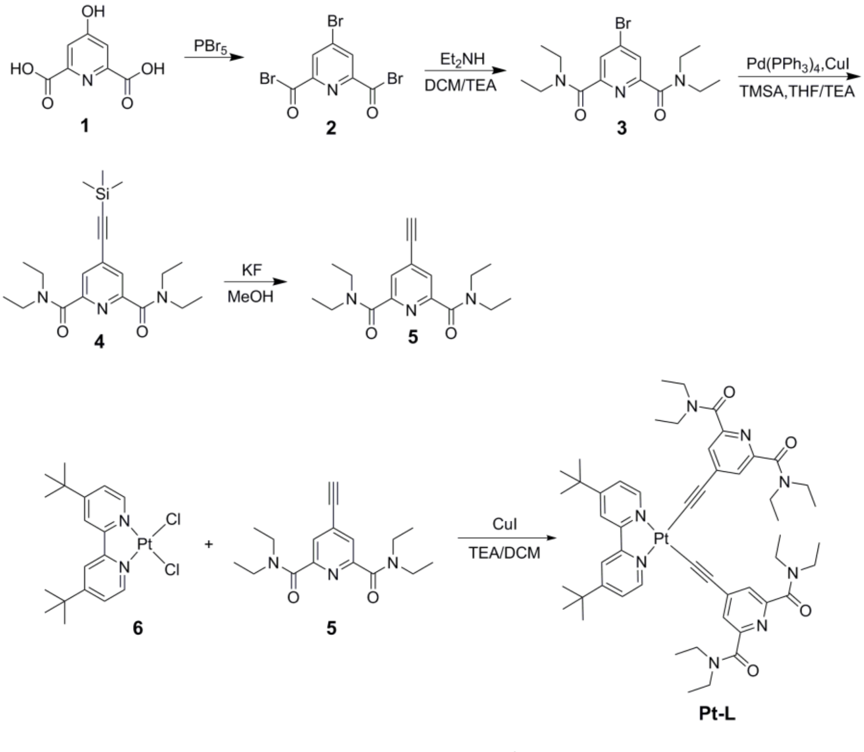

Scheme S1. Synthetic route of organic ligand.

The preparation of compound **3** and **6** were followed the literature procedure.[1] Ligand bis(2-(diphenylphosphino)phenyl) ether oxide (**DPEPO**) was purchased from Bide Pharmatech Ltd.

3 ^{1}H NMR (400 MHz, $CDCl_3$) δ 7.79 (s), 3.54 (q, *J* = 7.1 Hz), 3.32 (q, *J* = 7.1 Hz), 1.24 (t, *J* = 7.1 Hz), 1.15 (t, *J* = 7.1 Hz). ^{13}C NMR (100 MHz, $CDCl_3$) δ 166.82, 154.59, 134.68, 127.24, 43.40, 40.39, 14.36, 12.84.

Synthesis of 4-(Trimethylsilylethynyl)-2,6-bis(diethylcarbamoyl)-pyridine(4):

3 (1068 mg, 3.0 mmol, 1.0 equiv), CuI (57 mg, 0.3 mmol, 0.1 equiv) and $Pd(PPh_3)_4$ (277 mg, 0.24 mmol, 0.08 equiv) were added into a three-necked flask, and the reaction mixture was stirred in anhydrous TEA/THF (60 mL, v/v = 1:5) at room temperature under nitrogen atmosphere. Then trimethylsilylacetylene (884 mg, 9 mmol, 3 equiv, TMSA) was added dropwise into the mixture and the suspension was stirred for 24 h. The residue was filtered off with kieselguhr, and the filtrate was concentrated under reduced pressure. The crude product was purified by chromatography on a silica gel column (DCM) to afford **4** as a white solid.(787.8 mg, 70.3%), m.p.>250℃. ^{1}H NMR (400 MHz, $CDCl_3$) δ 7.61 (s, 2H), 3.54 (q, *J* = 7.1 Hz, 4H), 3.31 (q, *J* = 7.1 Hz, 4H), 1.24 (t, *J* = 7.1 Hz, 6H), 1.13 (t, *J* = 7.1 Hz, 6H), 0.25 (s, 9H). ^{13}C NMR (100 MHz, $CDCl_3$) δ 167.65, 153.87, 133.63, 102.09, 101.22, 43.37, 40.30, 14.38, 12.88, -0.28.

Synthesis of 4-Ethynyl-2,6-bis(diethylcarbamoyl)pyridine(5):

KF (348 mg, 6.0 mmol, 3.0 equiv) was added to a solution of 4 (747 mg, 2.0 mmol, 1.0 equiv) in MeOH (60 mL). The solution was furth**er s**tirred for 6 h at room temperature. The organic solvent was removed under reduced pressure, and the crude product was purified by chromatography on a silica gel column (v/v, DCM/MeOH=100:1) to afford **5** as a light yellow solid.(577 mg, 95.8%), m.p.>250℃. ^{1}H NMR (400 MHz, $CDCl_3$) δ 7.65 (s, 2H), 3.54 (q, *J* = 7.1 Hz, 4H), 3.37 (s, 1H), 3.31 (q, *J* = 7.0 Hz, 4H), 1.24 (t, *J* = 7.1 Hz, 6H), 1.13 (t, *J* = 7.0 Hz, 6H). ^{13}C NMR (100 MHz, $CDCl_3$) δ 167.47, 153.93, 132.74, 126.14, 83.54, 80.23, 43.38, 40.30, 14.35, 12.86.

Synthesis of Pt-L:

Under a nitrogen atmosphere, **6** (160.3 mg, 0.3 mmol, 1.0 equiv), **5** (266 mg, 0.75 mmol, 2.5 equiv), CuI (3.4 mg, 0.03 mmol, 0.1 equiv) and a mixture solvent of DCM/TEA (60 ml, v/v=4:1) were added into a 100 mL Schlenk flask. The mixture were stiring for 24h at ambient temperature. After the reaction, The solvents were removed in vacuo and the crude material was purified by chromatography on a silica gel column (v/v,CH_2Cl_2/CH_3OH =60:1) to give ligand as yellow powder (255mg,0.24mmol, 80.1%), m.p.>250℃. ^{1}H NMR (400 MHz, $CDCl_3$) δ 9.51 (d, *J* = 5.9 Hz, 2H), 7.97 (s, 2H), 7.66 (d, *J* = 6.0 Hz, 2H), 7.58 (s, 4H), 3.54 (q, *J* = 7.1 Hz, 8H), 3.33 (q, *J* = 6.9 Hz, 8H), 1.46 (s, 9H), 1.24 (t, *J* = 7.0 Hz, 12H), 1.13 (t, *J* = 7.0 Hz, 12H).^{13}C NMR (100 MHz, $CDCl_3$) δ 168.48, 164.31, 156.15, 153.44, 151.06, 138.10, 125.80, 125.05, 119.16, 99.60, 97.47, 43.22, 39.95, 35.97, 30.28, 14.33, 12.88. HR-MS (ESI) calcd. For $C_{52}H_{68}N_8O_4Pt$ $[Pt\text{-}L+H]^{1+}$:1064.5088, found 1064.5085.

Synthesis of $La_2(Pt\text{-}L)_2(ClO_4)_6$

Ligand **Pt-L** (31.9mg, 30μmol, 1.0 equiv) was treated with $La(ClO_4)_3$ $6H_2O$ (16.4mg, 30μmol, 1.0 equiv) in 5mL MeCN, the turbid suspension changed to homogeneous green solution immediately. The mixture was further stirred for 2h at 40℃. ^{1}H NMR showed the quantitative formation of La_2**(Pt-L)**$_2(ClO_4)_6$. The solvent was removed under reduced pressure to give the isolated product (45.3mg, 14.07μmol, 93.7% yield), m.p.>250℃. ^{1}H NMR (400 MHz, CD_3CN) δ 9.38 (d, *J* = 6.0 Hz, 2H), 8.38 (s, 2H), 7.79 (s, 6H), 3.75 (q, *J* = 7.0 Hz, 8H), 3.56 (d, *J* = 6.6 Hz, 8H), 1.47 (s, 18H), 1.41 (t, *J* = 7.1 Hz, 12H), 1.23 (t, *J* = 7.0 Hz, 12H). ^{13}C NMR (100 MHz, CD_3CN) δ 170.30, 166.61, 157.27, 151.31, 150.72, 141.00, 128.90, 125.89, 122.14, 108.35, 100.60, 45.47, 43.15, 36.80, 30.18, 14.09, 12.35.

Synthesis of Eu_2(Pt-L)$_2$(OTf)$_6$

The complexe of Eu_2(Pt-L)$_2$(OTf)$_6$ was prepared by the same procedure. ligand **Pt-L**(31.9mg, 30μmol, 1.0 equiv) was treated with Eu(OTf)$_3$(18.0mg, 30μmol, 1.0 equiv) in 5mL MeCN, the turbid suspension changed to clear light orange solution immediately. The mixture was further stirred for 2h at 40℃. ^{1}H NMR showed the quantitative formation of Eu_2**(Pt-L)**$_2$(OTf)$_6$. The solvent was removed under reduced pressure to give the isolated product (45.9mg, 13.80μmol, 92.0% yield), m.p.>250℃. ^{1}H NMR (400 MHz, CD_3CN) δ 8.32 (d, *J* = 6.1 Hz, 2H), 7.95 (s, 2H), 6.88 (d, *J* = 5.4 Hz, 2H), 1.06 (s, 18H). ^{13}C NMR (100 MHz, CD_3CN) δ 166.20, 156.83, 151.17, 150.42, 124.94, 121.77, 114.04, 110.86, 109.27, 94.84, 36.41, 29.81(The signals of pcam are not detectable, probably due to the paramagnetic property of Eu^{III}). ESI-TOF-MS for Eu_2**(Pt-L)**$_2$(OTf)$_6$.: The following picked signals are those at the highest intensities. *m/z* Calcd for $[Eu_2(Pt\text{-}L)_2(OTf)_4]^{2+}$ 1514.3264, found 1514.3241; Calcd for $[Eu_2(Pt\text{-}L)_2(OTf)_3]^{3+}$ 959.9001, found 959.8984; Calcd for $[Eu_2(Pt\text{-}L)_2(OTf)_2]^{4+}$ 682.6870, found 682.6859; Calcd for $[Eu_2(Pt\text{-}L)_2(OTf)]^{5+}$ 516.1589, found 516.1588.

Synthesis of Lu_2(Pt-L)$_2$(OTf)$_6$

ligand **Pt-L**(31.9mg, 30μmol, 1.0 equiv) was treated with Lu(OTf)$_3$(18.67mg, 30μmol, 1.0 equiv) in 5mL MeCN, the turbid suspension changed to clear light red solution immediately. The mixture was further stirred for 2h at 40 ℃. ^{1}H NMR showed the quantitative formation of Lu_2**(Pt-L)**$_2$(OTf)$_6$. The solvent was removed under reduced pressure to give the isolated product (46.1mg, 13.67μmol, 91.2% yield), m.p.>250℃. ^{1}H NMR (400 MHz, CD_3CN) δ 9.43 (d, *J* = 5.8 Hz, 2H), 8.41 (s, 2H), 7.98 (s, 2H), 7.76 (d, *J* = 6.0 Hz, 2H), 7.71 (s, 2H), 3.74 (s, 8H), 3.12 (s, 8H), 1.48 (s, 18H), 1.26 (s, 12H), 0.99 (s, 12H). ^{13}C NMR (100 MHz, CD_3CN) δ 170.09, 166.73, 157.35, 151.41, 149.66, 141.88, 129.78, 125.78, 123.08, 122.27, 119.90, 109.38, 100.61, 45.67, 44.19, 36.85, 30.19, 13.93, 12.11. ESI-TOF-MS for Lu_2**(Pt-L)$_2$**(OTf)$_6$.: The following picked signals are those at the highest intensities. *m/z* Calcd for $[Lu_2(Pt\text{-}L)_2(OTf)_4]^{2+}$ 1536.8461, found 1536.8428; Calcd for $[Lu_2(Pt\text{-}L)_2(OTf)_3]^{3+}$ 974.9133, found 974.9128; Calcd for $[Lu_2(Pt\text{-}L)_2(OTf)_2]^{4+}$ 693.9468, found 693.9467; Calcd for $Lu_2(Pt\text{-}L)_2(OTf)]^{5+}$ 525.3670, found 525.3668.

Synthesis of Lu_2(Pt-L)$_2$(DPEPO)$_2$(OTf)$_6$

ligand **Pt-L**(31.9mg, 30μmol, 1.0 equiv) was treated with Lu(OTf)$_3$(18.67mg, 30μmol, 1.0 equiv) and DPEPO(17.11mg, 30μmol, 1.0 equiv)in 5mL MeCN, the turbid suspension changed to clear light green solution within minites. The mixture was further stirred for 2h at 40℃. ^{1}H NMR showed the quantitative formation of Lu_2**(Pt-L)**$_2$(DPEPO)$_2$(OTf)$_6$. The solvent was removed under reduced pressure to give the isolated product (62.3mg, 13.81μmol, 92.1% yield), m.p.>250℃. ESI-TOF-MS for Lu_2**(Pt-L)**$_2$(DPEPO)$_2$(OTf)$_6$: The following picked signals are those at the highest intensities. *m/z* Calcd for $[Lu_2(Pt\text{-}L)_2(DPEPO)_2(OTf)_3]^{3+}$ 1355.3484, found 1355.3496; Calcd for $[Lu_2(Pt\text{-}L)_2(DPEPO)_2(OTf)_2]^{4+}$ 979.2732, found 979.2735; Calcd for $[Lu_2(Pt\text{-}L)_2(DPEPO)_2(OTf)]^{5+}$ 753.6281, found 753.6285; Calcd for $[Lu_2(Pt\text{-}L)_2(DPEPO)_2]^{6+}$ 603.1980, found 603.1988.

2.2 NMR spectra

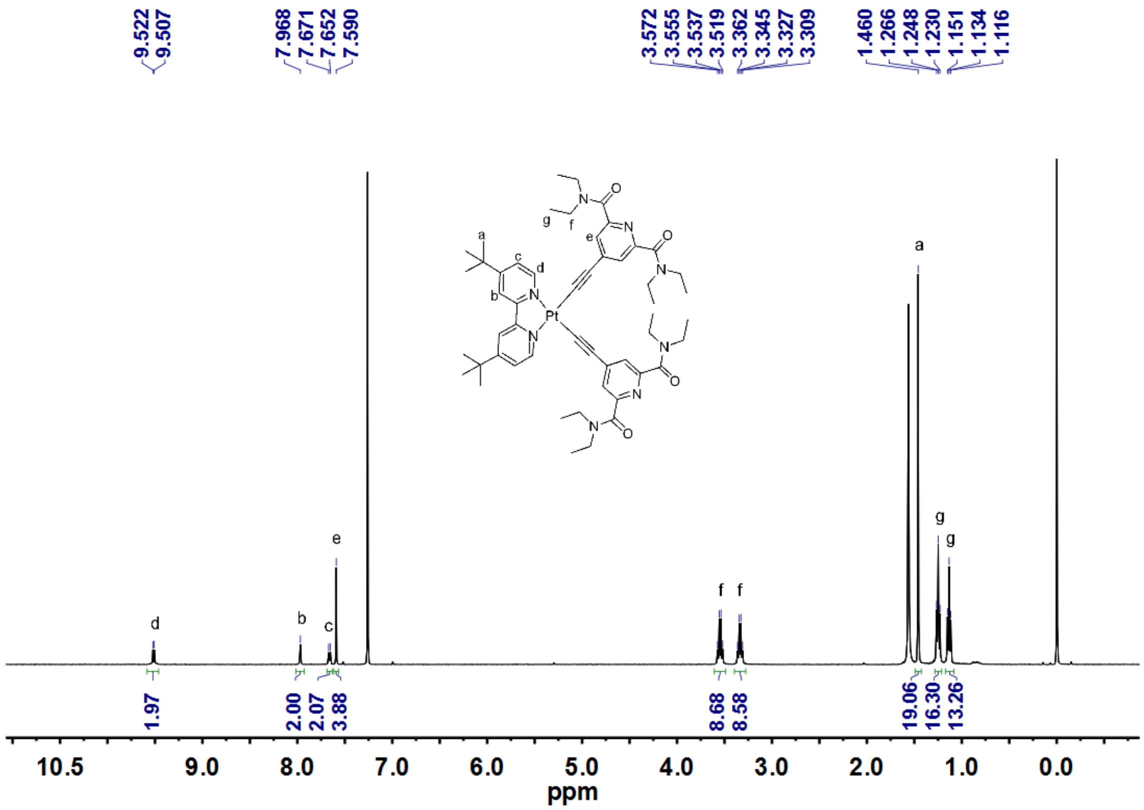

Figure S1. ^{1}H NMR spectrum of ligand **Pt-L** (400MHz, $CDCl_3$, 298 K).

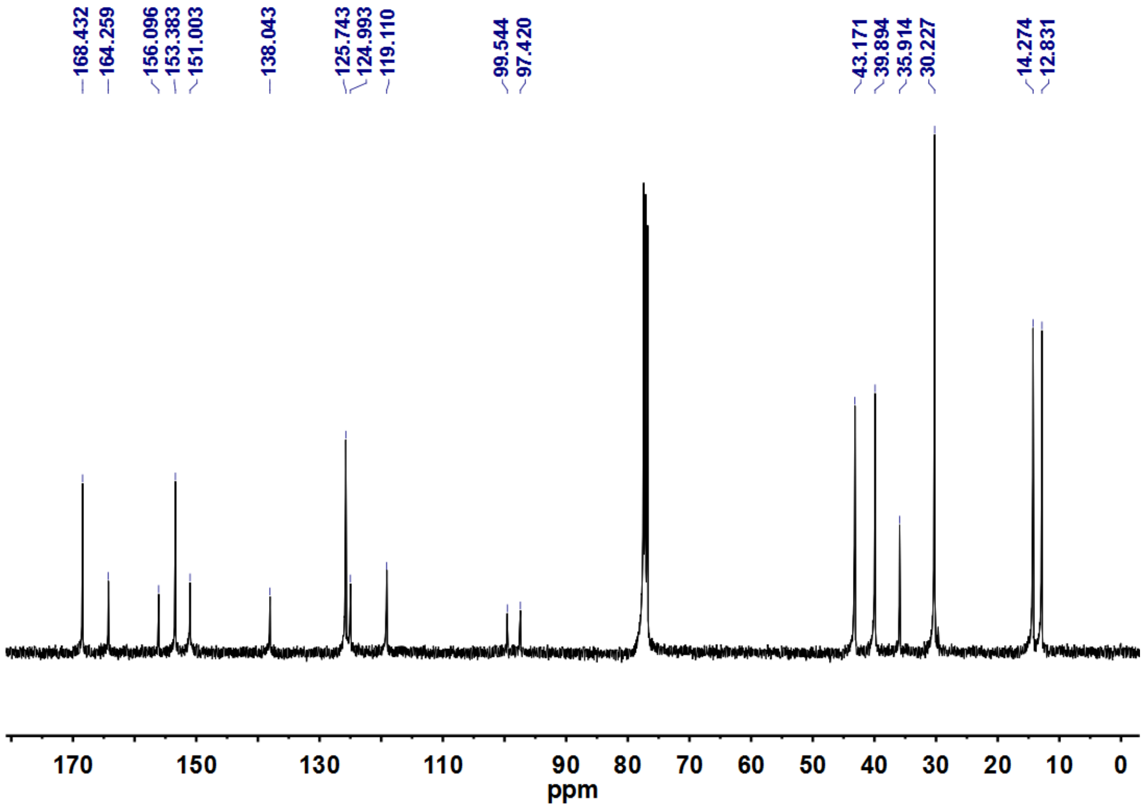

Figure S2. ^{13}C NMR spectrum of ligand **Pt-L** (100MHz, $CDCl_3$, 298 K).

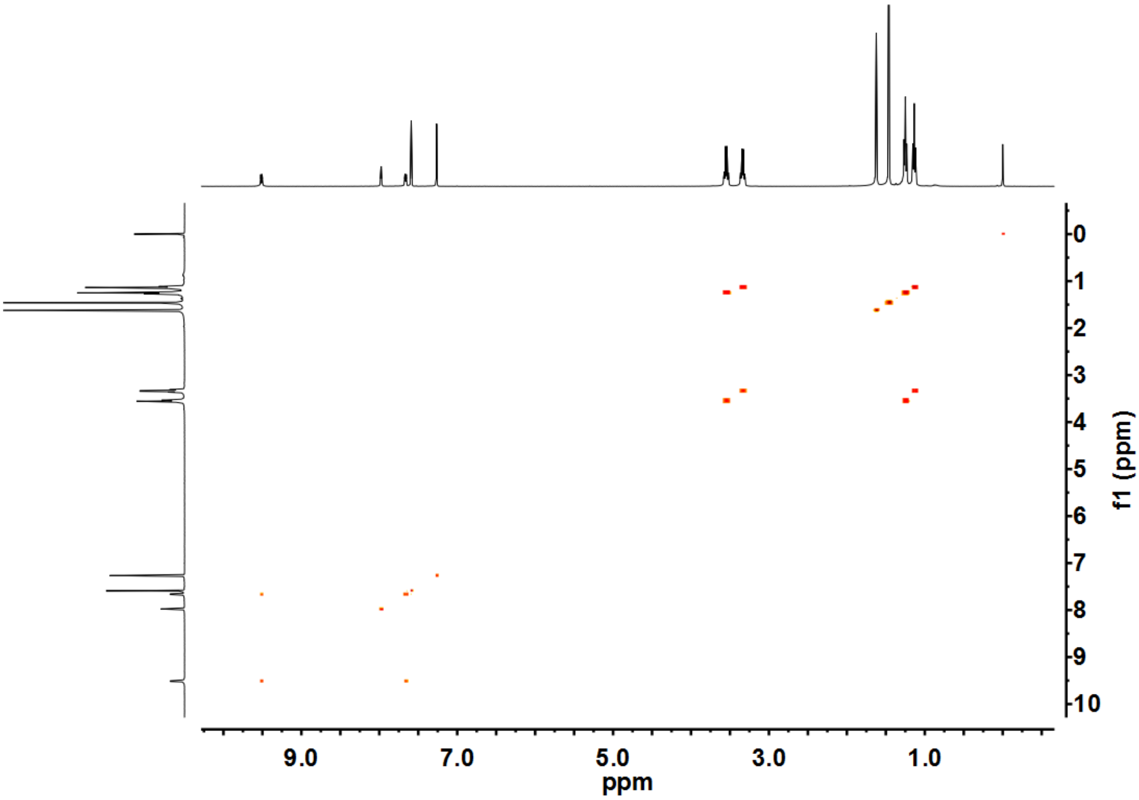

Figure S3. ^{1}H COSY spectrum of **Pt-L** (400 MHz, CD_3CN, 298 K).

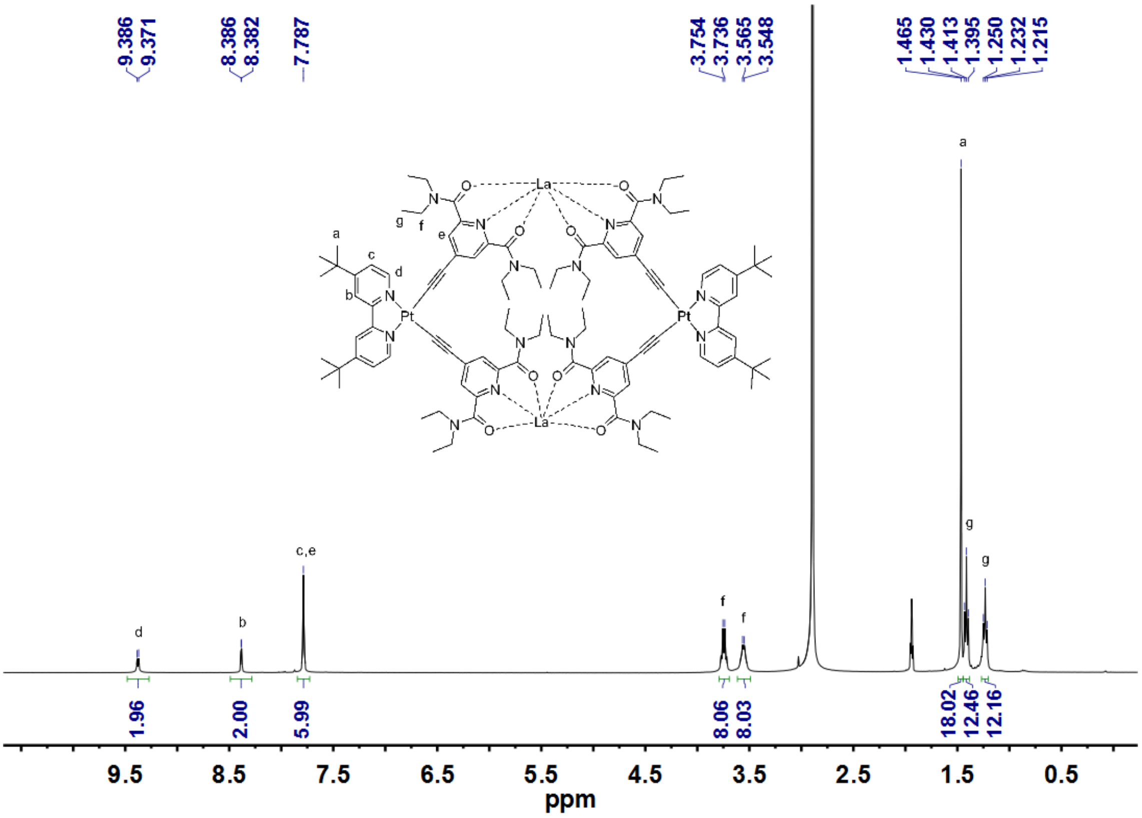

Figure S4. ^{1}H NMR spectrum of La_2(**Pt-L**)$_2$(ClO_4)$_6$ (400 MHz, CD_3CN, 298 K).

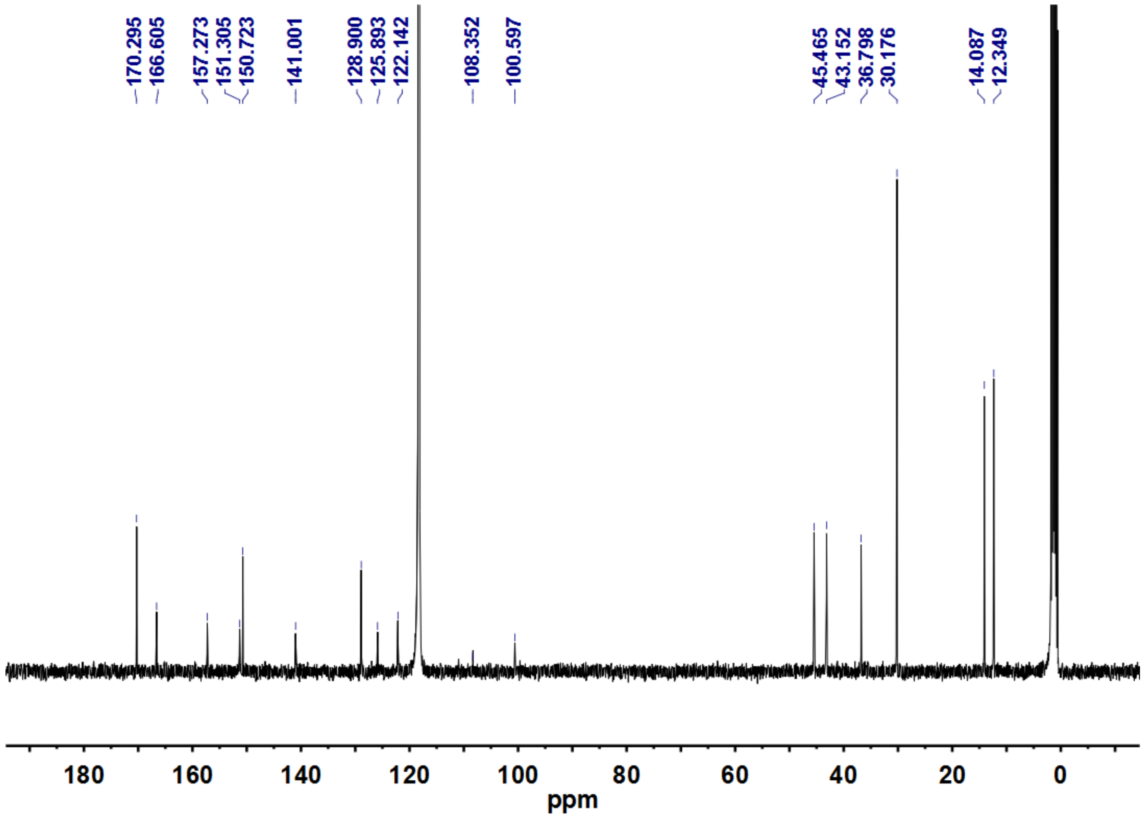

Figure S5. ^{13}C NMR spectrum of La$_2$(**Pt-L**)$_2$(ClO$_4$)$_6$ (100MHz, CD$_3$CN, 298 K).

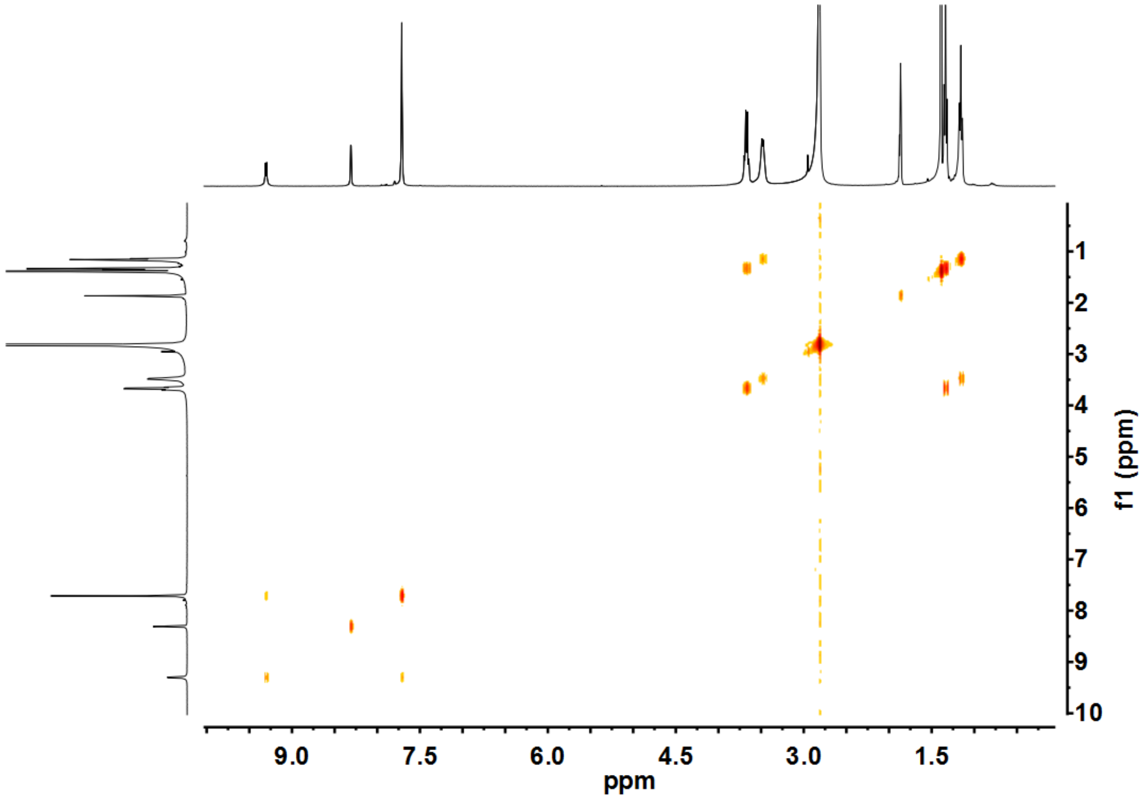

Figure S6. ^{1}H COSY spectrum of La$_2$(**Pt-L**)$_2$(ClO$_4$)$_6$ (400 MHz, CD$_3$CN, 298 K).

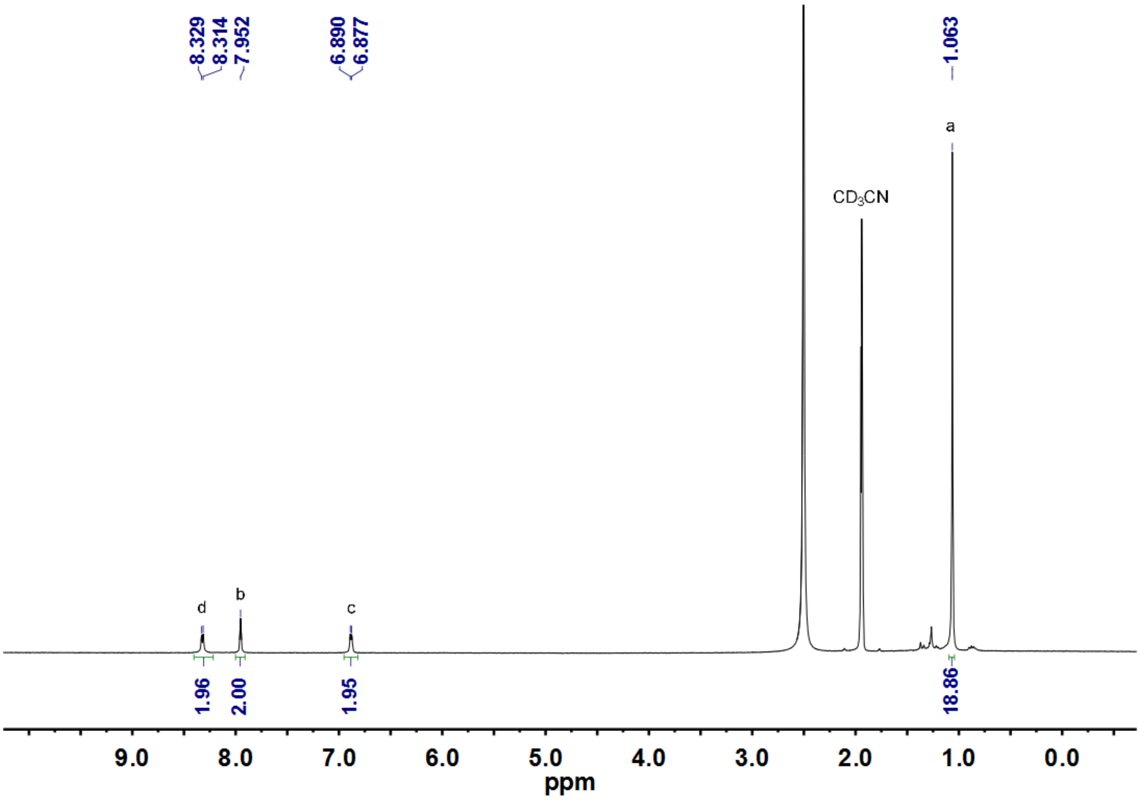

Figure S7. ^{1}H NMR spectrum of Eu$_2$(**Pt-L**)$_2$(OTf)$_6$ (400 MHz, CD$_3$CN, 298 K) (The signals of pcam are not detectable, probably due to the paramagnetic property of Eu^{III}).

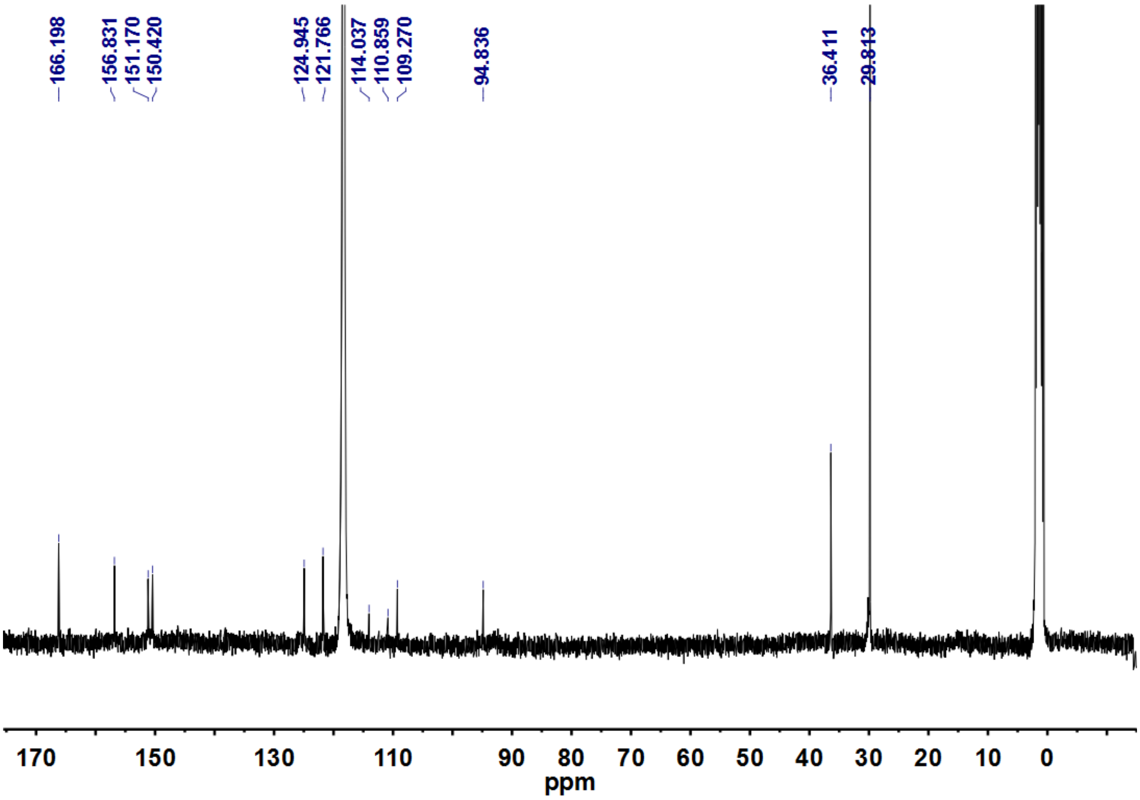

Figure S8. ^{13}C NMR spectrum of Eu$_2$(**Pt-L**)$_2$(OTf)$_6$ (100MHz, CD$_3$CN, 298 K) (The signals of pcam are not detectable, probably due to the paramagnetic property of Eu^{III}).

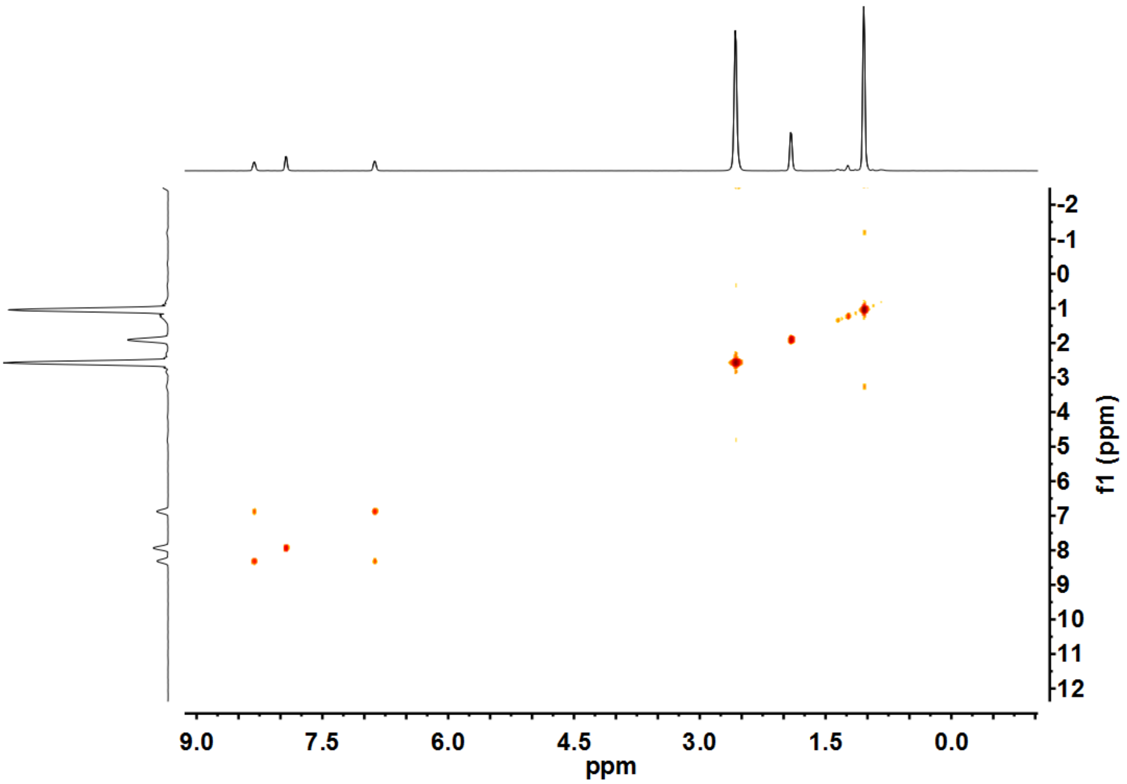

Figure S9. ^{1}H COSY spectrum of Eu_2(**Pt-L**)$_2$(OTf)$_6$ (400 MHz, CD_3CN, 298 K).

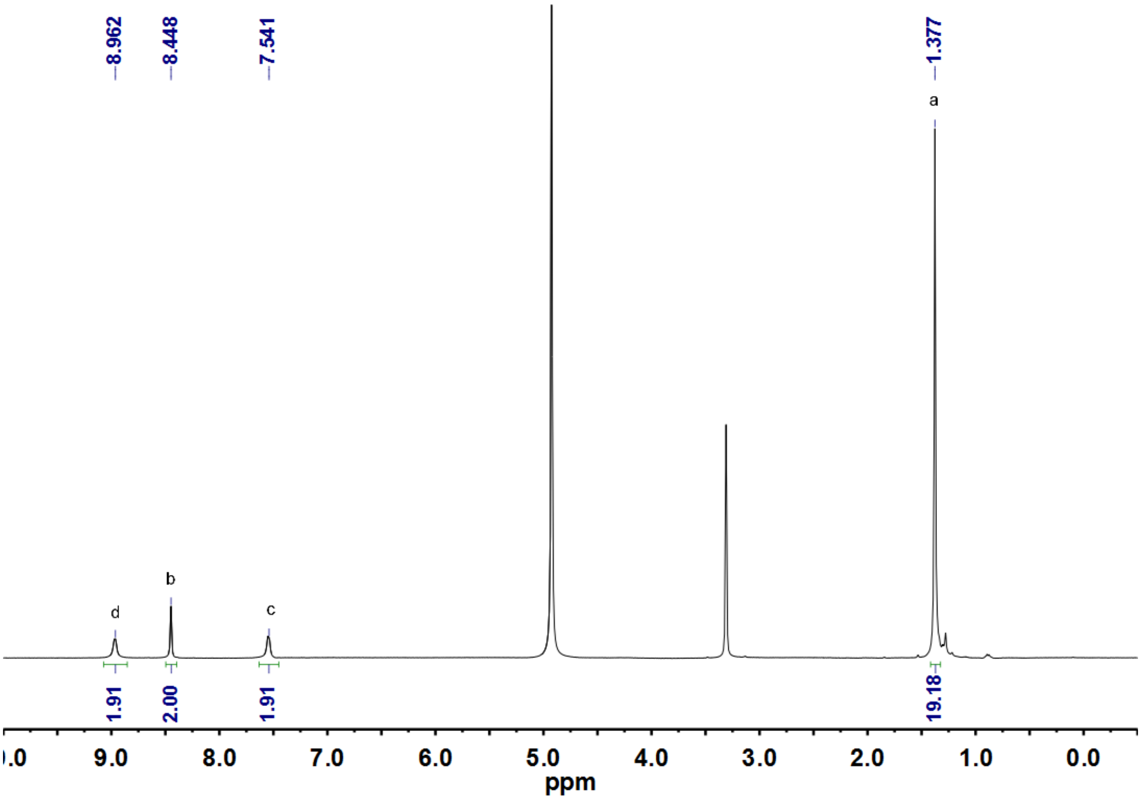

Figure S10. ^{1}H NMR spectrum of Eu_2(**Pt-L**)$_2$(OTf)$_6$ (400 MHz, CD_3OD, 298 K) (The signal of pcam are not detectable, probably due to the paramagnetic property of Eu^{III}).

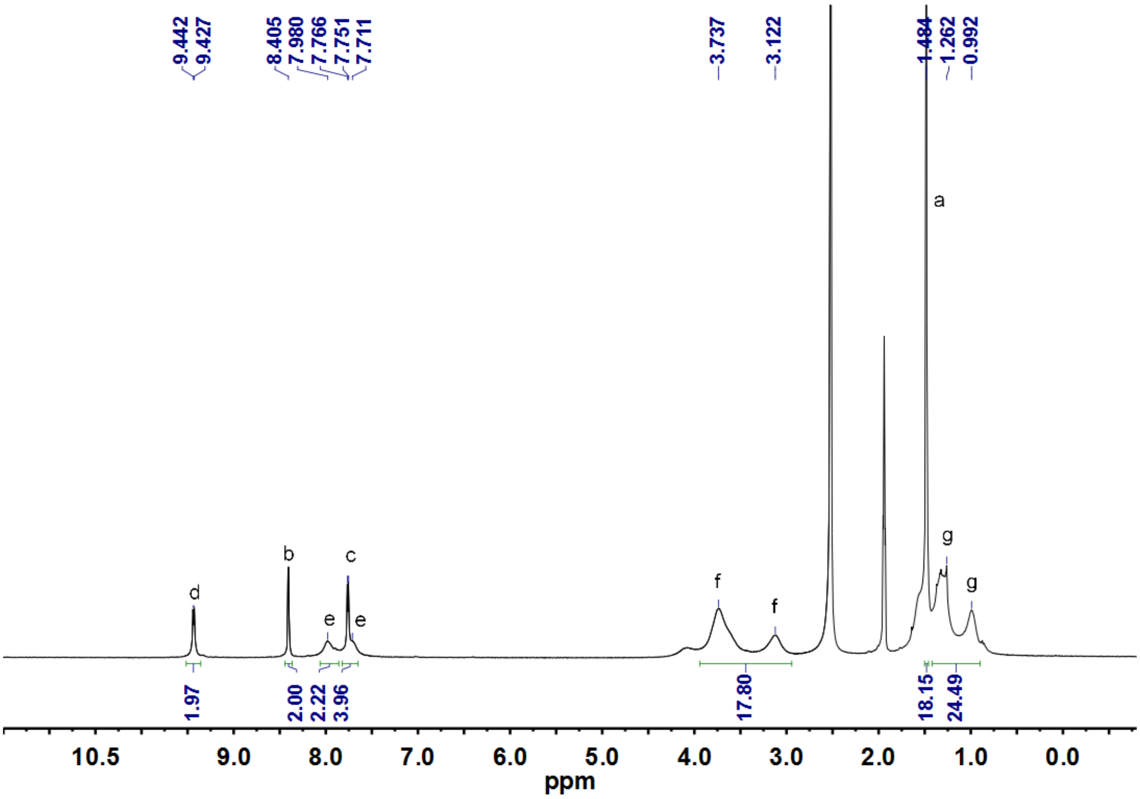

Figure S11. ^{1}H NMR spectrum of Lu_2(**Pt-L**)$_2$(OTf)$_6$ (400 MHz, CD_3CN, 298 K).

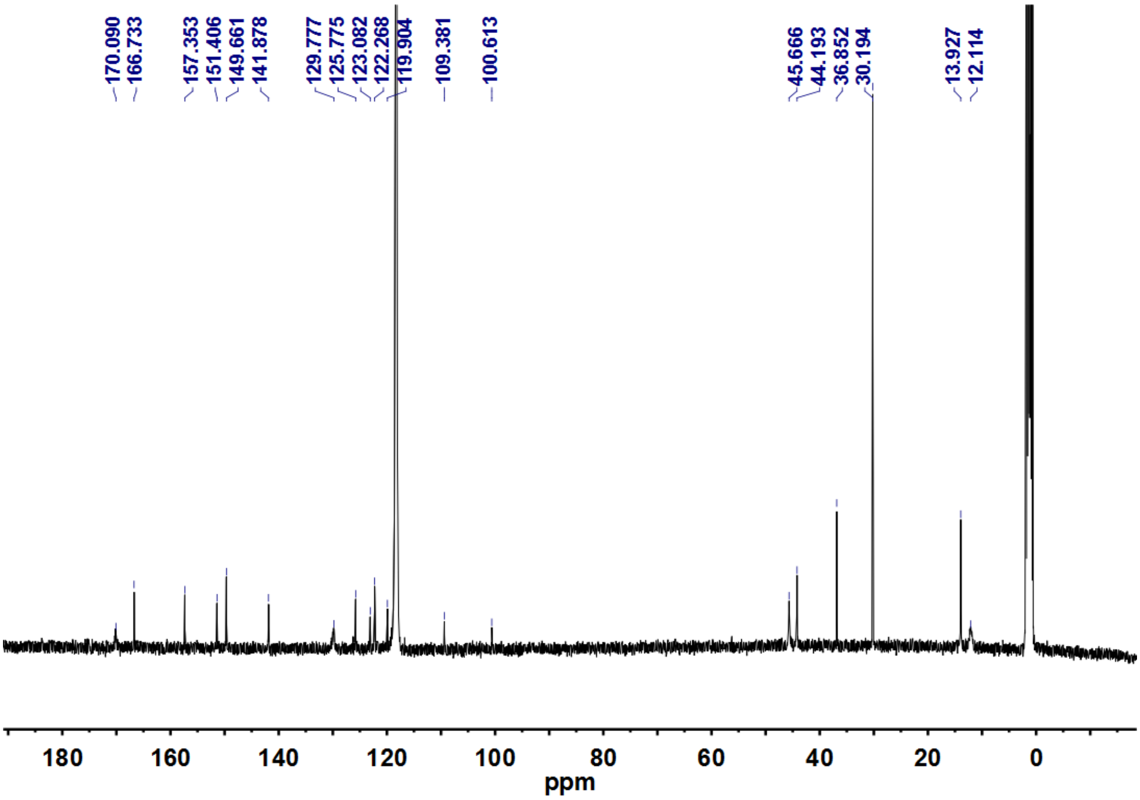

Figure S12. ^{13}C NMR spectrum of Lu_2(**Pt-L**)$_2$(OTf)$_6$ (100 MHz, CD_3CN, 298 K).

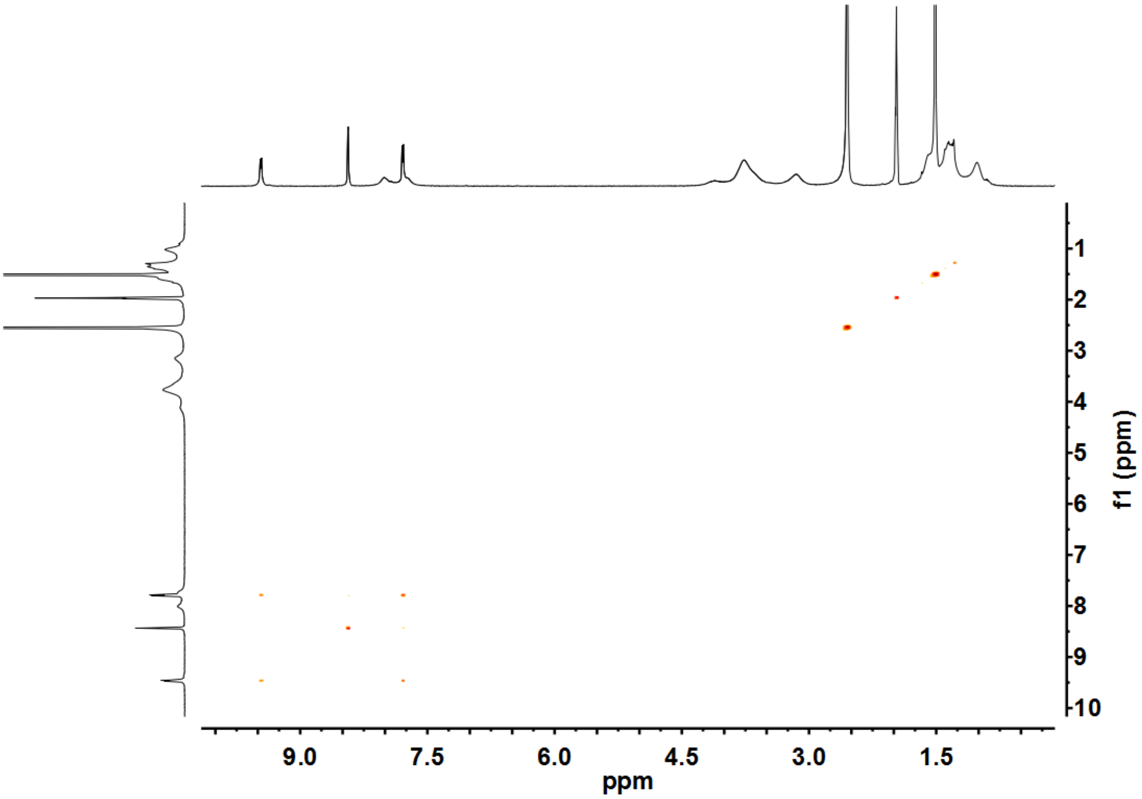

Figure S13. ^{1}H COSY NMR spectrum of Lu_2(**Pt-L**)$_2$(OTf)$_6$ (400 MHz, CD_3CN, 298 K).

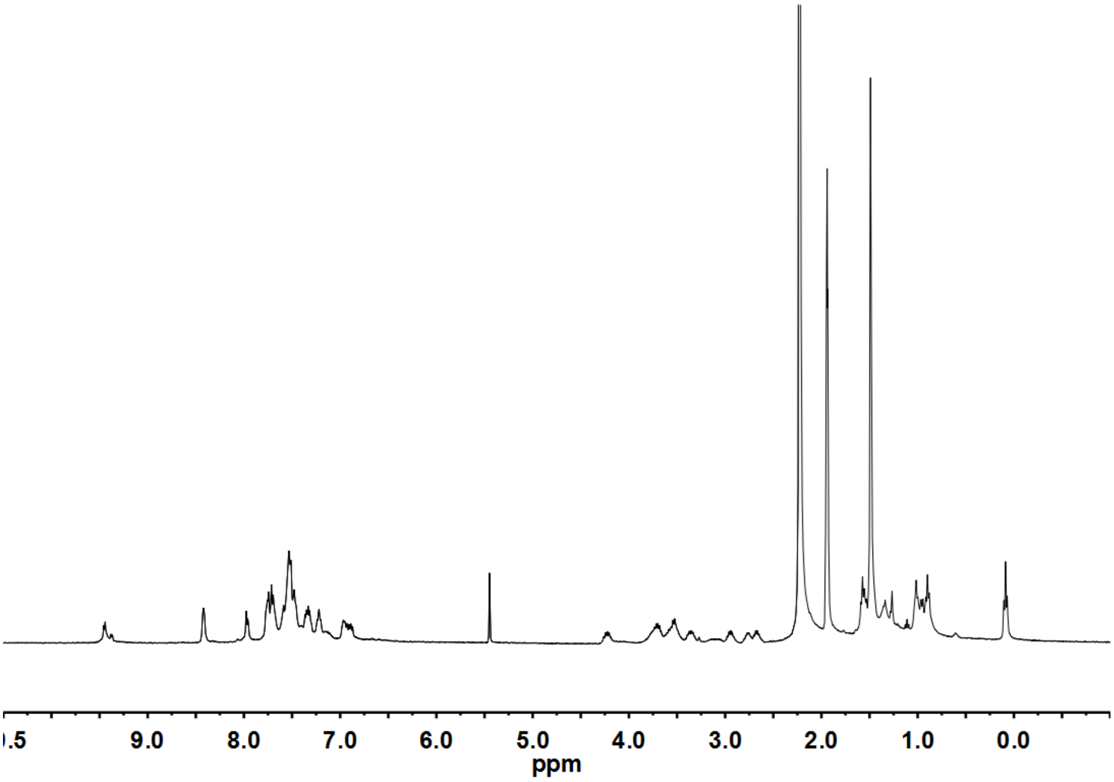

Figure S14. ^{1}H NMR spectrum of Lu_2(**Pt-L**)$_2$(DPEPO)$_2$(OTf)$_6$ by post-assembly modification (400 MHz, CD_3CN, 298 K).

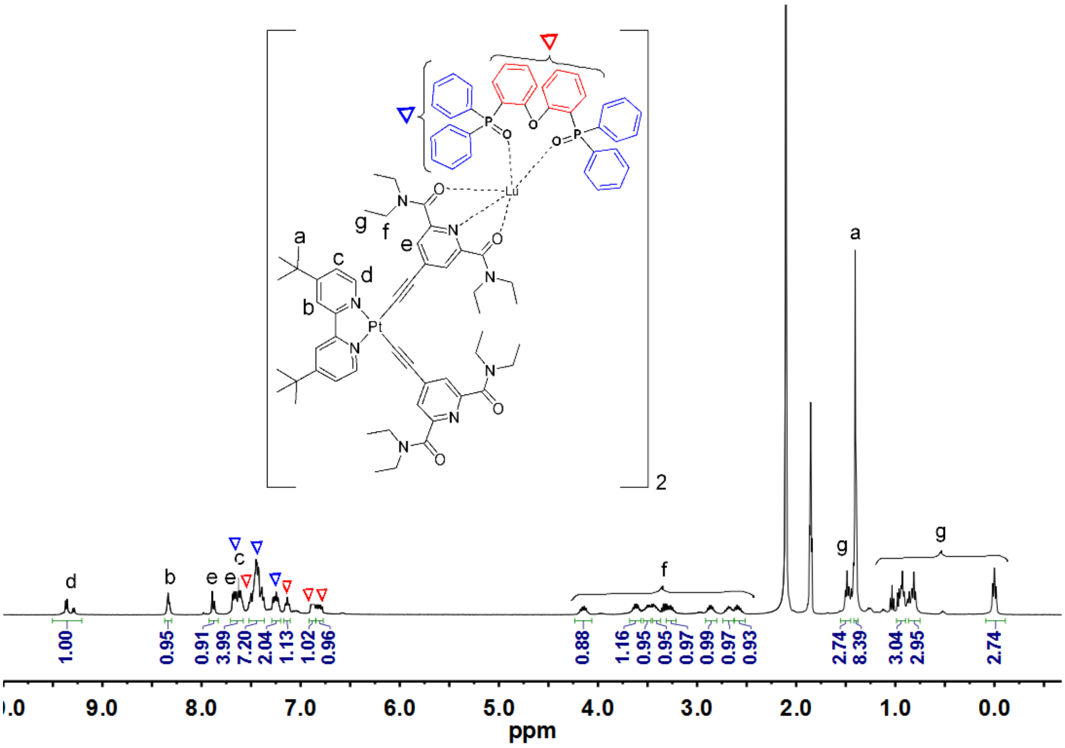

Figure S15. ^{1}H NMR spectrum of the redissolved Lu_2(**Pt-L**)$_2$(DPEPO)$_2$(OTf)$_6$ crystals (400 MHz, CD_3CN, 298 K).

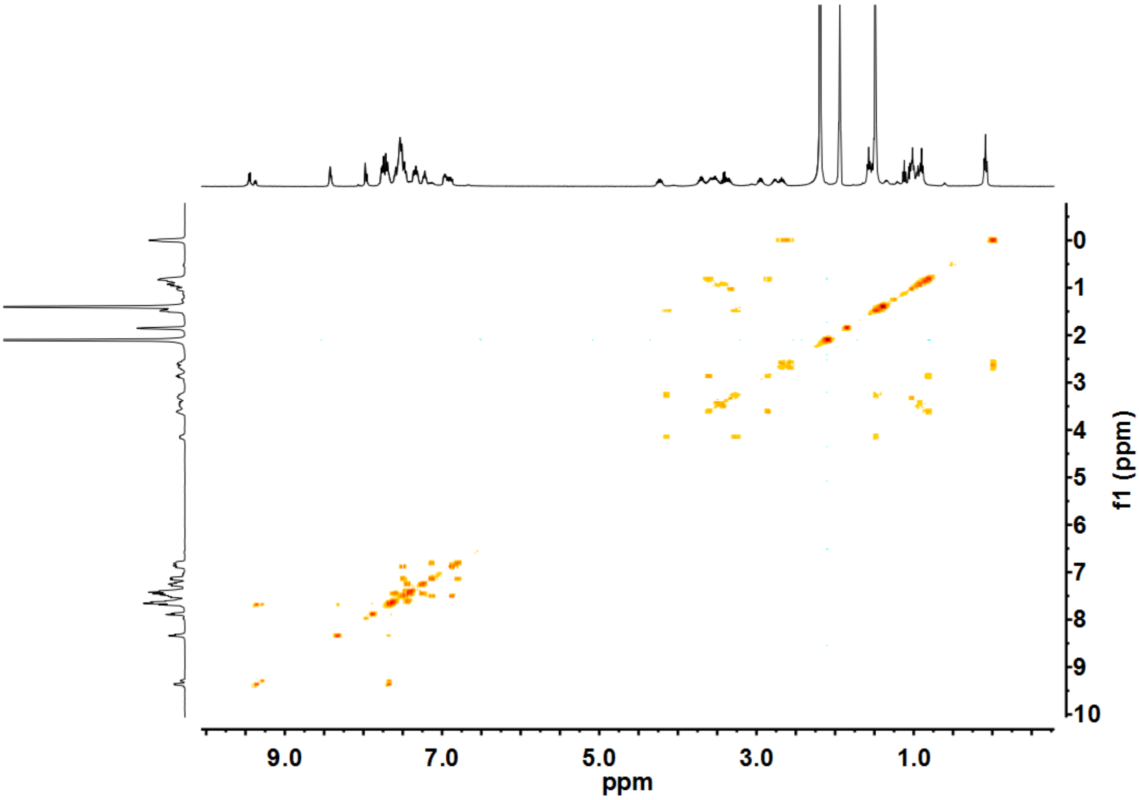

Figure S16. ^{1}H COSY spectrum of the redissolved Lu_2(**Pt-L**)$_2$(DPEPO)$_2$(OTf)$_6$ crystals (400 MHz, CD_3CN, 298 K).

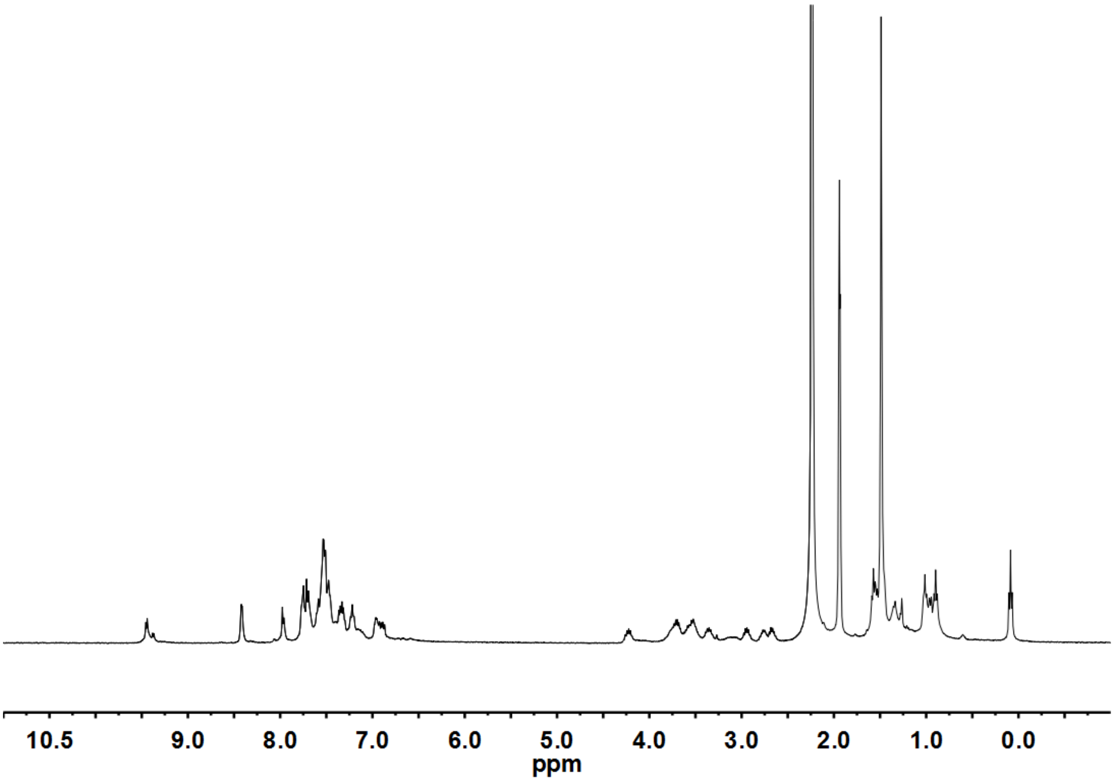

Figure S17. ^{1}H NMR spectrum of Lu_2(**Pt-L**)$_2$(DPEPO)$_2$(OTf)$_6$ by one pot reaction (400 MHz, CD_3CN, 298 K).

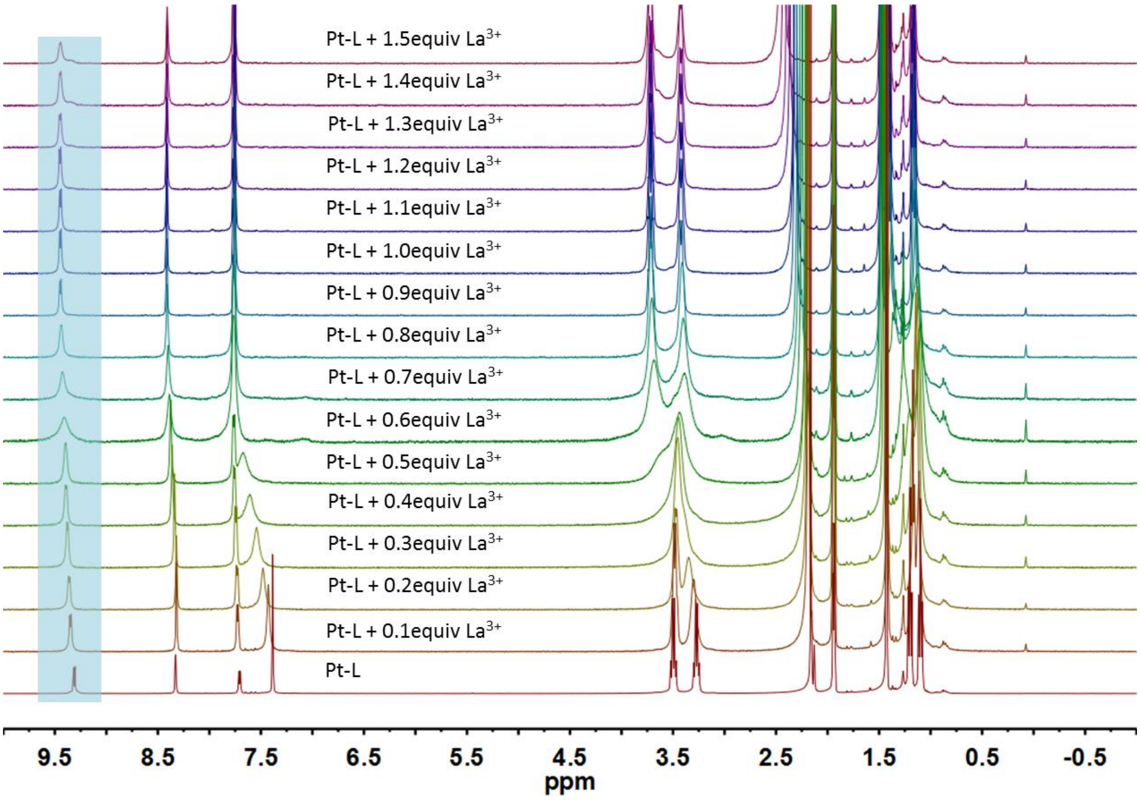

Figure S18. ^{1}H NMR (400 MHz, 298 K) titration spectra of titrating **Pt-L** with La(ClO$_4$)$_3$ in CD_3CN.

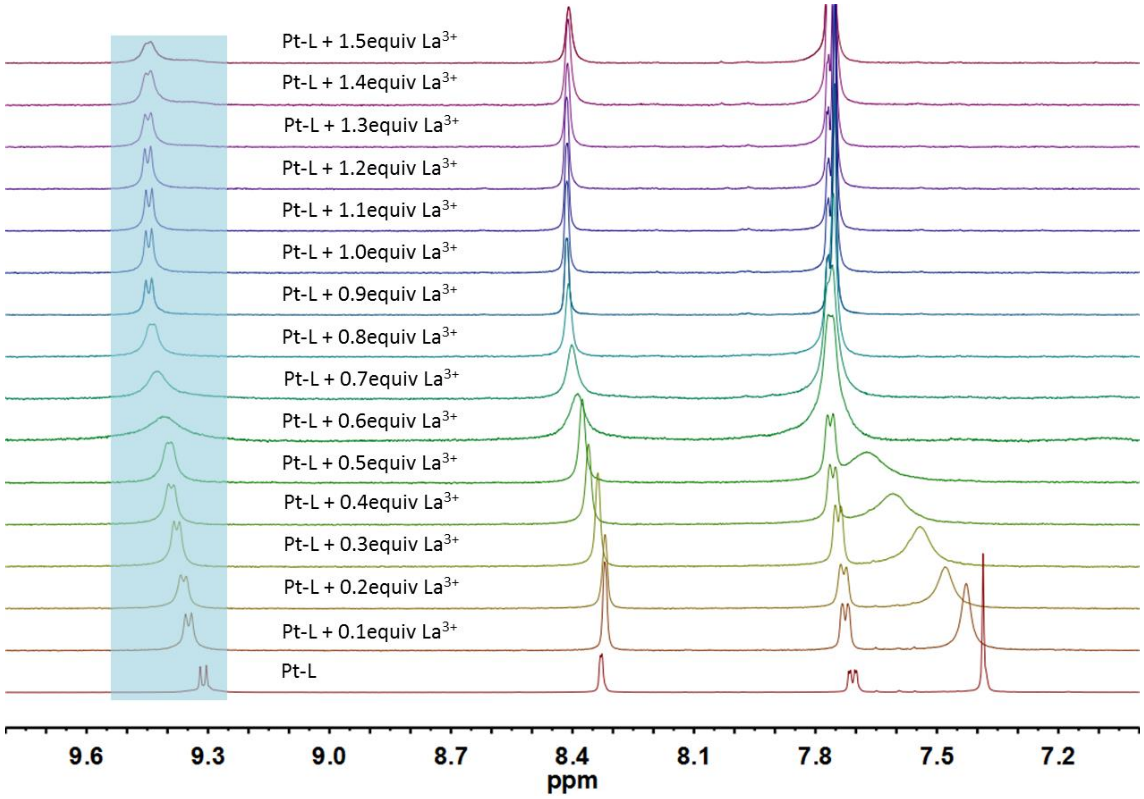

Figure S19. Highlight ^{1}H NMR spectra with gradually down field shifted.

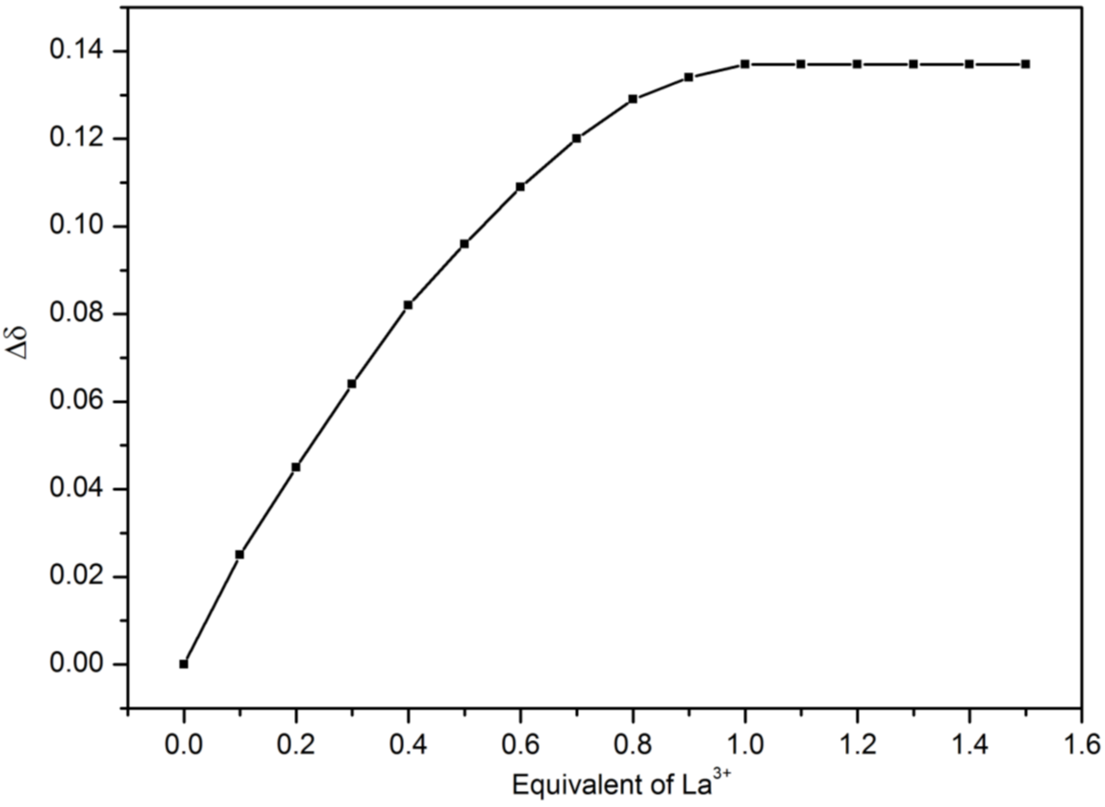

Figure S20. Chemical shift difference of the compounds with different equivalent of La$(ClO_4)_3$.

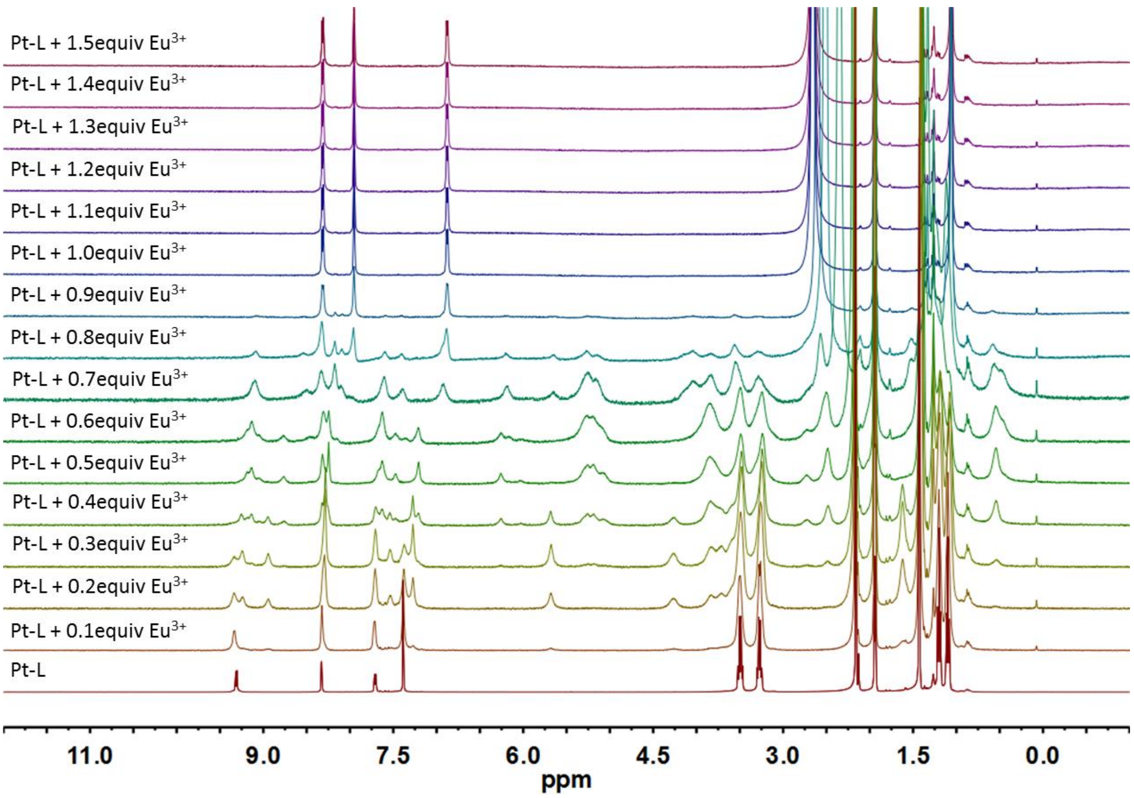

Figure S21. ^{1}H NMR (400 MHz, 298 K) titration spectra of titrating **Pt-L** with Eu(OTf)$_3$ in CD$_3$CN.

2.3 ^{1}H DOSY spectra

Stokes-Einstein equation:

$$D=\frac{K_B T}{6\pi\eta r} \qquad (1)$$

was applied to estimate the dynamic radius for heterometal-organic macrocycles in solution. *D* is diffusion coefficient obtained from DOSY spectrum, K_B is Boltzmann constant, *T* is the absolute temperature, viscosity η was tested to be 0.343 mPa•s, and *r* is the estimated dynamic radius.

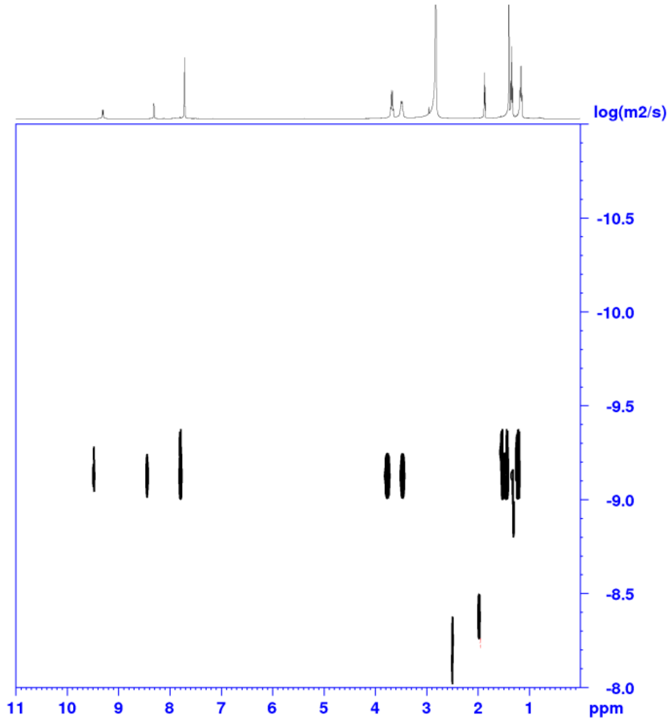

```
Current Data Parameters
NAME          zqy406-13dosy
EXPNO                     5
PROCNO                    1

F2 - Acquisition Parameters
Date_              20180128
Time                  10.05
INSTRUM               spect
PROBHD     5 mm PABBO BB/
PULPROG           stebpgp1s
TD                    16384
SOLVENT               CD3CN
NS                       16
DS                        2
SWH                6393.862 Hz
FIDRES             0.390250 Hz
AQ                1.2812288 sec
RG                   124.06
DW                   78.200 usec
DE                     6.50 usec
TE                    298.0 K
D1               1.00000000 sec
D16              0.00020000 sec
D20              0.06000000 sec

======== CHANNEL f1 ========
SFO1            400.1332010 MHz
NUC1                     1H
P1                     9.90 usec
P2                    19.80 usec
PLW1            16.00000000 W

====== GRADIENT CHANNEL =====
GPNAM[6]          sine.100
GPNAM[7]          sine.100
GPZ6                 100.00 %
GPZ7                 -17.13 %
P19                  600.00 usec
P30                 1700.00 usec

F1 - Acquisition parameters
TD                       16
SFO1               400.1332 MHz
FIDRES           250.000000 Hz
SW                    4.998 ppm
FnMODE                   QF

F2 - Processing parameters
SI                     8192
SF              400.1300000 MHz
WDW                      EM
SSB         0
LB                     0.30 Hz
GB          0
PC                     1.00

F1 - Processing parameters
SI                       16
MC2                      QF
SF              400.1300000 MHz
WDW                      no
SSB         0
LB          0 Hz
GB          0
```

Figure S22. ^{1}H DOSY spectra of La$_2$(**Pt-L**)$_2$(ClO$_4$)$_6$ (400 MHz, CD$_3$CN, 298 K). (D=7.01×10^{-10} m^2 s^{-1}).

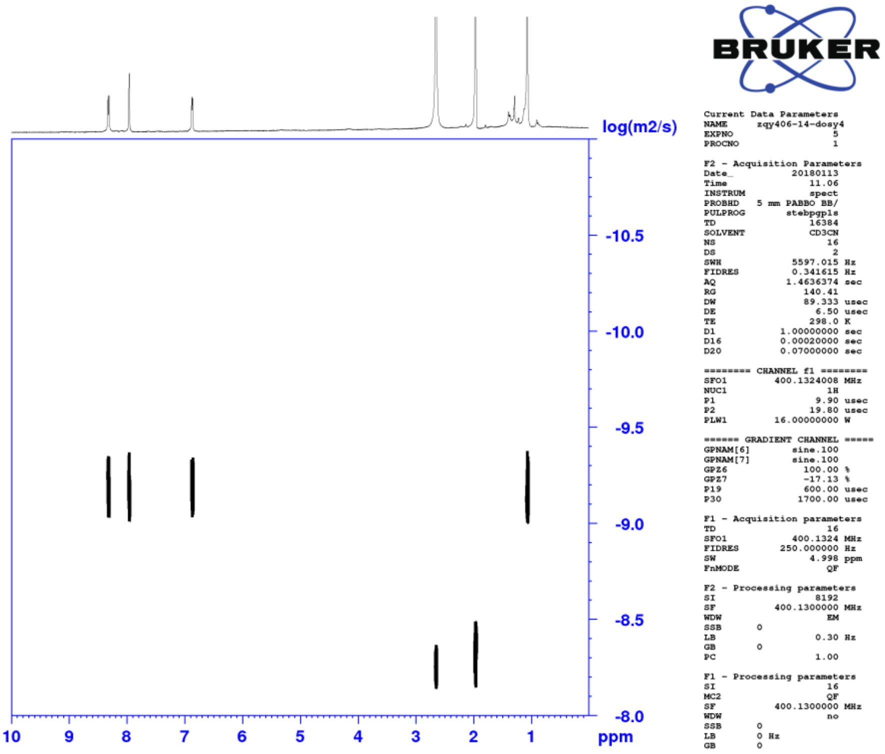

```
Current Data Parameters
NAME       zqy406-14-dosy4
EXPNO                    5
PROCNO                   1

F2 - Acquisition Parameters
Date_             20180113
Time                 11.06
INSTRUM              spect
PROBHD    5 mm PABBO BB/
PULPROG           stebpgp1s
TD                   16384
SOLVENT              CD3CN
NS                      16
DS                       2
SWH               5597.015 Hz
FIDRES            0.341615 Hz
AQ               1.4636374 sec
RG                  140.41
DW                  89.333 usec
DE                    6.50 usec
TE                   298.0 K
D1              1.00000000 sec
D16             0.00020000 sec
D20             0.07000000 sec

======== CHANNEL f1 ========
SFO1          400.1324008 MHz
NUC1                    1H
P1                    9.90 usec
P2                   19.80 usec
PLW1           16.00000000 W

====== GRADIENT CHANNEL =====
GPNAM[6]          sine.100
GPNAM[7]          sine.100
GPZ6                100.00 %
GPZ7                -17.13 %
P19                 600.00 usec
P30                1700.00 usec

F1 - Acquisition parameters
TD                      16
SFO1              400.1324 MHz
FIDRES          250.000000 Hz
SW                   4.998 ppm
FnMODE                  QF

F2 - Processing parameters
SI                    8192
SF             400.1300000 MHz
WDW                     EM
SSB      0
LB                    0.30 Hz
GB       0
PC                    1.00

F1 - Processing parameters
SI                      16
MC2                     QF
SF             400.1300000 MHz
WDW                     no
SSB      0
LB       0 Hz
GB       0
```

Figure S23. ^{1}H DOSY spectra of Eu$_2$(**Pt-L**)$_2$(OTf)$_6$ (400 MHz, CD$_3$CN, 298 K) (D=6.93×10^{-10} m^2 s^{-1}).

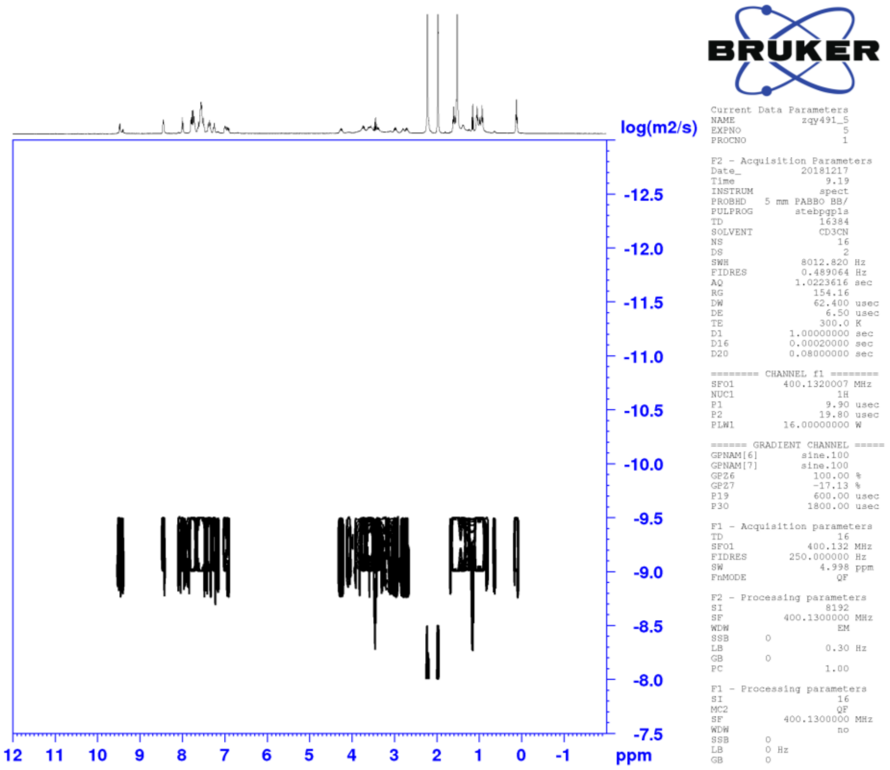

```
Current Data Parameters
NAME             zqy491_5
EXPNO                   5
PROCNO                  1

F2 - Acquisition Parameters
Date_            20181217
Time                 9.19
INSTRUM             spect
PROBHD    5 mm PABBO BB/
PULPROG          stebpgp1s
TD                  16384
SOLVENT             CD3CN
NS                     16
DS                      2
SWH              8012.820 Hz
FIDRES           0.489064 Hz
AQ              1.0223616 sec
RG                 154.16
DW                 62.400 usec
DE                   6.50 usec
TE                  300.0 K
D1             1.00000000 sec
D16            0.00020000 sec
D20            0.08000000 sec

======== CHANNEL f1 ========
SFO1         400.1320007 MHz
NUC1                   1H
P1                   9.90 usec
P2                  19.80 usec
PLW1          16.00000000 W

====== GRADIENT CHANNEL =====
GPNAM[6]         sine.100
GPNAM[7]         sine.100
GPZ6               100.00 %
GPZ7               -17.13 %
P19                600.00 usec
P30               1800.00 usec

F1 - Acquisition parameters
TD                     16
SFO1              400.132 MHz
FIDRES         250.000000 Hz
SW                  4.998 ppm
FnMODE                 QF

F2 - Processing parameters
SI                   8192
SF            400.1300000 MHz
WDW                    EM
SSB      0
LB                   0.30 Hz
GB       0
PC                   1.00

F1 - Processing parameters
SI                     16
MC2                    QF
SF            400.1300000 MHz
WDW                    no
SSB      0
LB       0 Hz
GB       0
```

Figure S24. ^{1}H DOSY spectra of Lu$_2$(**Pt-L**)$_2$(DPEPO)$_2$(OTf)$_6$ (400 MHz, CD$_3$CN, 298 K) (D=6.61×10^{-10} m^2 s^{-1}).

3. Photophysical property

3.1 UV-Vis absorption and Fluorescence Spectra

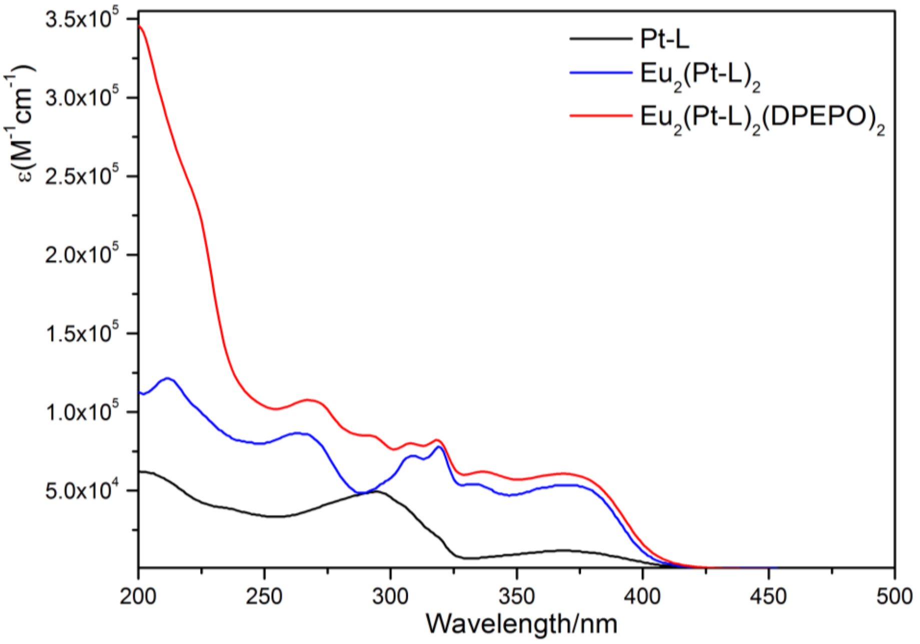

Figure S25. UV/Vis absorption spectra of **Pt-L**, Eu_2(**Pt-L**)$_2$(OTf)$_6$ and Eu_2(**Pt-L**)$_2$(DPEPO)$_2$(OTf)$_6$ in CH_3CN.

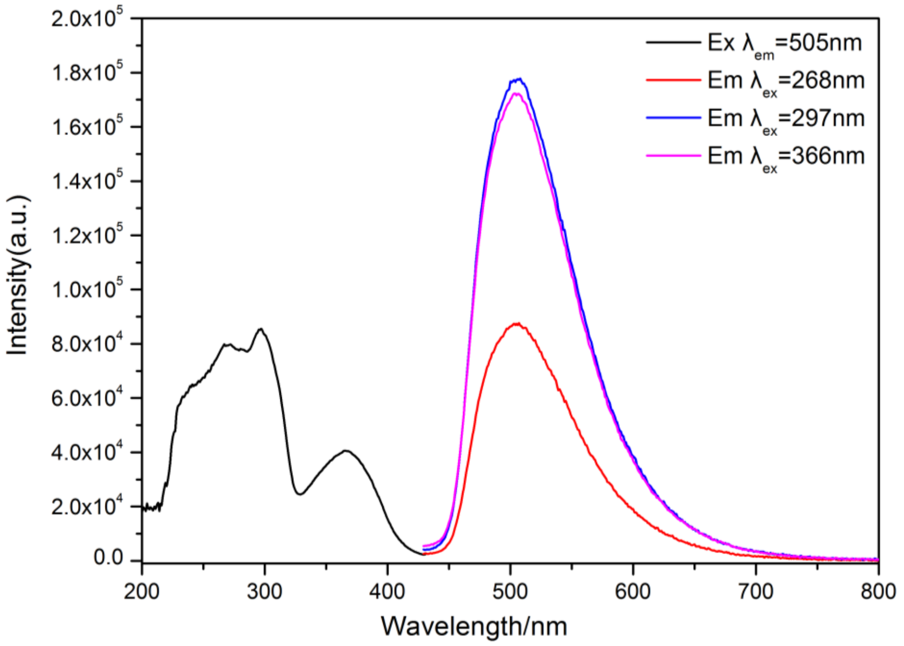

Figure S26. Excitation and emission spectrum of ligand **Pt-L** at different wavelengths in CH_3CN (c= 1×10^{-5} M, slits =4-4).

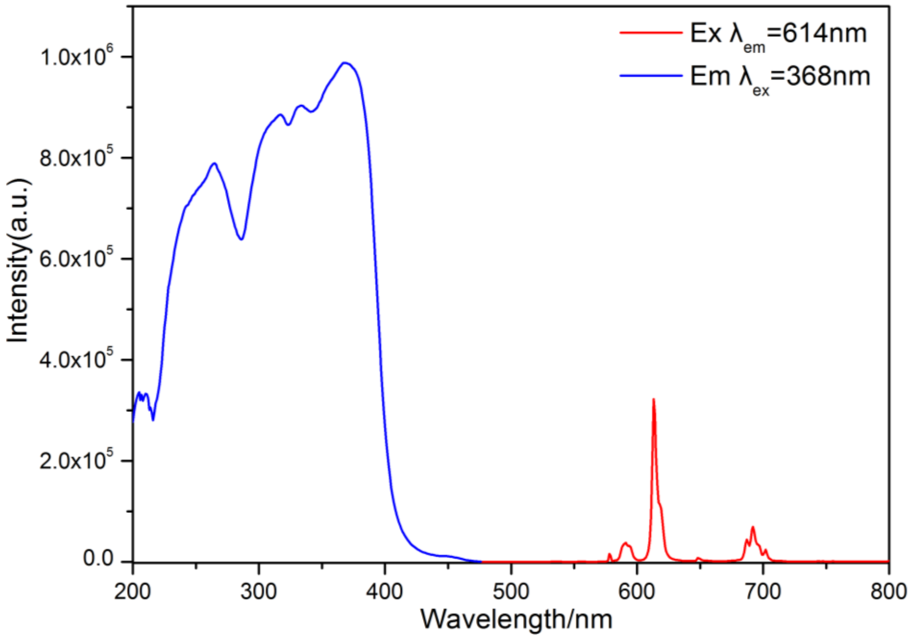

Figure S27. Excitation spectrum and emission spectrum of Eu_2(**Pt-L**)$_2$(OTf)$_6$ in CH_3CN (c= 1×10^{-5} M, slits =0.9-0.9).

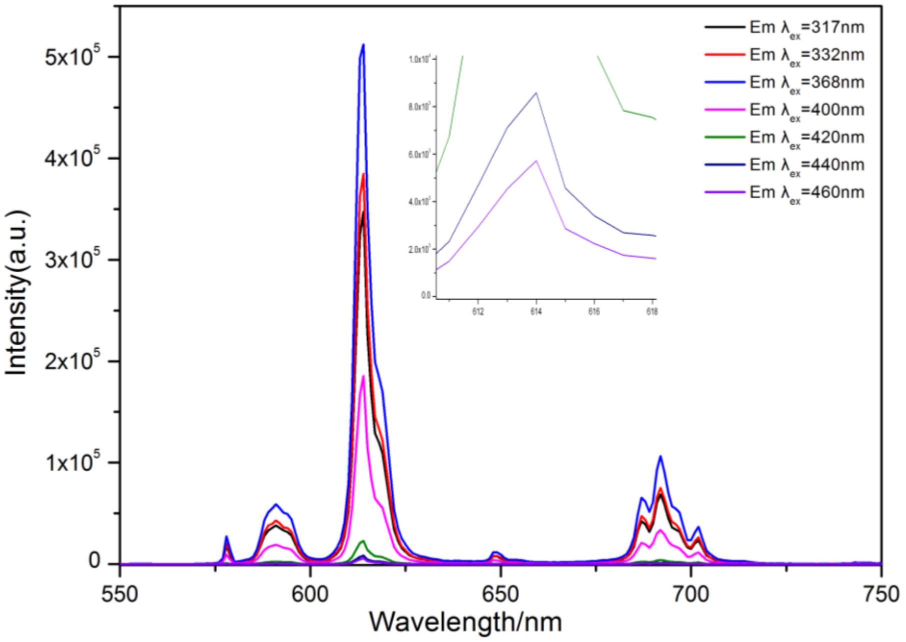

Figure S28. Excitation and emission spectrum of Eu_2(**Pt-L**)$_2$(OTf)$_6$ at different wavelengths in CH_3CN (c= 1×10^{-5} M, slits =0.9-0.9, λ_{em}=614nm).

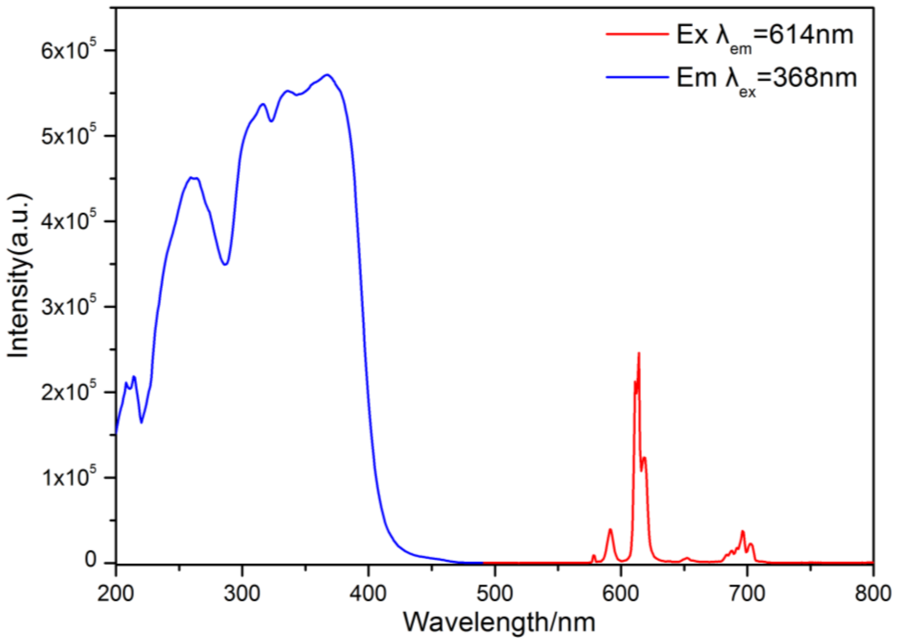

Figure S29. Excitation spectrum and emission spectrum of Eu_2(**Pt-L**)$_2$(DPEPO)$_2$(OTf)$_6$ in CH_3CN, (c= 1×10^{-5} M, slits =0.6-0.6).

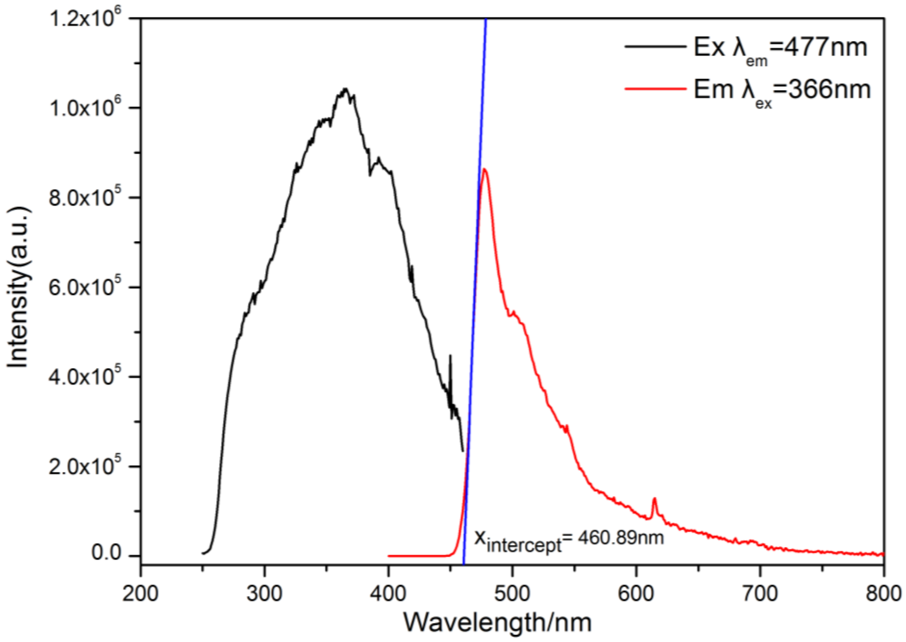

Figure S30.The excitation and emission spectra of Gd_2(**Pt-L**)$_2$(OTf)$_6$ (powder, 77 k, slits =6-6).

3.2 Lifetime measurement

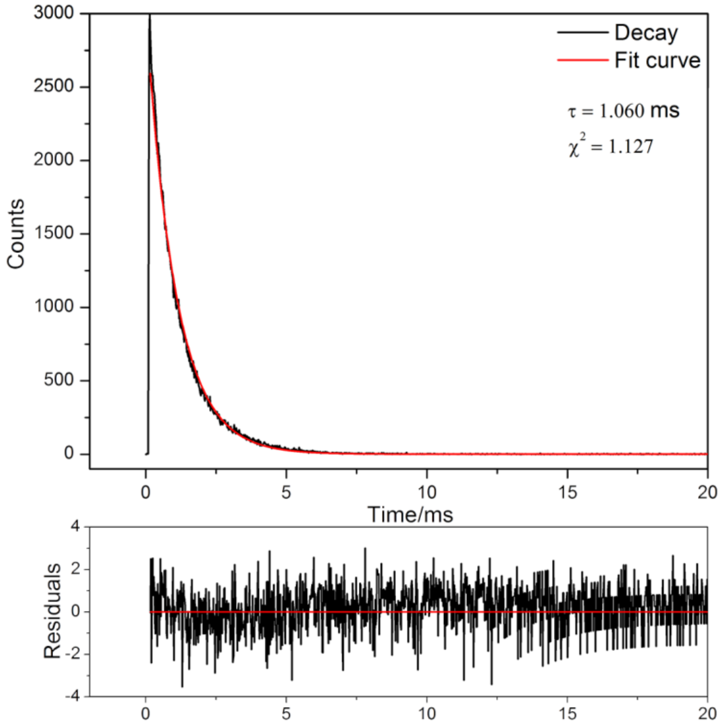

Figure S31. Excited state decay curve (black line) with mono exponential fit (red line) of Eu_2(**Pt-L**)$_2$ (1×10^{-5} M in CH_3CN, λ_{ex} = 368 nm, λ_{em} = 614 nm).

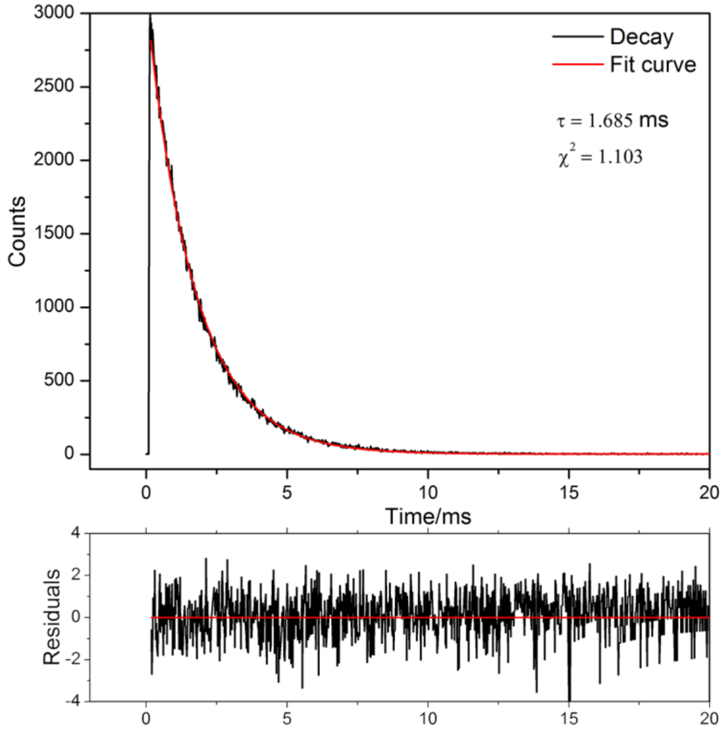

Figure S32. Excited state decay curve (black line) with mono exponential fit (red line) of Eu_2(**Pt-L**)$_2$(DPEPO)$_2$ (1×10^{-5} M in CH_3CN, λ_{ex} = 368 nm, λ_{em} = 614 nm).

The intrinsic quantum yields of europium can be determined by the following two equations:[2]

$$\Phi = \frac{A_{RAD}}{A_{RAD}+A_{ND}} = \frac{\tau_{obs}}{\tau_{rad}} \qquad (2)$$

$$A_{RAD} = \frac{1}{\tau_{rad}} = A_{MD,O}\, n^3 \left(\frac{I_{tot}}{I_{MD}}\right) \qquad (3)$$

Where, A_{RAD} and A_{NR} are radiative and non-radiative decay rate, respectively. τ_{obs} and τ_{rad} are observed and radiative lifetimes, respectively. n is the refractive index of the medium, while I_{tot} is the integrated emission of the $^5D_0 \rightarrow {}^7F_J$ (J = 0 - 6) transition, and I_{MD} is the integrated emission of the $^5D_0 \rightarrow {}^7F_1$ transition. $A_{MD,0}$ = 14.65 s^{-1} is the spontaneous emission probability emission probability of magnetic dipole $^5D_0 \rightarrow {}^7F_1$ transition.

The efficiency of lanthanide sensitization (Φ_{sens}) is the ratio between $\Phi_{overall}$ (determined experimentally) and Φ_{Ln}:[3]

$$\Phi_{sense} = \frac{\Phi_{\mathrm{overall}}}{\Phi_{Ln}} \qquad (4)$$

Table S1. Summary of photophysical data for the ligand and heterometal-organic macrocycles.

Complex	$\varepsilon/10^4$ [$M^{-1}cm^{-1}$]	λ_{ex}^{max} [nm]	λ_{em}^{ax} [nm]	τ_{obs}	q[a]	$\Phi_{overall}$[b] [%]	Φ_{Ln} [%]	Φ_{sens}[c] [%]
Pt-L	1.18	366	505	5.78ns	-	1.4	-	-
$Eu_2(Pt\text{-}L)_2$	5.44	368	614	1.06ms	2.95	30.4	49.8	61.0
$Eu_2(Pt\text{-}L)_2(DPEPO)_2$	6.07	368	614	1.69ms	0.34	79.4	89.9	88.3

[a] Number of coordinated solvent molecules; [b] Overall luminescence quantum yield; [c] Efficiency of ligand sensitization.

3.3 Quantum yield

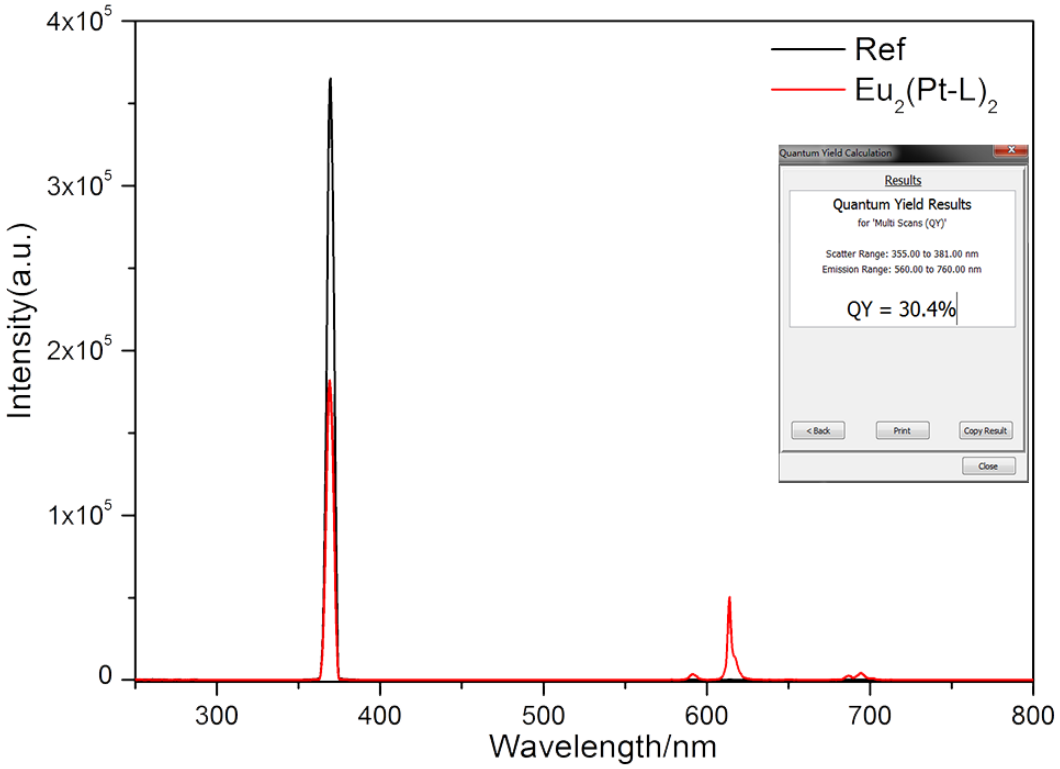

Quantum Yield Results
for 'Multi Scans (QY)'

Scatter Range: 355.00 to 381.00 nm
Emission Range: 560.00 to 760.00 nm

QY = 30.4%

Figure S33. Quantum yield of Eu_2(**Pt-L**)$_2$ in CH_3CN (298K, c=1×10^{-5} M, λ_{ex}=368nm).

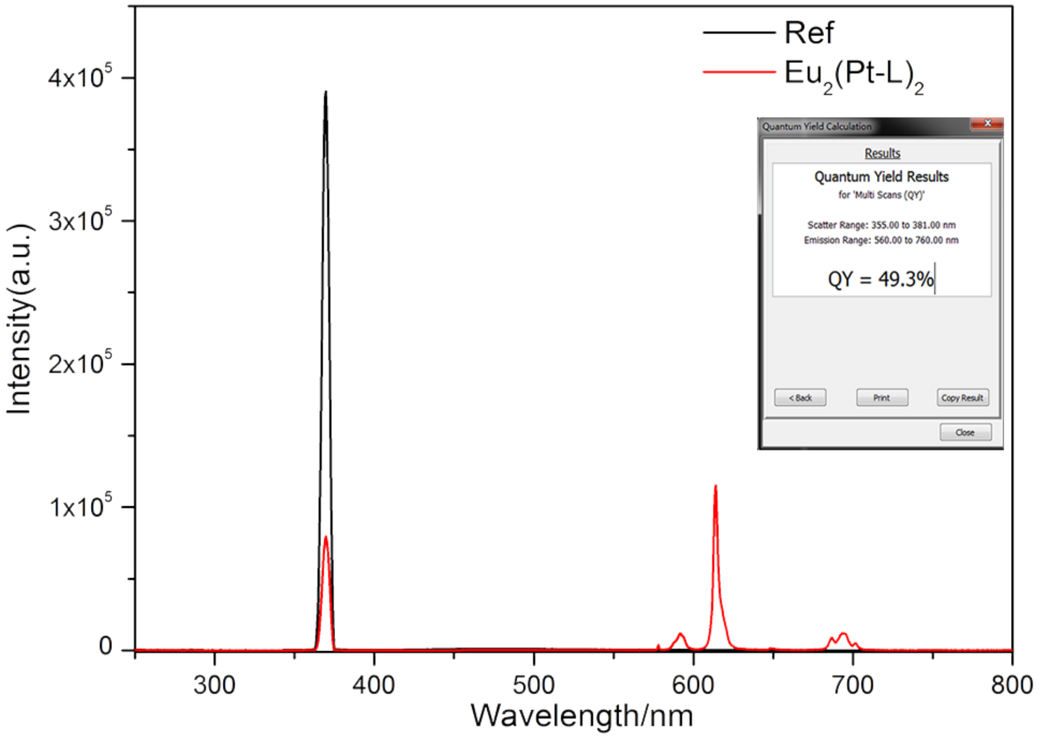

Quantum Yield Results
for 'Multi Scans (QY)'

Scatter Range: 355.00 to 381.00 nm
Emission Range: 560.00 to 760.00 nm

QY = 49.3%

Figure S34. Quantum yield of Eu_2(**Pt-L**)$_2$ in solid state (298K, powder, λ_{ex}=368nm).

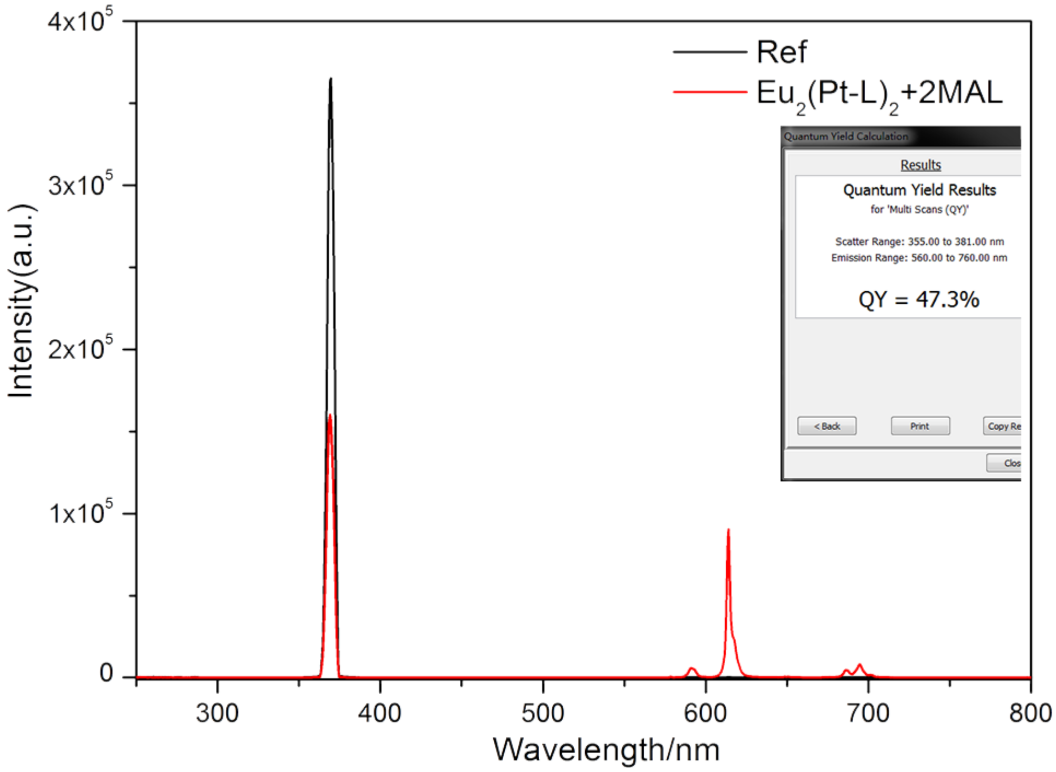

Quantum Yield Results

for 'Multi Scans (QY)'

Scatter Range: 355.00 to 381.00 nm

Emission Range: 560.00 to 760.00 nm

QY = 47.3%

Figure S35. Quantum yield of Eu_2(**Pt-L**)$_2$ with 2equiv MAL in CH_3CN (298K, c=1×10^{-5} M, λ_{ex}=368nm).

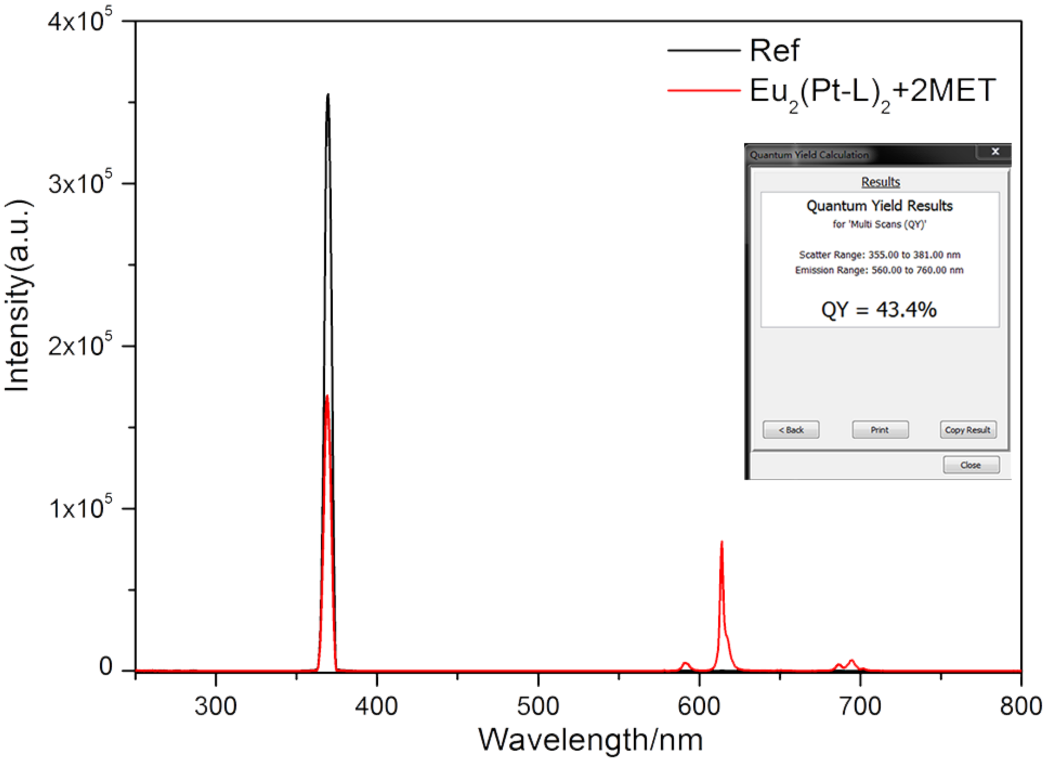

Quantum Yield Results

for 'Multi Scans (QY)'

Scatter Range: 355.00 to 381.00 nm

Emission Range: 560.00 to 760.00 nm

QY = 43.4%

Figure S36. Quantum yield of Eu_2(**Pt-L**)$_2$ with 2equiv MET in CH_3CN (298K, c=1×10^{-5} M, λ_{ex}=368nm).

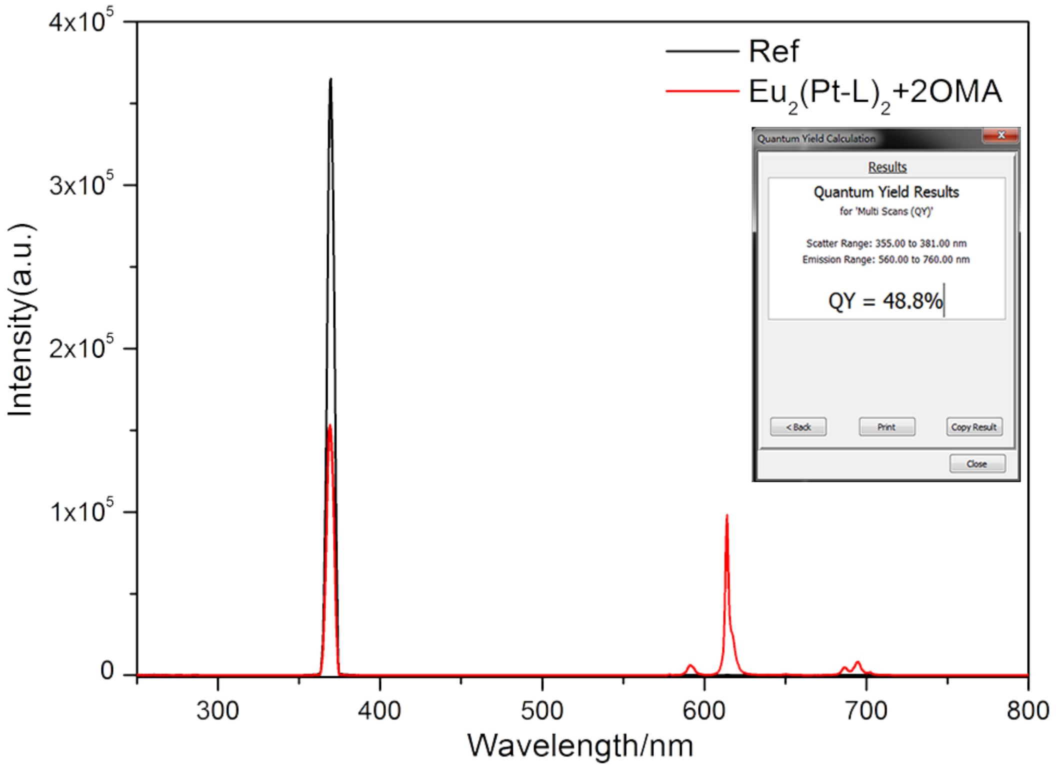

Quantum Yield Results
for 'Multi Scans (QY)'

Scatter Range: 355.00 to 381.00 nm
Emission Range: 560.00 to 760.00 nm

QY = 48.8%

Figure S37. Quantum yield of Eu_2(**Pt-L**)$_2$ with 2equiv OMA in CH_3CN (298K, c=1×10^{-5} M, λ_{ex}=368nm).

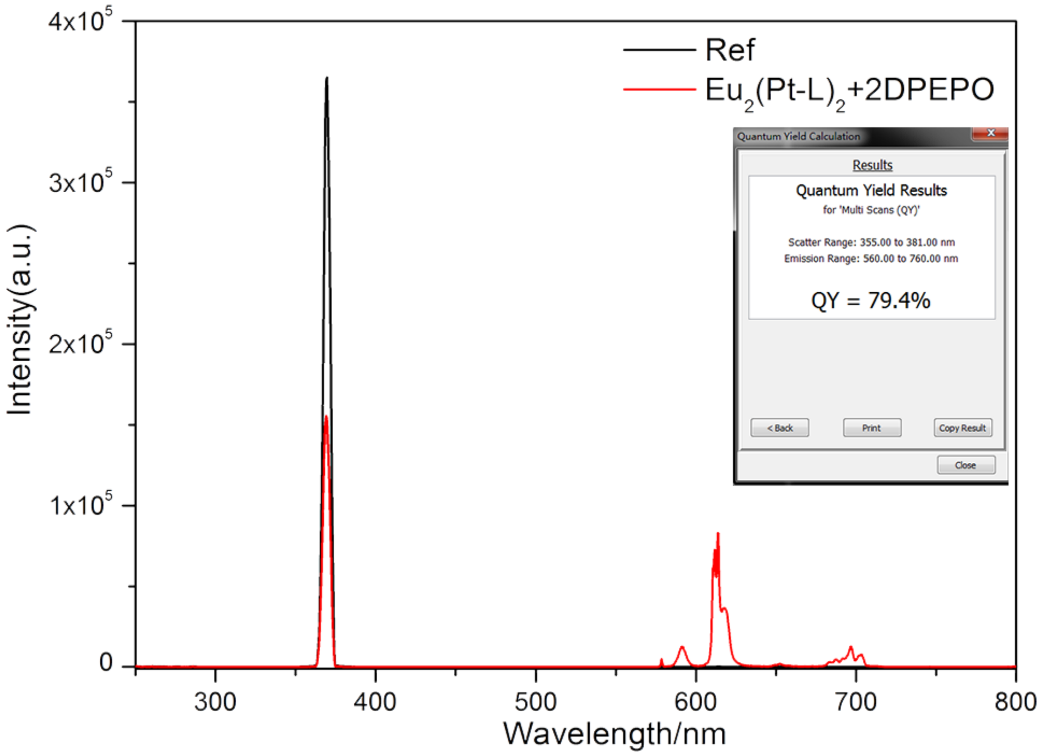

Quantum Yield Results
for 'Multi Scans (QY)'

Scatter Range: 355.00 to 381.00 nm
Emission Range: 560.00 to 760.00 nm

QY = 79.4%

Figure S38. Quantum yield of Eu_2(**Pt-L**)$_2$(DPEPO)$_2$ in CH_3CN (298K, c=1×10^{-5} M, λ_{ex}=368nm).

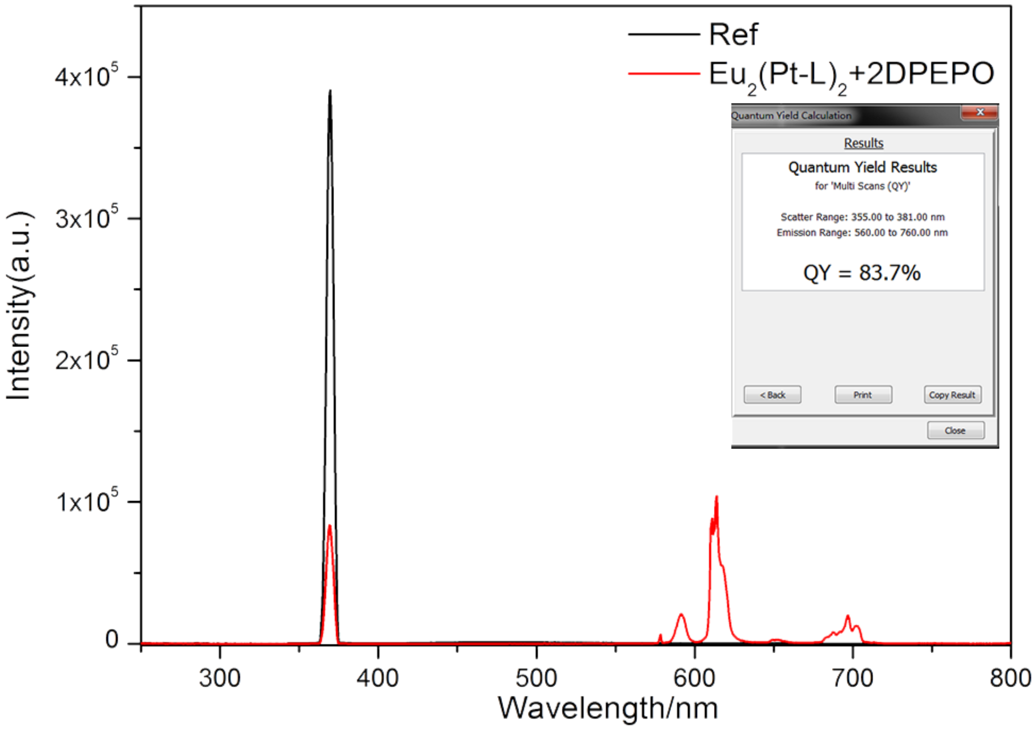

Quantum Yield Results
for 'Multi Scans (QY)'

Scatter Range: 355.00 to 381.00 nm
Emission Range: 560.00 to 760.00 nm

QY = 83.7%

Figure S39. Quantum yield of Eu_2(**Pt-L**)$_2$(DPEPO)$_2$ in solid state (298K, powder, λ_{ex}=368nm).

3.3 Number of coordinated solvent molecules

Here, empirical equation is used to determine the number of solvent molecules q coordinated to Eu^{III} centers in compounds.

$$q=A(\tau_{methanol}^{-1} - \tau_{deutero\text{-}methanol}^{-1} - B) \qquad (5)$$

Where, empirically coefficients A = 2.1 and B = 0 were determined in methanol and Methanol-d4 condition. The calculated q values is 2.95 for Eu_2(**Pt-L**)$_2$, And 0.34 for Eu_2(**Pt-L**)$_2$(DPEPO)$_2$.

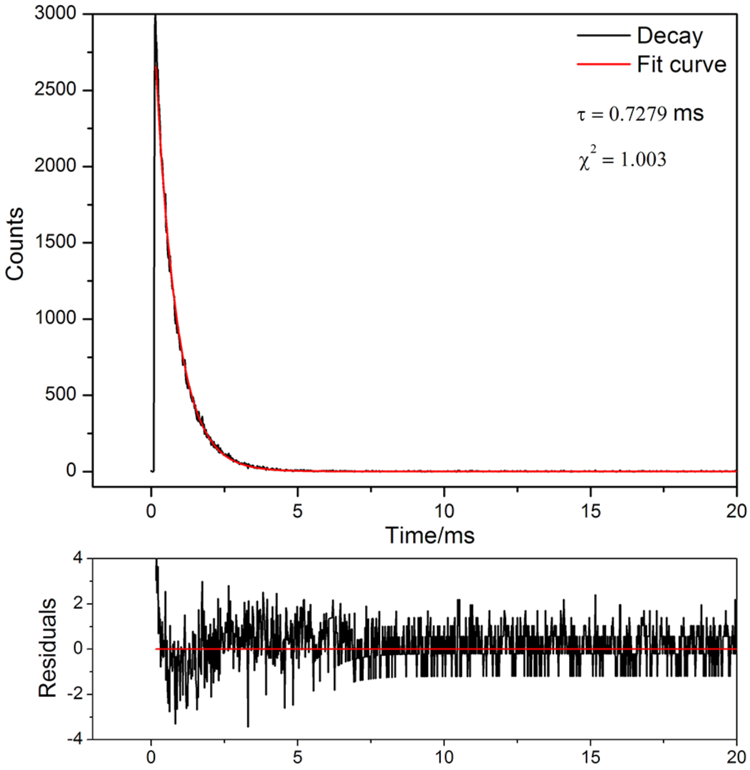

Figure S40. Excited state decay curve (black line) with mono exponential fit (red line) of Eu_2(**Pt-L**)$_2$ (2×10^{-5} M in CD_3OD, λ_{ex} = 368 nm, λ_{em} = 614 nm).

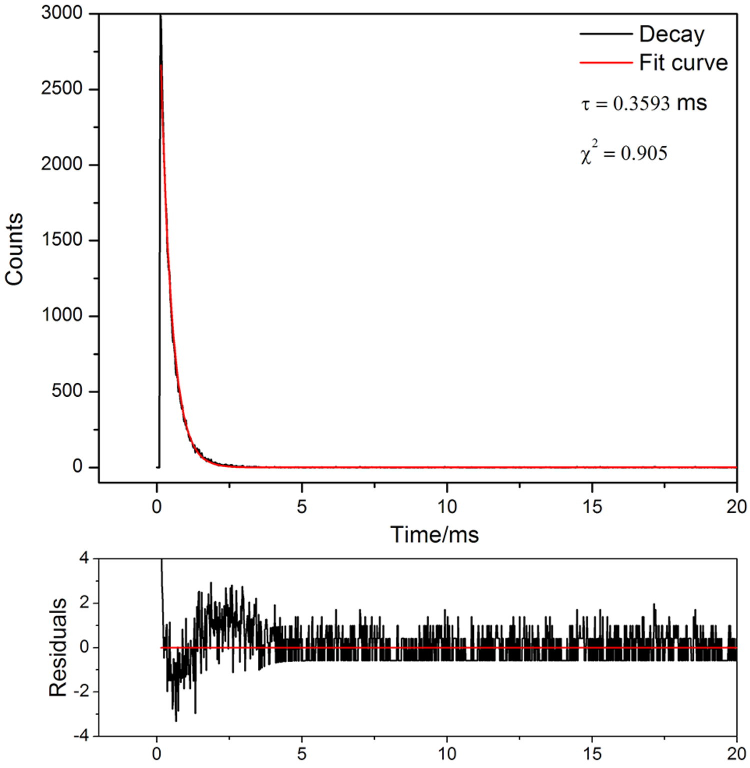

Figure S41. Excited state decay curve (black line) with mono exponential fit (red line) of Eu_2(**Pt-L**)$_2$ (2×10^{-5} M in CD_3OH, λ_{ex} = 368 nm, λ_{em} = 614 nm).

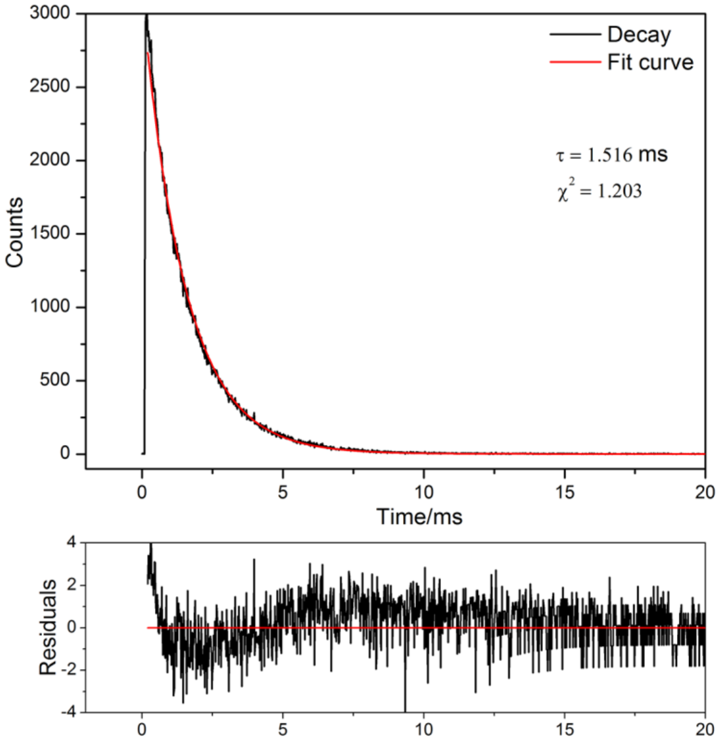

Figure S42. Excited state decay curve (black line) with mono exponential fit (red line) of Eu_2(**Pt-L**)$_2$(DPEPO)$_2$ (2×10^{-5} M in CD_3OD, λ_{ex} = 368 nm, λ_{em} = 614 nm).

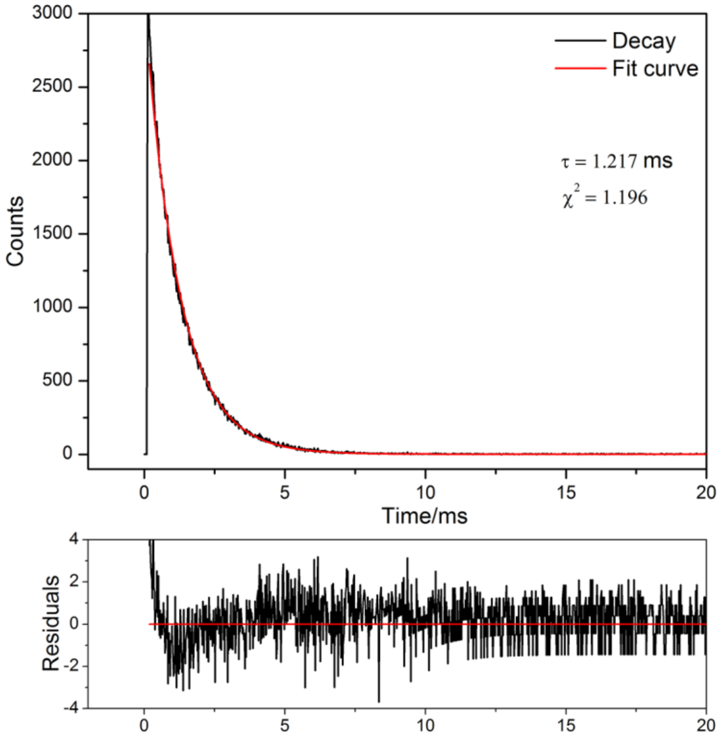

Figure S43. Excited state decay curve (black line) with mono exponential fit (red line) of Eu_2(**Pt-L**)$_2$(DPEPO)$_2$ (2×10^{-5} M in CD_3OH, λ_{ex} = 368 nm, λ_{em} = 614 nm).

4. Organophosphorus sensing

4.1 Fluorescent titration

Benesi-Hildebrand equation:

$$\frac{1}{F-F_0}=\frac{1}{K_a(F_{max}-F_0)[A]^2}+\frac{1}{F_{max}-F_0} \qquad (6)$$

was used to estimate the binding constant. Where: A is the concentration of OPs. F_0 and F are the fluorescence intensity of Eu_2(**Pt-L**)$_2$ in the absence and presence of OPs, respectively. F_{max} is the fluorescence intensity obtained with excess of OPs. K_a is the binding constant.

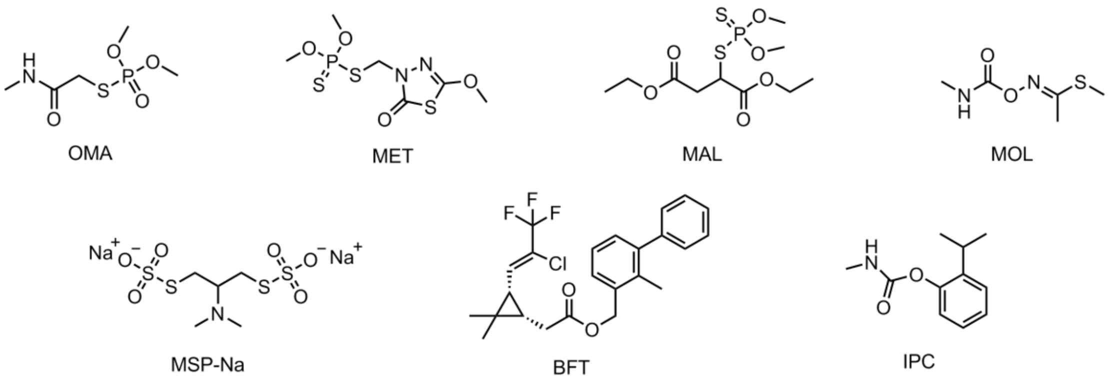

Scheme S2. The chemical structures of the pesticides studied.

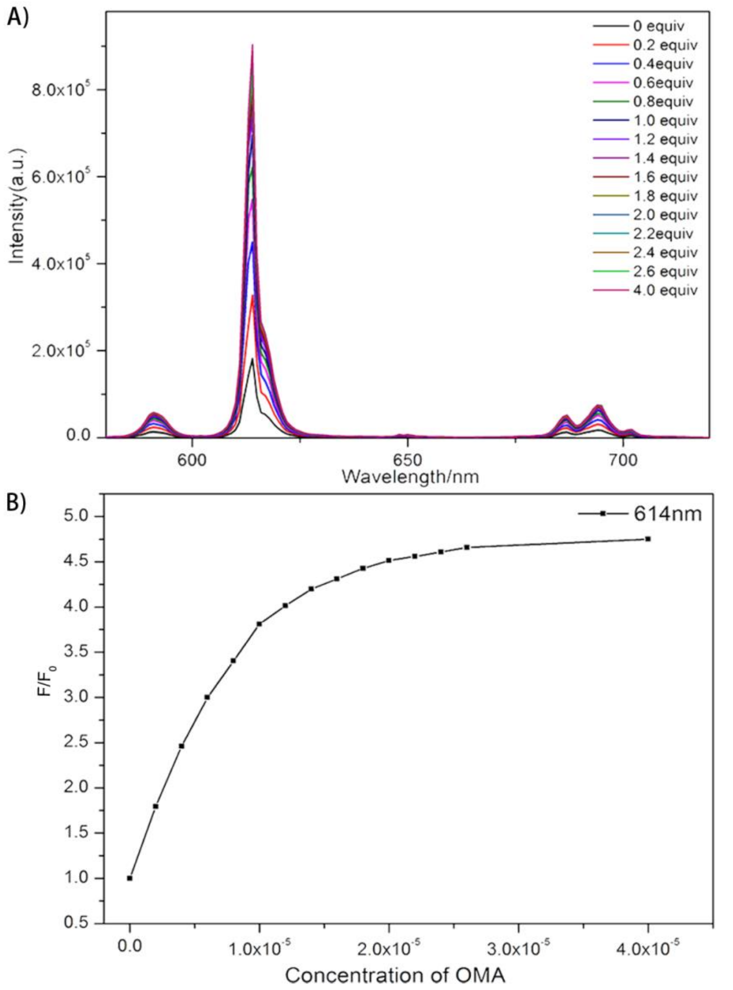

Figure S44. (A) Fluorescent titration spectra of Eu_2(**Pt-L**)$_2$ in CH_3CN (1×10^{-5}M, λ_{ex} = 368 nm) upon addition of different equiv of OMA. (B) Changes of the fluorescence emission at 614 nm of Eu_2(**Pt-L**)$_2$ containing different equiv of OMA.

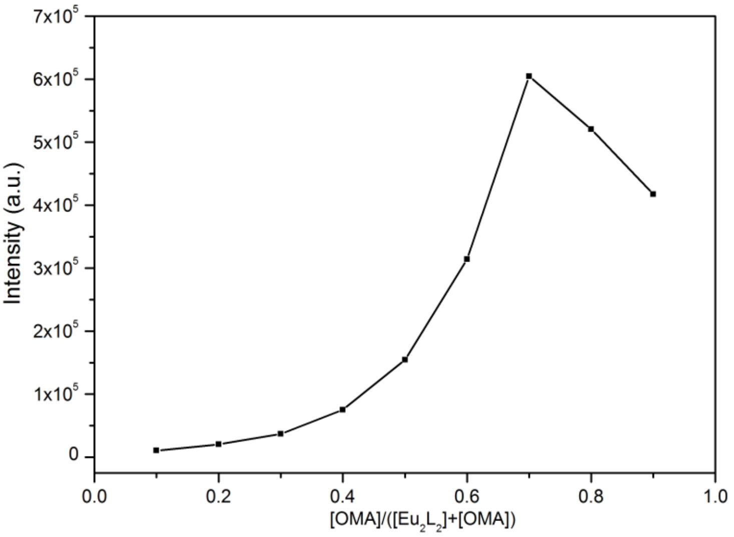

Figure S45. Job’s plot confirming the 2:1 binding stoichiometry of OMA with Eu_2(**Pt-L**)$_2$.

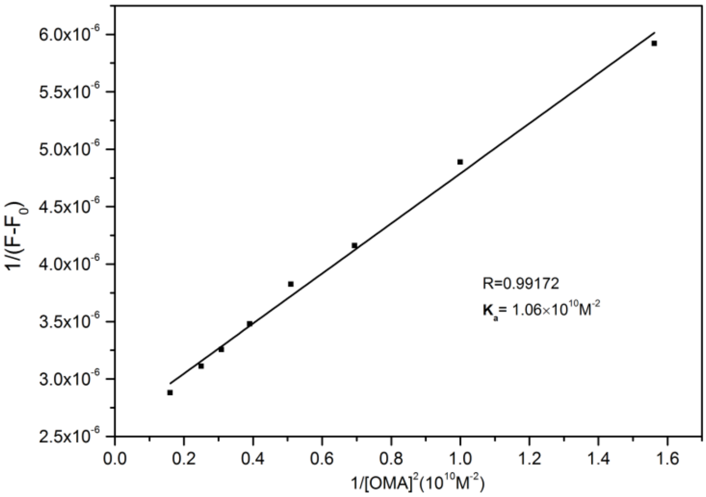

Figure S46. The Benesi-Hildebrand plot for determining K_a of OMA with Eu_2(**Pt-L**)$_2$.

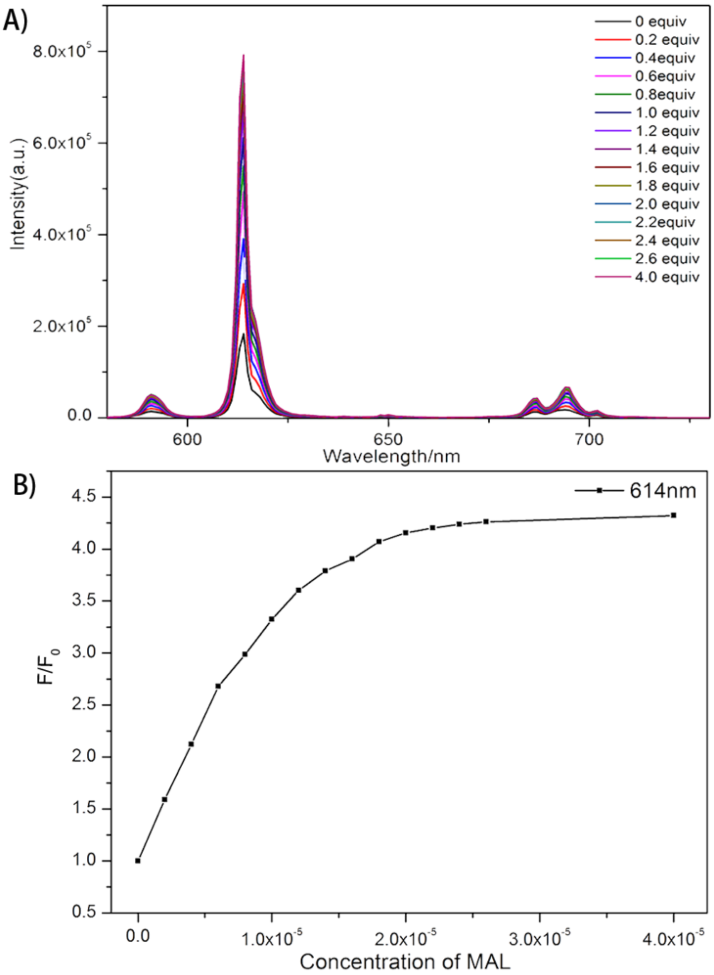

Figure S47. (A) Fluorescent titration spectra of Eu_2L_2 in CH_3CN (1×10^{-5}M, λ_{ex} = 368 nm) upon addition of different equiv of MAL. (B) Changes of the fluorescence emission at 614 nm of Eu_2(**Pt-L**)$_2$ containing different equiv of MAL.

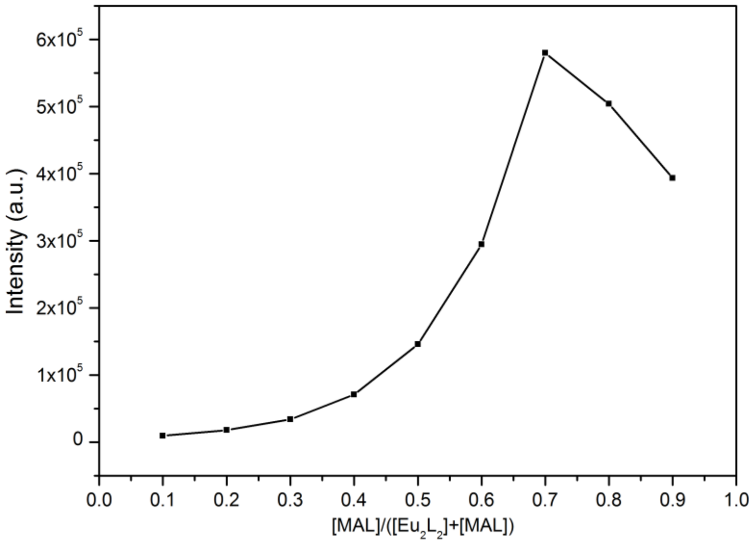

Figure S48. Job’s plot confirming the 2: 1binding stoichiometry of MAL with Eu_2(**Pt-L**)$_2$.

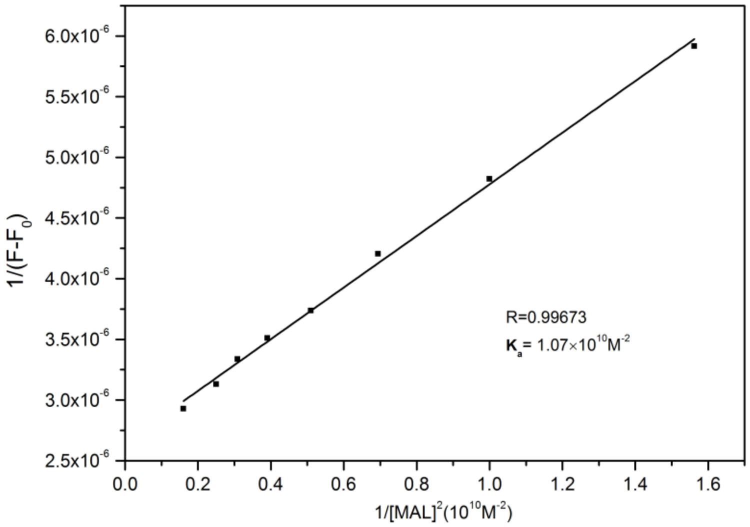

Figure S49. The Benesi-Hildebrand plot for determining K_a of MAL with Eu_2(**Pt-L**)$_2$.

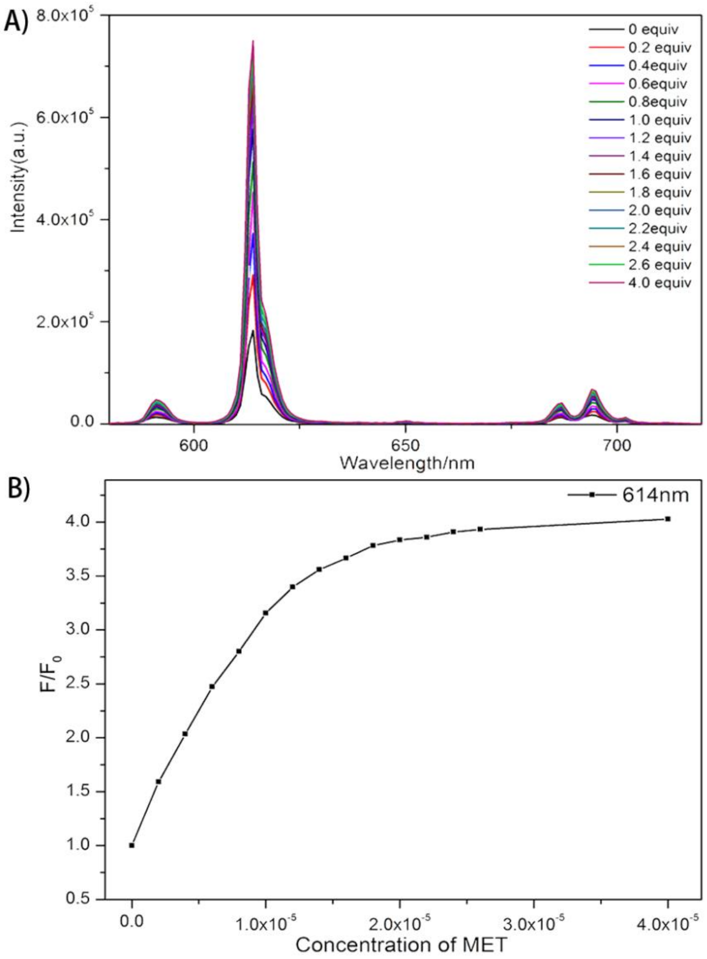

Figure S50. (A) Fluorescent titration spectra of Eu_2(**Pt-L**)$_2$ in CH_3CN (1×10^{-5}M, λ_{ex} = 368 nm) upon addition of different equiv of MET. (B) Changes of the fluorescence emission at 614 nm of Eu_2(**Pt-L**)$_2$ containing different equiv of MET.

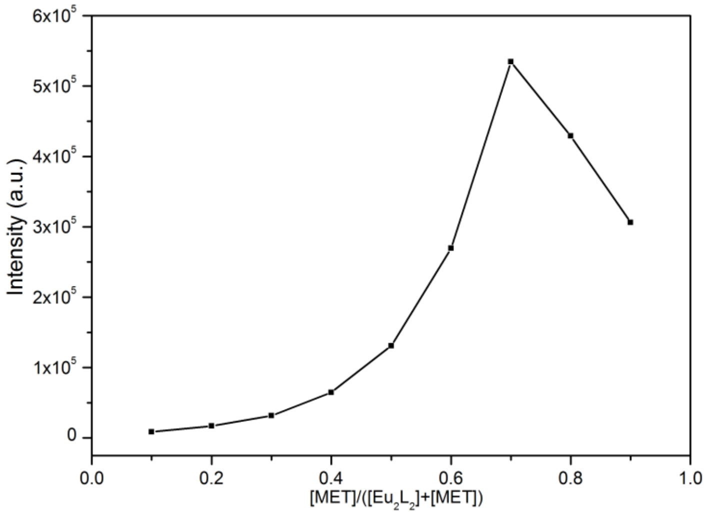

Figure S51. Job's plot confirming the 2: 1binding stoichiometry of MET with Eu_2(**Pt-L**)$_2$.

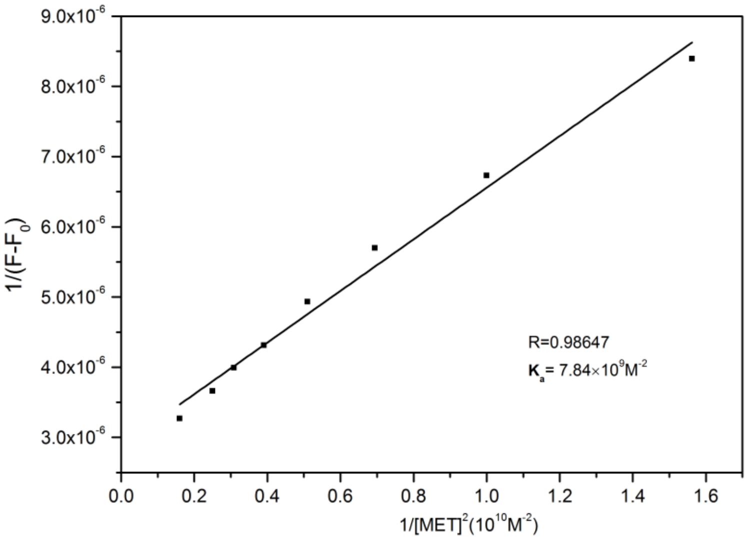

Figure S52. The Benesi-Hildebrand plot for determining K_a of MET with Eu_2(**Pt-L**)$_2$.

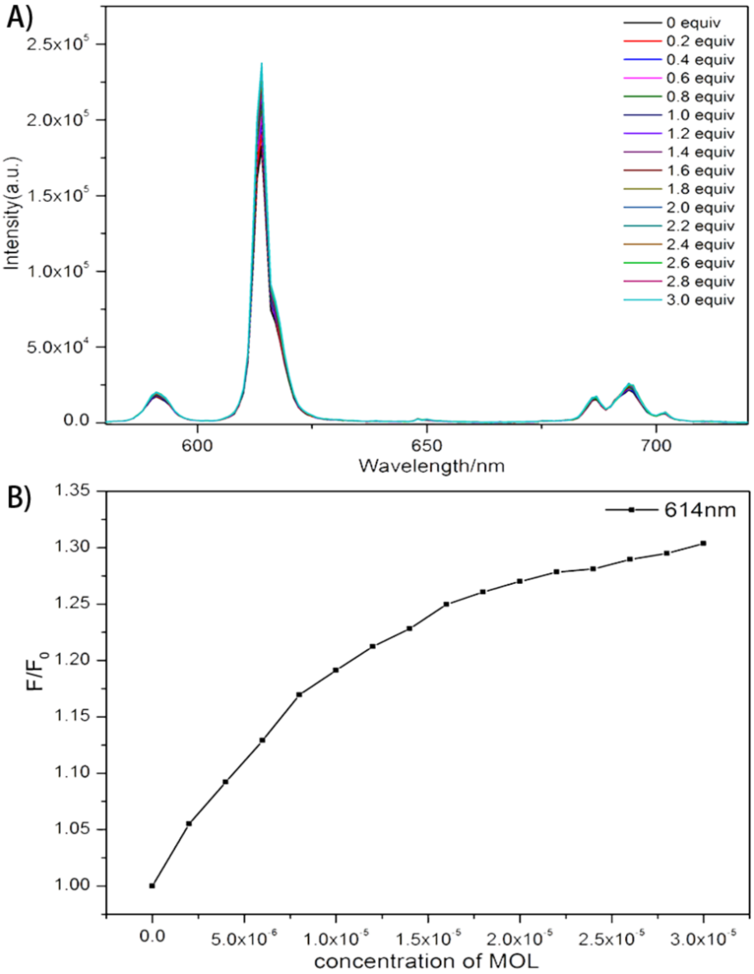

Figure S53. (A) Fluorescent titration spectra of Eu_2(**Pt-L**)$_2$ in CH_3CN (1×10^{-5}M, λ_{ex} = 368 nm) upon addition of different equiv of MOL. (B) Changes of the fluorescence emission at 614 nm of Eu_2(**Pt-L**)$_2$ containing different equiv of MOL.

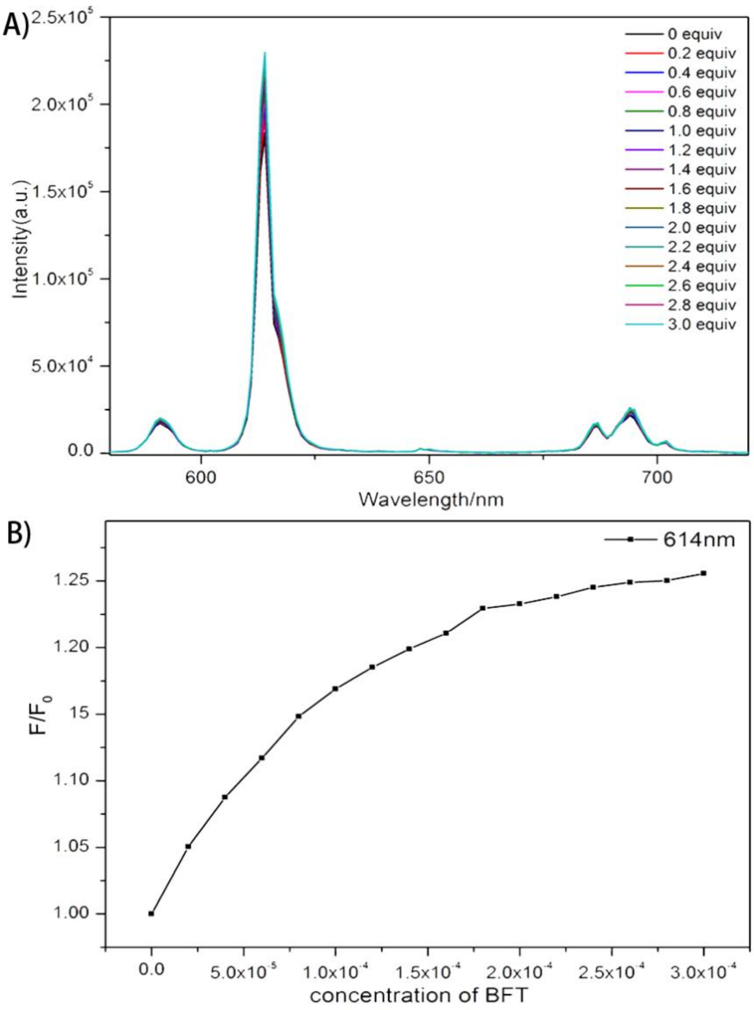

Figure S54. (A) Fluorescent titration spectra of Eu_2(**Pt-L**)$_2$ in CH_3CN (1×10^{-5}M, λ_{ex}=368 nm) upon addition of different equiv of BFT. (B) Changes of the fluorescence emission at 614 nm of Eu_2(**Pt-L**)$_2$ containing different equiv of BFT.

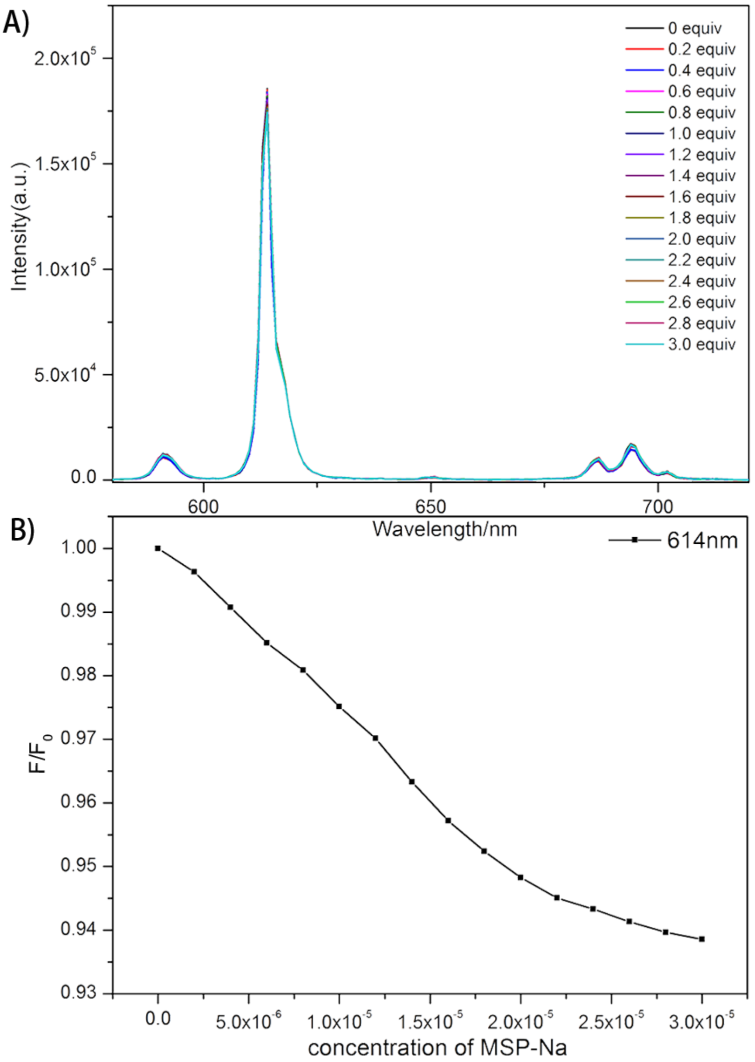

Figure S55. (A) Fluorescent titration spectra of Eu_2(**Pt-L**)$_2$ in CH_3CN (1×10^{-5}M, λ_{ex} = 368 nm) upon addition of different equiv of MSP-Na. (B) Changes of the fluorescence emission at 614 nm of Eu_2(**Pt-L**)$_2$ containing different equiv of MSP-Na.

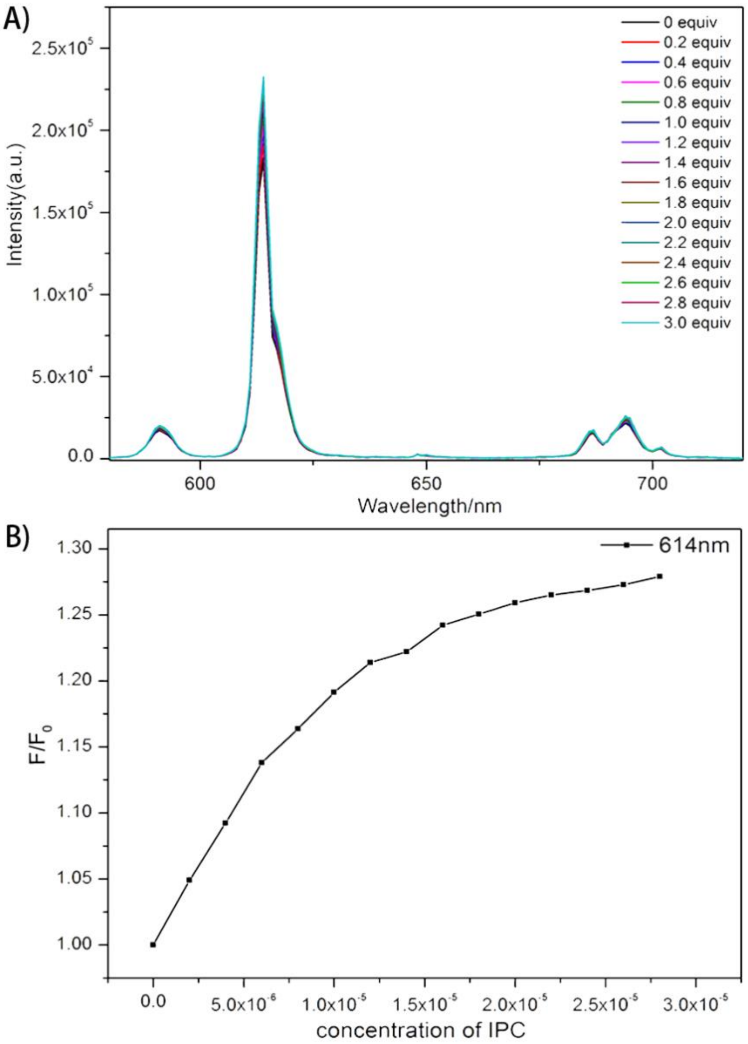

Figure S56. (A) Fluorescent titration spectra of Eu_2(**Pt-L**)$_2$ in CH_3CN (1×10^{-5}M, λ_{ex} = 368 nm) upon addition of different equiv of IPC. (B) Changes of the fluorescence emission at 614 nm of Eu_2(**Pt-L**)$_2$ containing different equiv of IPC.

4.2 UV-Vis titration

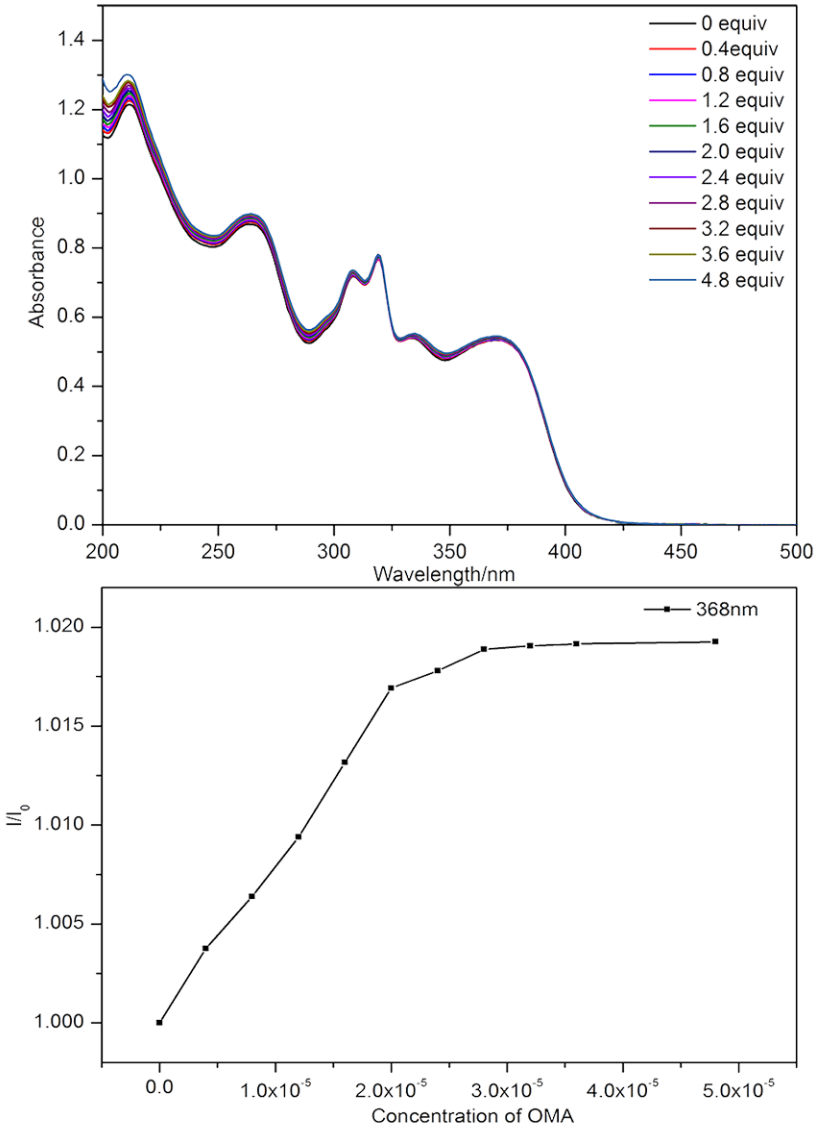

Figure S57. UV-Vis titration spectra of Eu_2(**Pt-L**)$_2$ in CH_3CN (1×10^{-5}M) upon addition of different equiv of OMA and Changes of the UV-Vis absorbance at 368 nm of Eu_2(**Pt-L**)$_2$ containing different equiv of OMA.

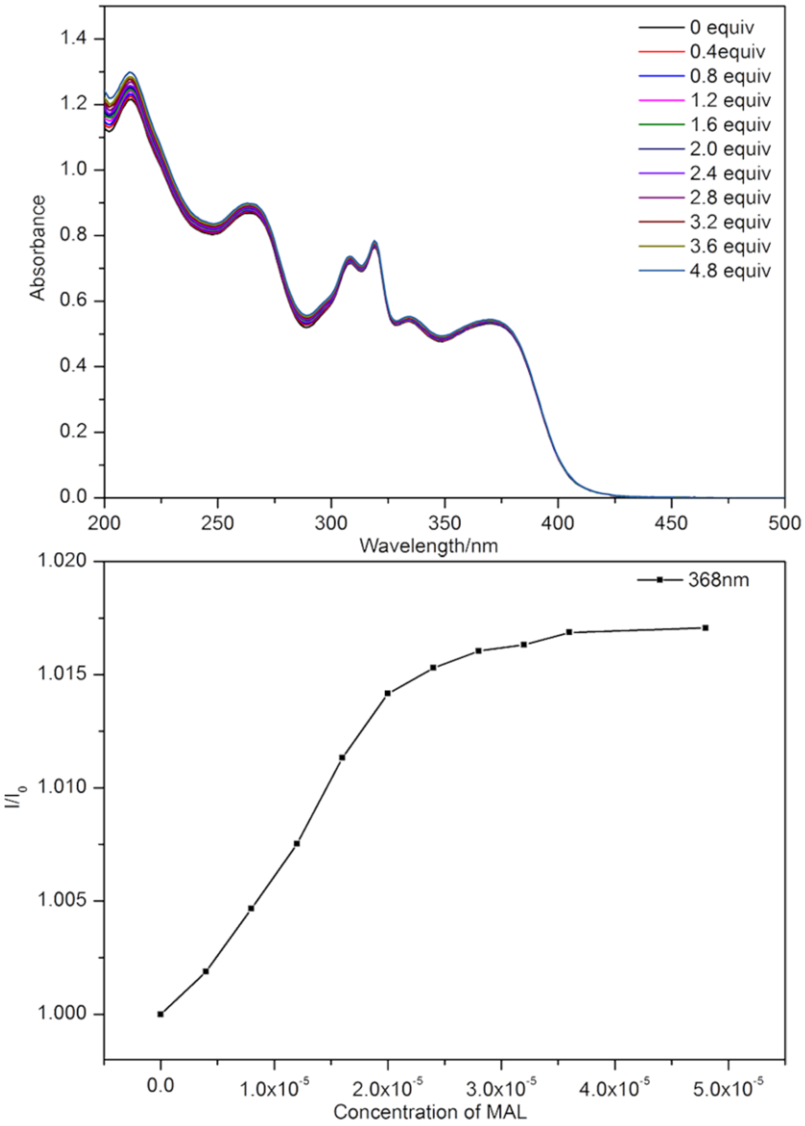

Figure S58. UV-Vis titration spectra of Eu_2(**Pt-L**)$_2$ in CH_3CN (1×10^{-5}M) upon addition of different equiv of MAL and Changes of the UV-Vis absorbance at 368 nm of Eu_2(**Pt-L**)$_2$ containing different equiv of MAL.

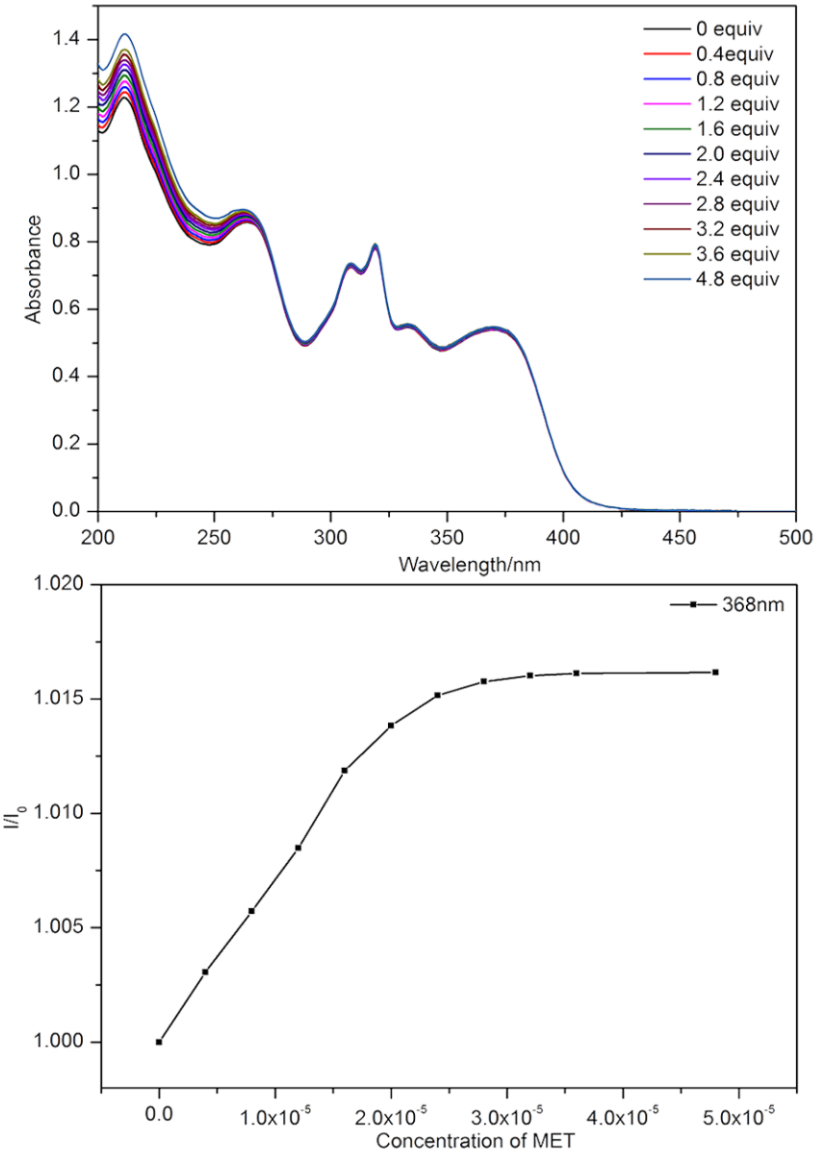

Figure S59. UV-Vis titration spectra of Eu_2(**Pt-L**)$_2$ in CH_3CN (1×10^{-5}M) upon addition of different equiv of MET and Changes of the UV-Vis absorbance at 368 nm of Eu_2(**Pt-L**)$_2$ containing different equiv of MET.

4.3 Lifetime measurement

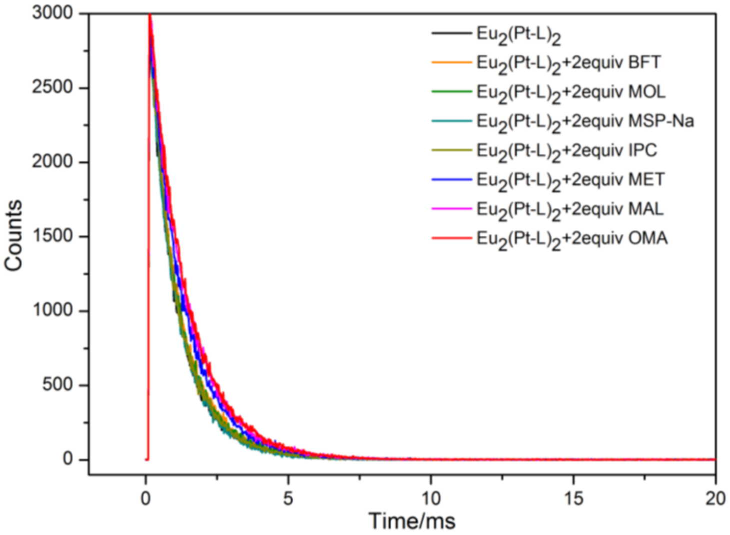

Figure S60. Excited state decay curve of Eu_2(**Pt-L**)$_2$ complexes with the addition of 2 equiv pesticides.

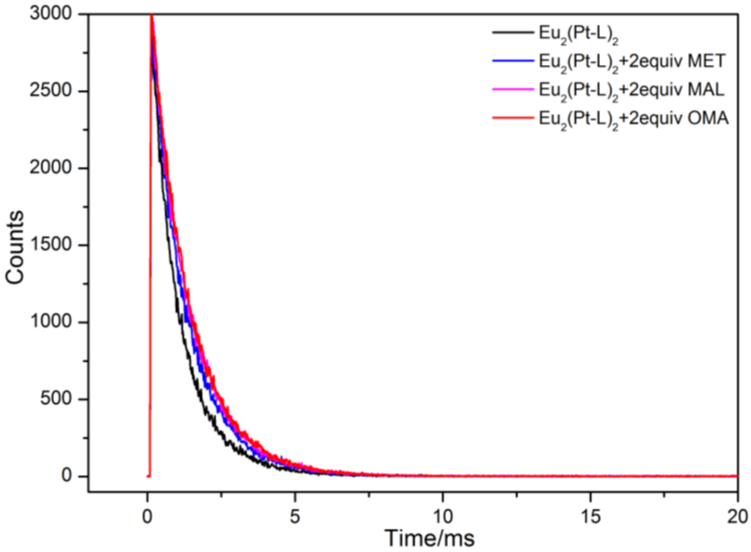

Figure S61. Excited state decay curve of Eu_2(**Pt-L**)$_2$ complexes with the addition of 2.0 equiv pesticides.

Table S2. Excited state decay curve of Eu_2(**Pt-L**)$_2$ complexes with the addition of 2.0 equiv pesticides.

	Eu_2L_2	**Eu_2L_2+ BFT**	**Eu_2L_2+ MOL**	**Eu_2L_2+ MSP-Na**	**Eu_2L_2+IPC**	**Eu_2L_2+ MET**	**Eu_2L_2+ MAL**	**Eu_2L_2+ OMA**
τ	1.060	1.099	1.101	1.017	1.095	1.225	1.281	1.306
χ^2	1.127	1.371	1.353	1.104	1.325	1.007	1.146	1.049

4.4 Limit of detection (LOD)

$$\mathrm{LOD}=3\delta/S \qquad (7)$$

$$\delta=\sqrt{\frac{\Sigma(F_0-\overline{F_0})^2}{N-1}}=483.5781(N=20) \qquad (8)$$

Where: S is the slope of the calibration curve, Standard deviation (δ) is calculated from twenty times measurements of blank solutions.

Table S3. Detection limit of Eu_2(**Pt-L**)$_2$ for OPs.

	OMA	MAL	MET
LOD (nM)	19	21	26

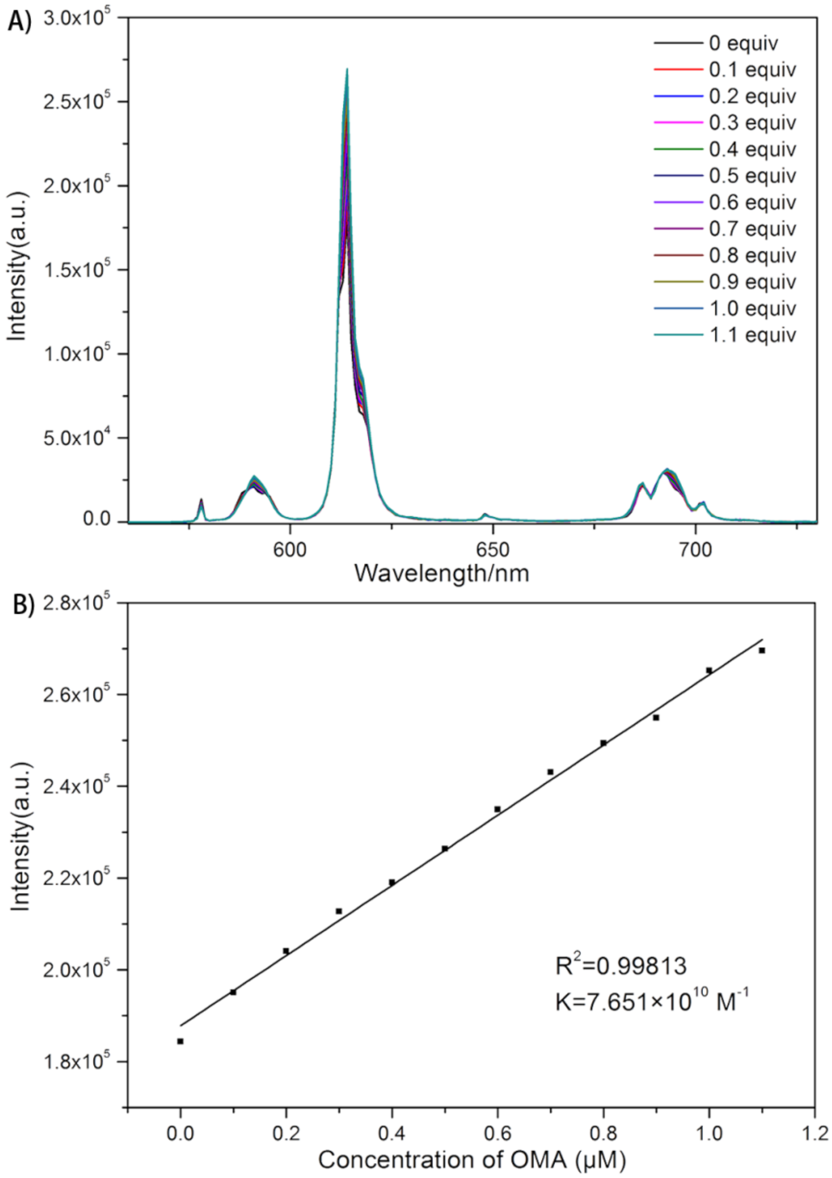

Figure S62. (A) Fluorescent titration spectra of Eu_2(**Pt-L**)$_2$ in CH_3CN (1×10^{-5}M, λ_{ex} = 368 nm) upon addition of different equiv of OMA. (B) Fitted curve of luminescent intensity versus OMA concentration.

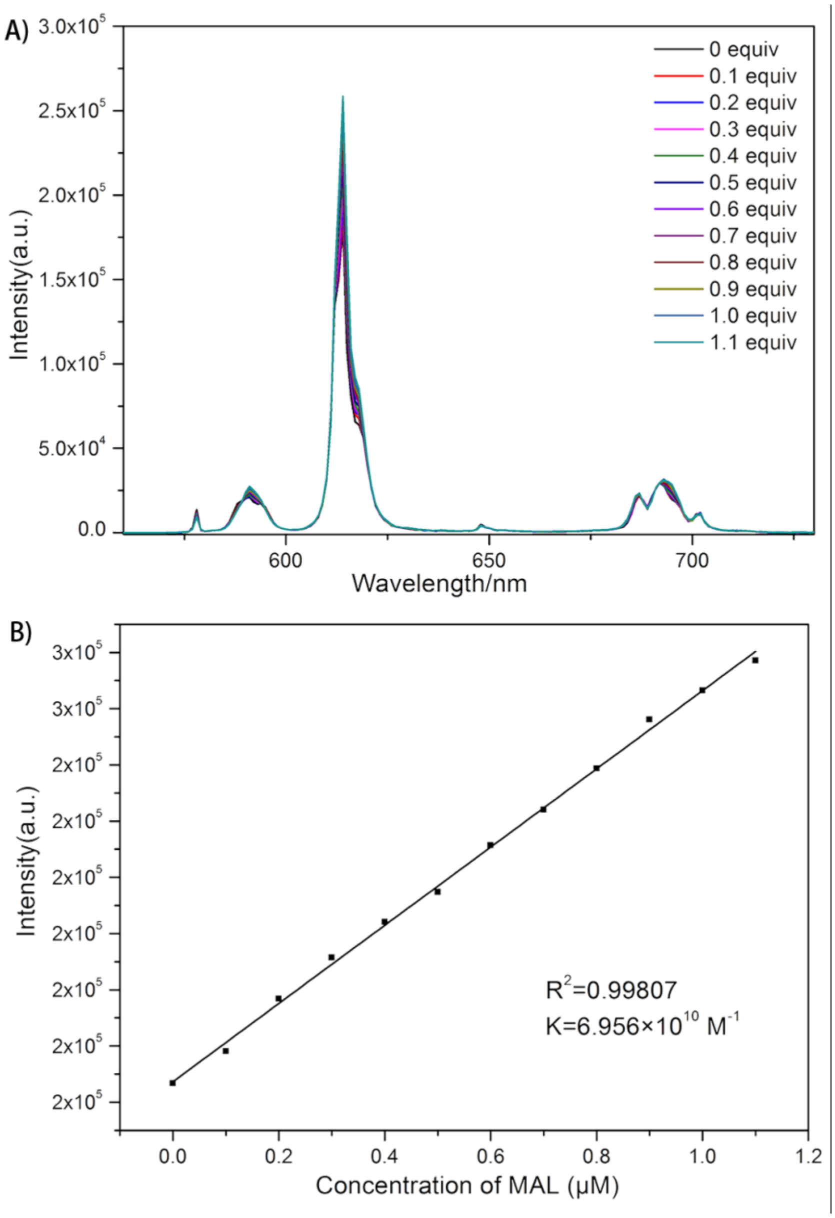

Figure S63. (A) Fluorescent titration spectra of $Eu_2(\mathbf{Pt\text{-}L})_2$ in CH_3CN (1×10^{-5}M, λ_{ex} = 368 nm) upon addition of different equiv of MAL. (B) Fitted curve of luminescent intensity versus MAL concentration.

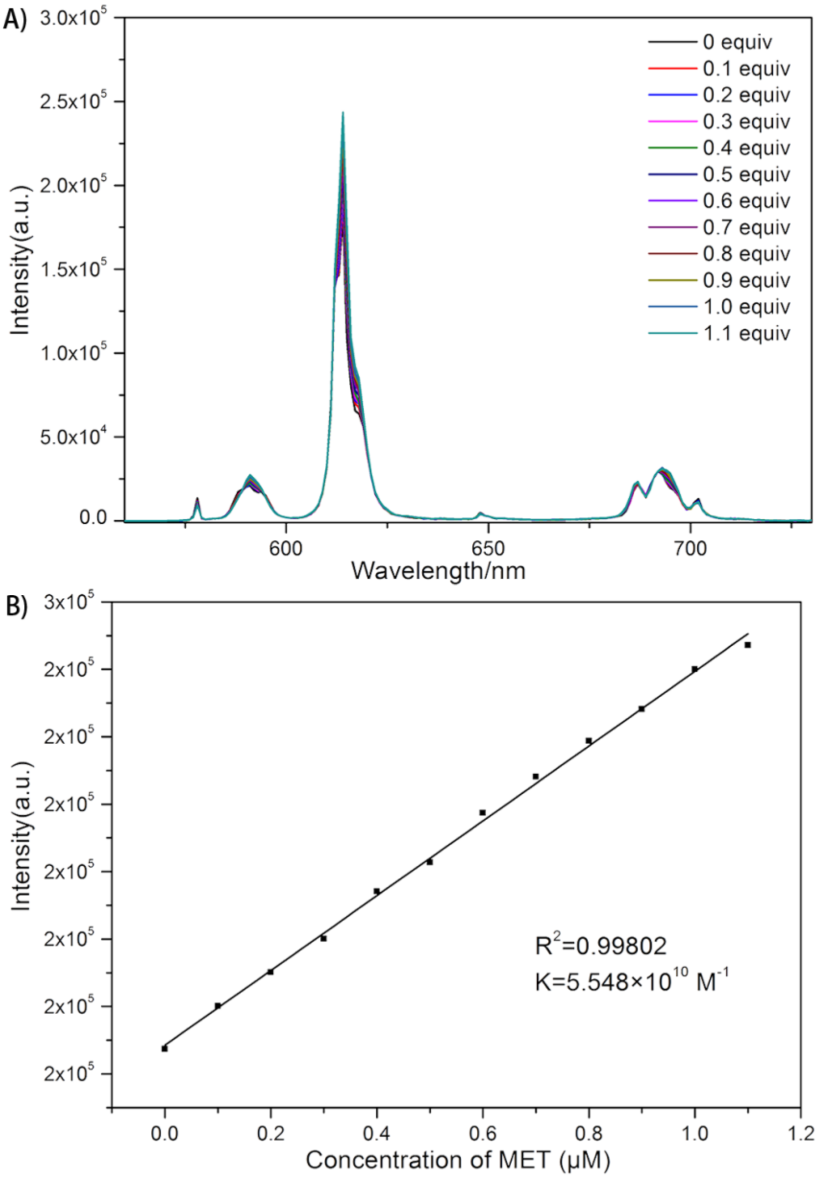

Figure S64. (A) Fluorescent titration spectra of Eu_2(**Pt-L**)$_2$ in CH_3CN (1×10^{-5}M, λ_{ex} = 368 nm) upon addition of different equiv of MET. (B) Fitted curve of luminescent intensity versus MET concentration.

5. Mass spectra

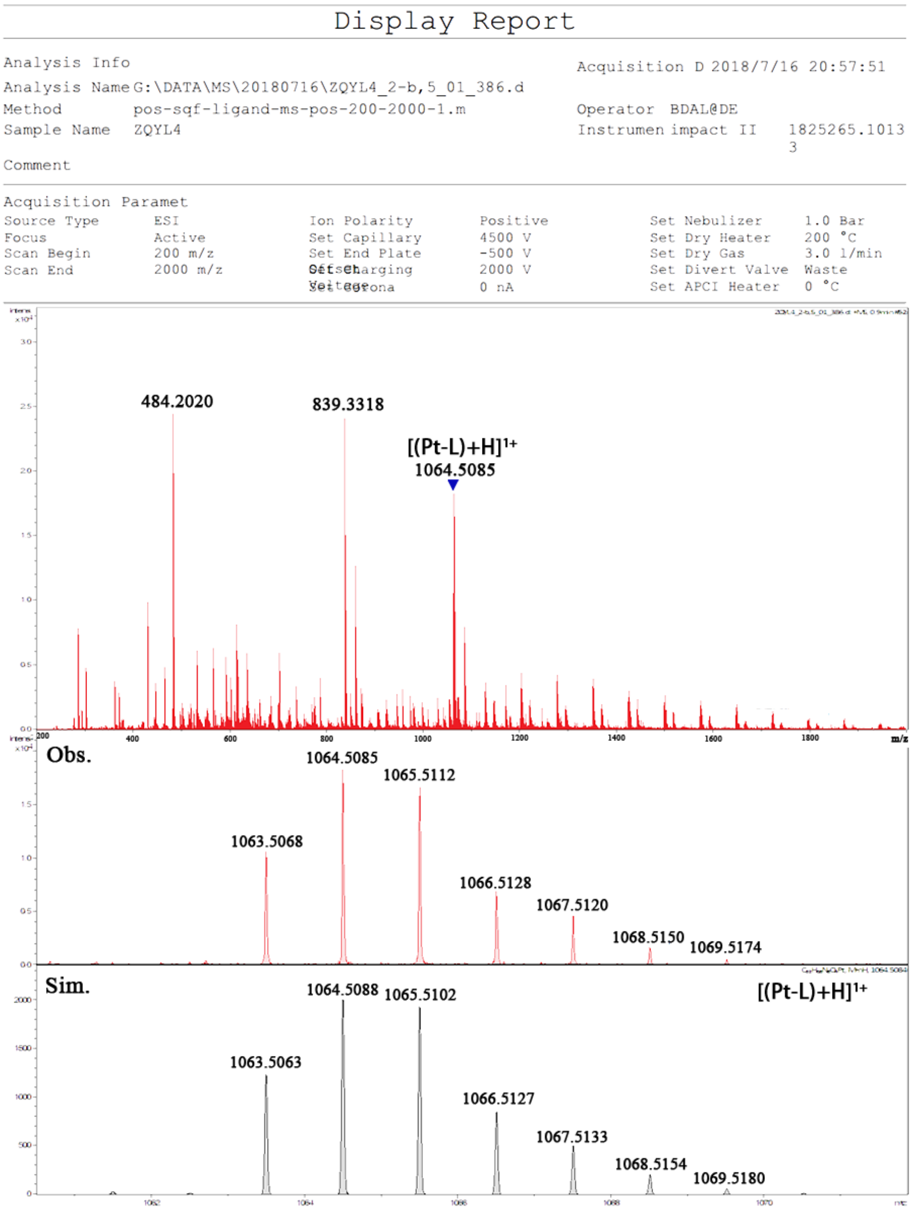

```
                              Display Report

Analysis Info                                       Acquisition D 2018/7/16 20:57:51
Analysis Name G:\DATA\MS\20180716\ZQYL4_2-b,5_01_386.d
Method        pos-sqf-ligand-ms-pos-200-2000-1.m    Operator  BDAL@DE
Sample Name   ZQYL4                                 Instrumen impact II    1825265.1013
                                                                           3
Comment

Acquisition Paramet
Source Type    ESI         Ion Polarity     Positive     Set Nebulizer      1.0 Bar
Focus          Active      Set Capillary    4500 V       Set Dry Heater     200 °C
Scan Begin     200 m/z     Set End Plate    -500 V       Set Dry Gas        3.0 l/min
Scan End       2000 m/z    Set Charging     2000 V       Set Divert Valve   Waste
                           Voltage
                           Set Corona       0 nA         Set APCI Heater    0 °C
```

Figure S65. ESI-TOF-MS spectra for **Pt-L**.

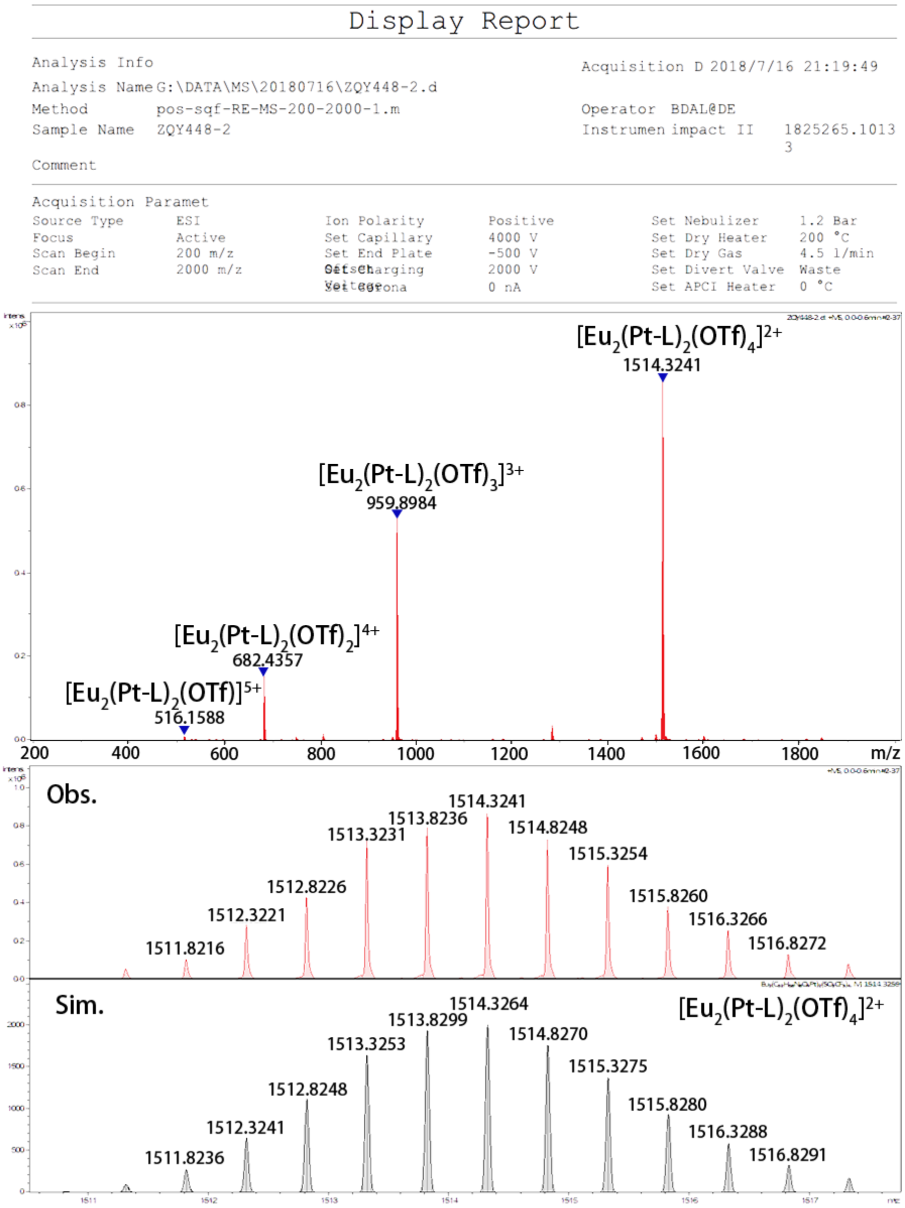

```
Display Report

Analysis Info                                          Acquisition D 2018/7/16 21:19:49
Analysis Name G:\DATA\MS\20180716\ZQY448-2.d
Method        pos-sqf-RE-MS-200-2000-1.m               Operator  BDAL@DE
Sample Name   ZQY448-2                                 Instrumen impact II   1825265.1013
                                                                             3
Comment

Acquisition Paramet
Source Type   ESI          Ion Polarity    Positive    Set Nebulizer     1.2 Bar
Focus         Active       Set Capillary   4000 V      Set Dry Heater    200 °C
Scan Begin    200 m/z      Set End Plate   -500 V      Set Dry Gas       4.5 l/min
Scan End      2000 m/z     Offset Charging 2000 V      Set Divert Valve  Waste
                           Voltage Corona  0 nA        Set APCI Heater   0 °C
```

Figure S66. ESI-TOF-MS spectra for $Eu_2(\textbf{Pt-L})_2(OTf)_6$.

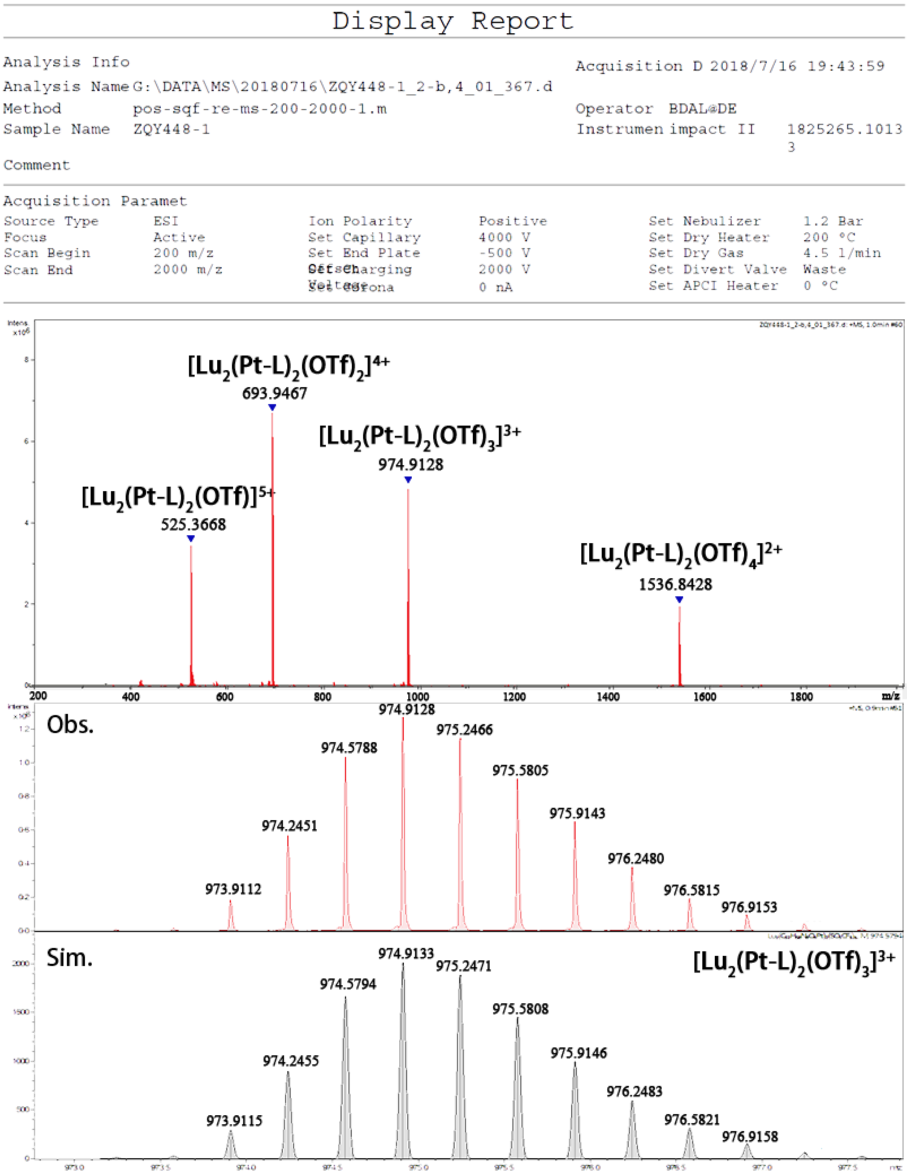

```
                         Display Report

Analysis Info                                       Acquisition D 2018/7/16 19:43:59
Analysis Name G:\DATA\MS\20180716\ZQY448-1_2-b,4_01_367.d
Method        pos-sqf-re-ms-200-2000-1.m            Operator  BDAL@DE
Sample Name   ZQY448-1                              Instrumen impact II    1825265.1013
                                                                           3
Comment

Acquisition Paramet
Source Type     ESI          Ion Polarity        Positive        Set Nebulizer      1.2 Bar
Focus           Active       Set Capillary       4000 V          Set Dry Heater     200 °C
Scan Begin      200 m/z      Set End Plate       -500 V          Set Dry Gas        4.5 l/min
Scan End        2000 m/z     Set Charging        2000 V          Set Divert Valve   Waste
                             Voltage
                             Set Corona          0 nA            Set APCI Heater    0 °C
```

Figure S67. ESI-TOF-MS spectra for $Lu_2(\textbf{Pt-L})_2(OTf)_6$.

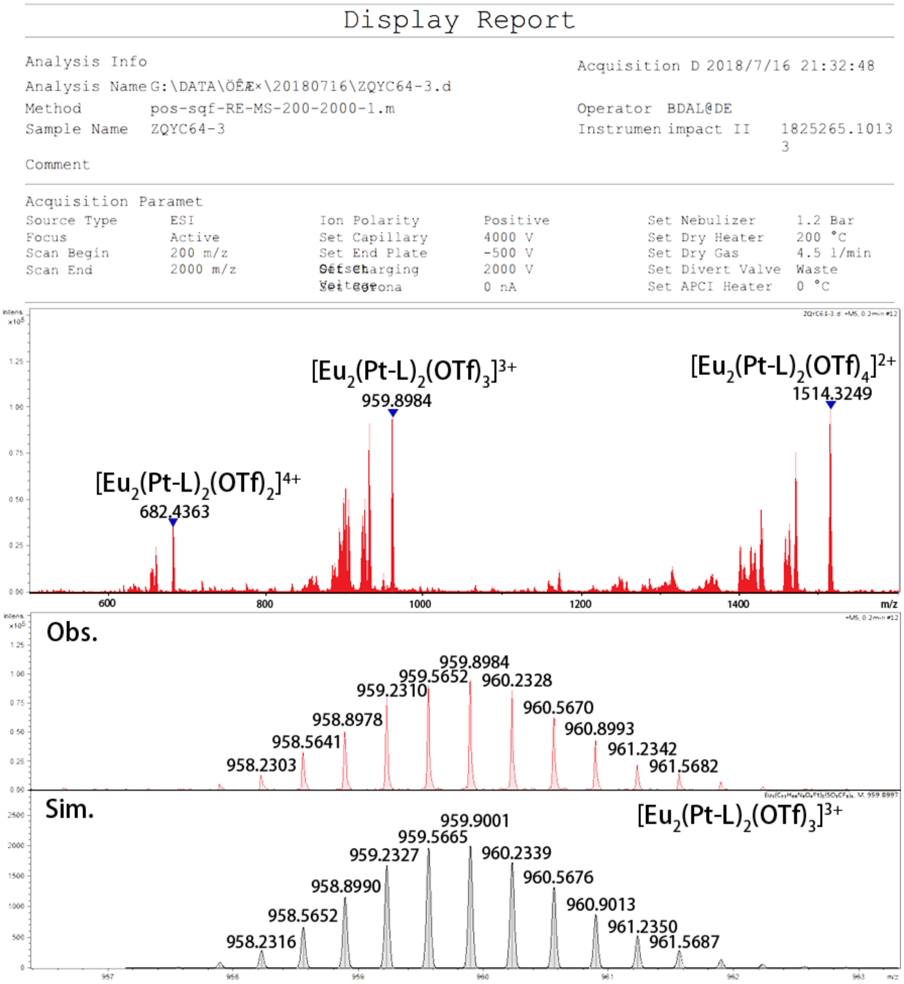

```
Display Report

Analysis Info                                   Acquisition D 2018/7/16 21:32:48
Analysis Name G:\DATA\ÖÊÆ×\20180716\ZQYC64-3.d
Method        pos-sqf-RE-MS-200-2000-1.m          Operator  BDAL@DE
Sample Name   ZQYC64-3                            Instrumen impact II    1825265.1013
                                                                         3
Comment

Acquisition Paramet
Source Type      ESI          Ion Polarity     Positive        Set Nebulizer      1.2 Bar
Focus            Active       Set Capillary    4000 V          Set Dry Heater     200 °C
Scan Begin       200 m/z      Set End Plate    -500 V          Set Dry Gas        4.5 l/min
Scan End         2000 m/z     Offset
                              Set Charging     2000 V          Set Divert Valve   Waste
                              Voltage
                              Set Corona       0 nA            Set APCI Heater    0 °C
```

Figure S68. ESI-TOF-MS spectra for Eu_2(**Pt-L**)$_2$(OTf)$_6$ in CH_3OH.

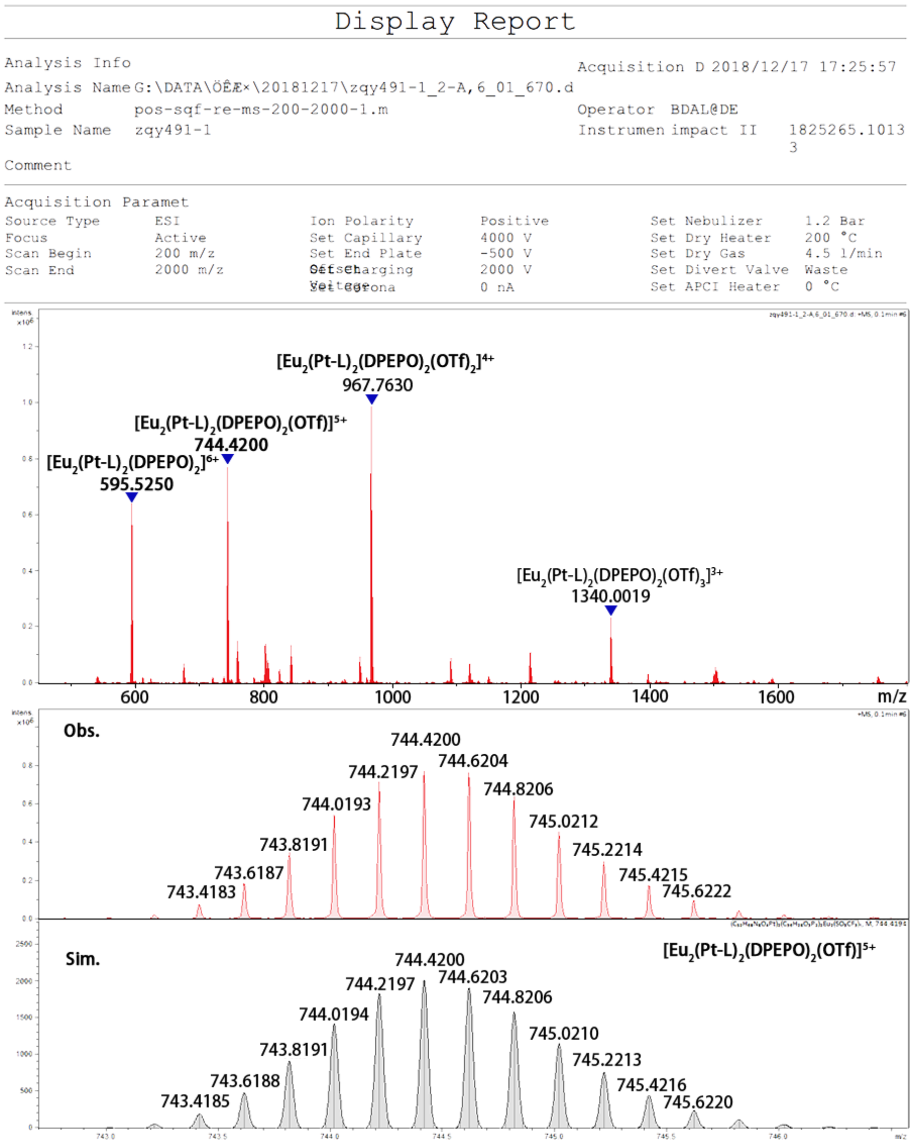

```
                              Display Report

Analysis Info                                  Acquisition D 2018/12/17 17:25:57
Analysis Name G:\DATA\ÖÊÆ×\20181217\zqy491-1_2-A,6_01_670.d
Method        pos-sqf-re-ms-200-2000-1.m       Operator  BDAL@DE
Sample Name   zqy491-1                         Instrumen impact II    1825265.1013
                                                                      3
Comment

Acquisition Paramet
Source Type   ESI        Ion Polarity       Positive     Set Nebulizer     1.2 Bar
Focus         Active     Set Capillary      4000 V       Set Dry Heater    200 °C
Scan Begin    200 m/z    Set End Plate      -500 V       Set Dry Gas       4.5 l/min
Scan End      2000 m/z   Set Charging       2000 V       Set Divert Valve  Waste
                         Voltage
                         Set Corona         0 nA         Set APCI Heater   0 °C
```

Figure S69. ESI-TOF-MS spectra for Eu$_2$(**Pt-L**)$_2$(DPEPO)$_2$(OTf)$_6$.

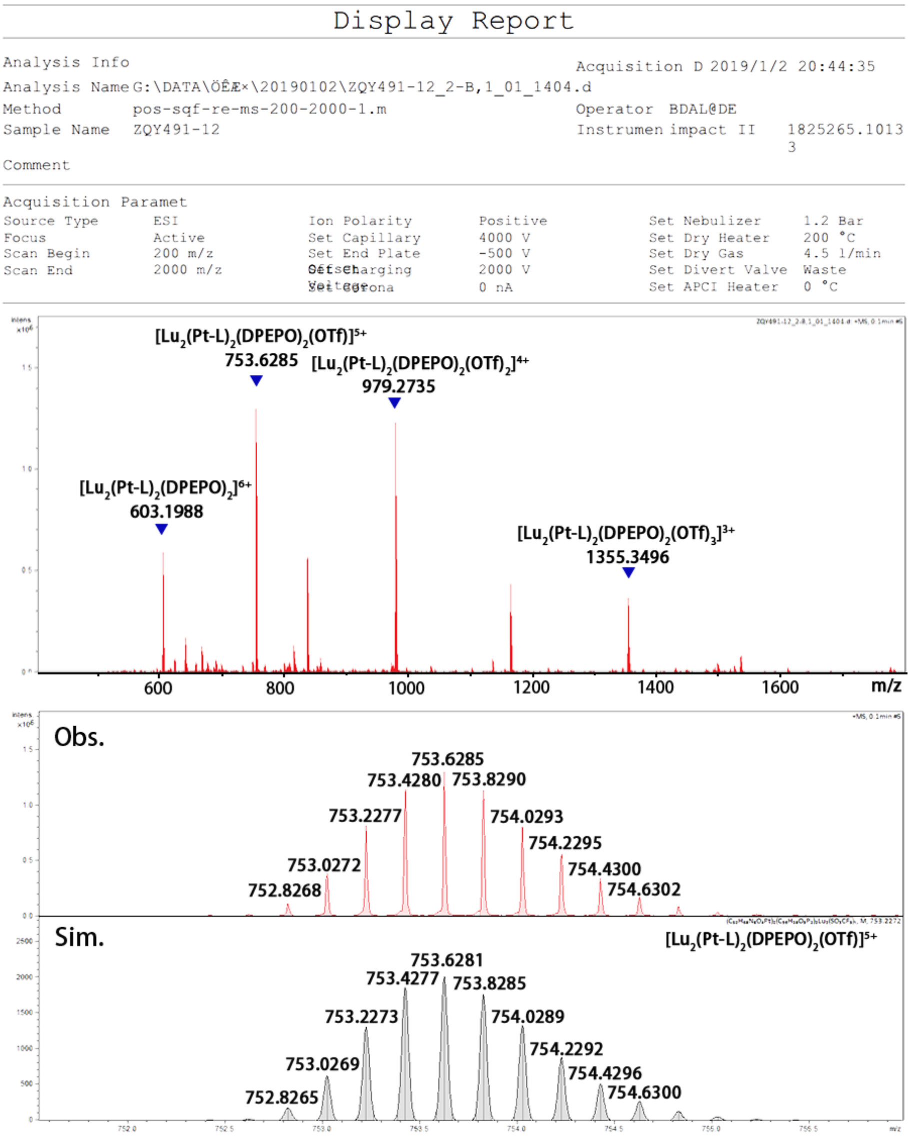

```
                         Display Report

Analysis Info                                    Acquisition D 2019/1/2 20:44:35
Analysis NameG:\DATA\ÖÊÆ×\20190102\ZQY491-12_2-B,1_01_1404.d
Method        pos-sqf-re-ms-200-2000-1.m         Operator  BDAL@DE
Sample Name   ZQY491-12                          Instrumen impact II    1825265.1013
                                                                        3
Comment

Acquisition Paramet
Source Type      ESI          Ion Polarity     Positive      Set Nebulizer      1.2 Bar
Focus            Active       Set Capillary    4000 V        Set Dry Heater     200 °C
Scan Begin       200 m/z      Set End Plate    -500 V        Set Dry Gas        4.5 l/min
Scan End         2000 m/z     Set Charging     2000 V        Set Divert Valve   Waste
                              Set Corona       0 nA          Set APCI Heater    0 °C
```

Figure S70. ESI-TOF-MS spectra for Lu_2(**Pt-L**)$_2$(DPEPO)$_2$(OTf)$_6$.

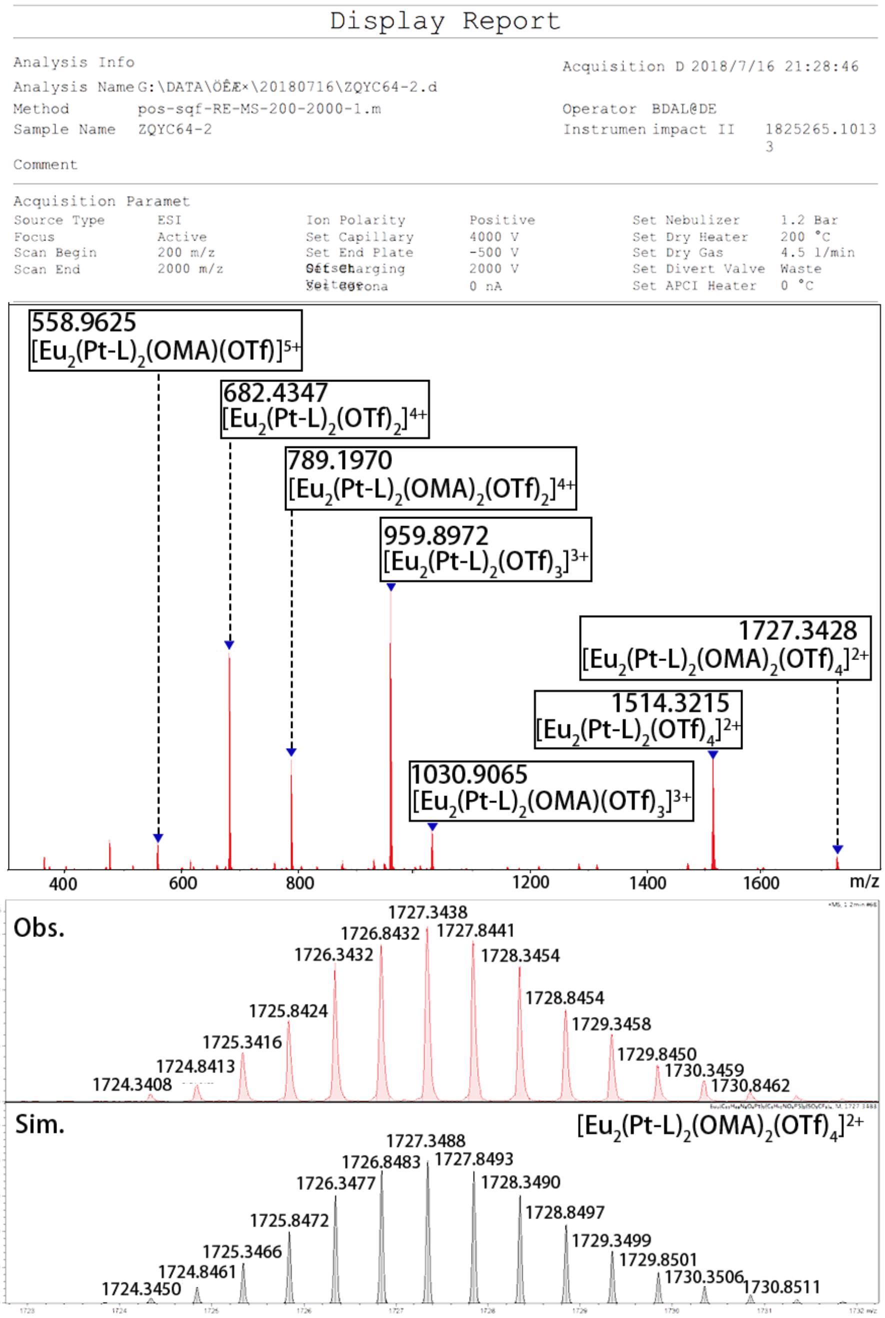

```
                          Display Report

Analysis Info                                   Acquisition D 2018/7/16 21:28:46
Analysis Name G:\DATA\ÖÊÆ×\20180716\ZQYC64-2.d
Method        pos-sqf-RE-MS-200-2000-1.m        Operator  BDAL@DE
Sample Name   ZQYC64-2                          Instrumen impact II   1825265.1013
                                                                      3
Comment

Acquisition Paramet
Source Type     ESI          Ion Polarity     Positive        Set Nebulizer      1.2 Bar
Focus           Active       Set Capillary    4000 V          Set Dry Heater     200 °C
Scan Begin      200 m/z      Set End Plate    -500 V          Set Dry Gas        4.5 l/min
Scan End        2000 m/z     Set Charging     2000 V          Set Divert Valve   Waste
                             Voltage
                             Set Corona       0 nA            Set APCI Heater    0 °C
```

Figure S71. ESI-TOF-MS spectra for Eu_2(**Pt-L**)$_2$(OTf)$_6$ containing 2.0 equiv of OMA.

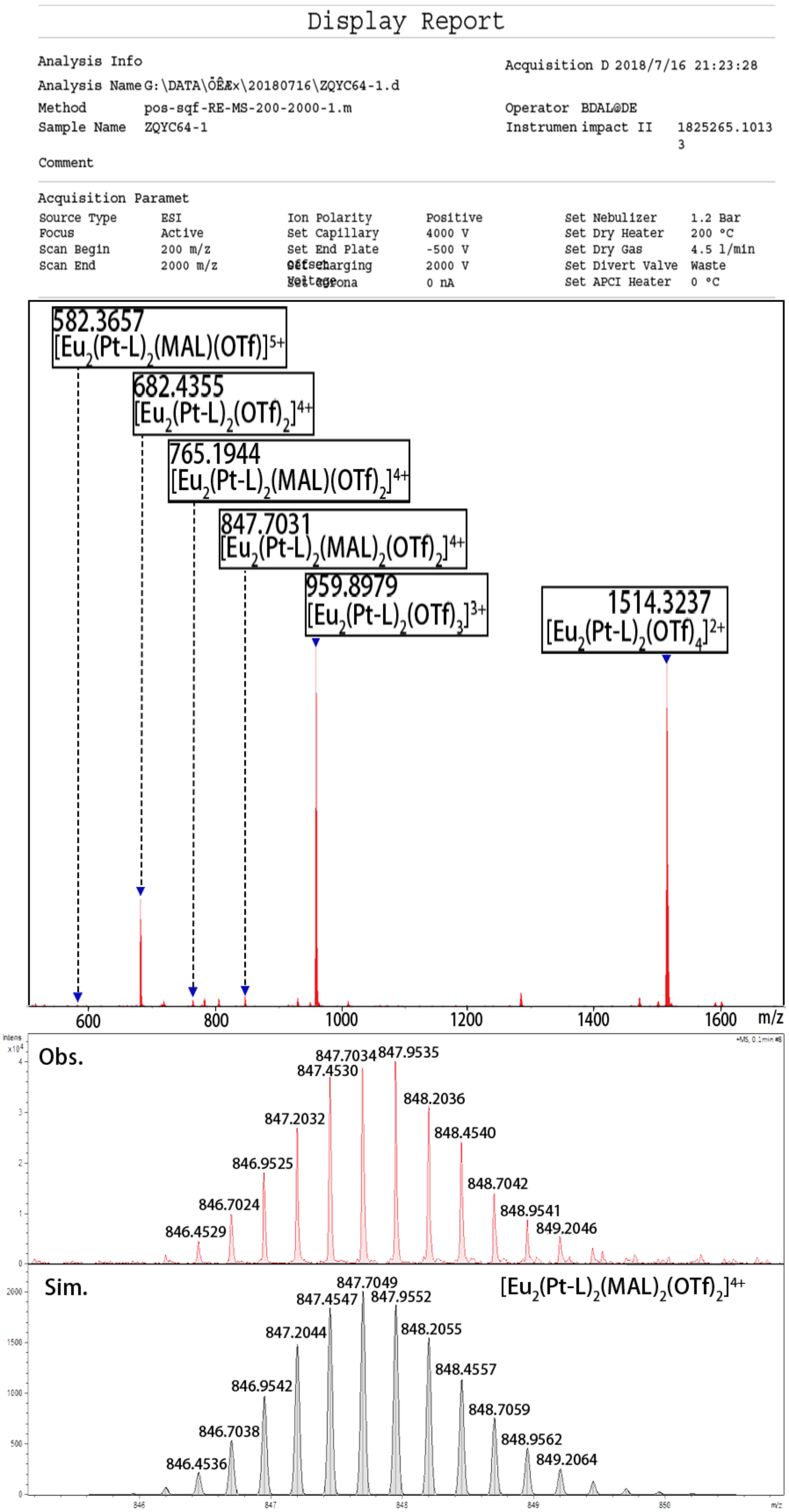

```
                         Display Report

Analysis Info                                   Acquisition D 2018/7/16 21:23:28
Analysis Name G:\DATA\ÕÊÆx\20180716\ZQYC64-1.d
Method        pos-sqf-RE-MS-200-2000-1.m        Operator  BDAL@DE
Sample Name   ZQYC64-1                          Instrumen impact II   1825265.1013
                                                                      3
Comment

Acquisition Paramet
Source Type    ESI        Ion Polarity        Positive   Set Nebulizer     1.2 Bar
Focus          Active     Set Capillary       4000 V     Set Dry Heater    200 °C
Scan Begin     200 m/z    Set End Plate       -500 V     Set Dry Gas       4.5 l/min
Scan End       2000 m/z   Offset
                          Set Charging        2000 V     Set Divert Valve  Waste
                          Voltage
                          Set Corona          0 nA       Set APCI Heater   0 °C
```

Figure S72. ESI-TOF-MS spectra for Eu_2(**Pt-L**)$_2$(OTf)$_6$ containing 2.0 equiv of MAL.

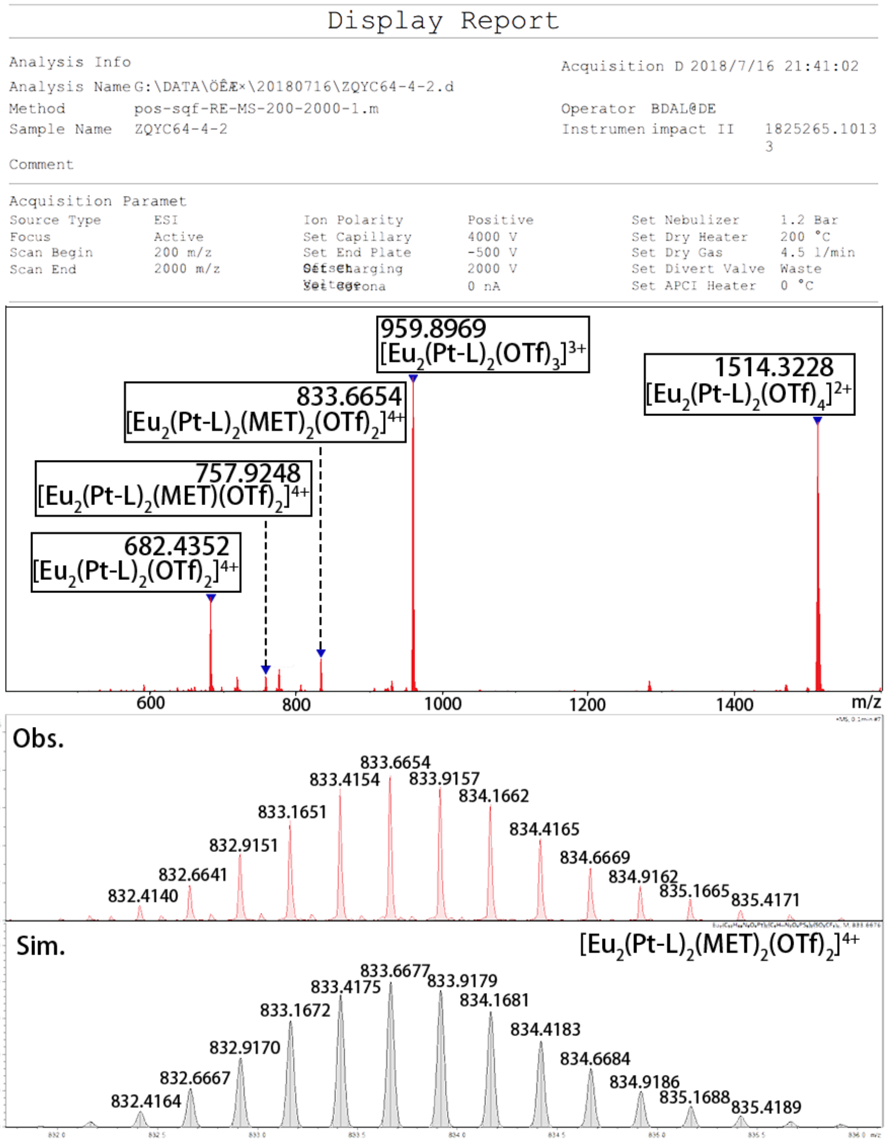

```
                              Display Report

Analysis Info                                    Acquisition D 2018/7/16 21:41:02
Analysis Name G:\DATA\ÖÊÆ×\20180716\ZQYC64-4-2.d
Method        pos-sqf-RE-MS-200-2000-1.m         Operator  BDAL@DE
Sample Name   ZQYC64-4-2                         Instrumen impact II   1825265.1013
                                                                       3
Comment

Acquisition Paramet
Source Type    ESI        Ion Polarity     Positive   Set Nebulizer     1.2 Bar
Focus          Active     Set Capillary    4000 V     Set Dry Heater    200 °C
Scan Begin     200 m/z    Set End Plate    -500 V     Set Dry Gas       4.5 l/min
Scan End       2000 m/z   Set Charging     2000 V     Set Divert Valve  Waste
                          Voltage
                          Set Corona       0 nA       Set APCI Heater   0 °C
```

Figure S73. ESI-TOF-MS spectra for Eu_2(**Pt-L**)$_2$(OTf)$_6$ containing 2.0 equiv of MET.

6. Single crystal X-ray diffraction studies

The X-ray diffraction studies for heterometal-organic macrocycles were carried out on Bruker D8 VENTURE photon II diffractometer with Iμs 3.0 microfocus X-ray source using APEX III program.[4] Data reduction was performed with the saint and SADABS package. Both structures were solved by direct methods and refined by full-matrix least-squares on F2 with anisotropic displacement using the SHELX software package.[5] solvent molecules were highly disordered and could not be reasonably located. These residual intensities were removed by PLATON/SQUEEZE routine.[6]

Table S4. Crystal data and structure refinement for La$_2$(**Pt-L**)$_2$(ClO$_4$)$_6$.

Identification code	La$_2$(**Pt-L**)$_2$(ClO$_4$)$_6$	
Empirical formula	C104 H136 Cl6 La2 N16 O34 Pt2	
Formula weight	3034.98	
Temperature	100(2) K	
Wavelength	0.71073 Å	
Crystal system	Triclinic	
Space group	P-1	
Unit cell dimensions	a = 14.1633(9) Å	a= 73.946(3) °.
	b = 15.5448(10) Å	b= 71.033(3) °.
	c = 18.1762(12) Å	g = 88.863(3) °.
Volume	3626.1(4) Å3	
Z	1	
Density (calculated)	1.390 Mg/m3	
Absorption coefficient	2.680 mm-1	
F(000)	1516	
Crystal size	0.10 x 0.08 x 0.07 mm3	
Theta range for data collection	2.386 to 24.782 °.	
Index ranges	-16<=h<=16, -18<=k<=18, -21<=l<=21	
Reflections collected	93911	
Independent reflections	12437 [R(int) = 0.1001]	
Completeness to theta = 24.782 °	99.7 %	
Absorption correction	None	
Refinement method	Full-matrix least-squares on F2	
Data / restraints / parameters	12437 / 4 / 678	
Goodness-of-fit on F2	1.041	
Final R indices [I>2sigma(I)]	R1 = 0.0660, wR2 = 0.1532	
R indices (all data)	R1 = 0.1047, wR2 = 0.1857	
Extinction coefficient	n/a	
Largest diff. peak and hole	2.375 and -3.317 e.Å-3	

Table S5. Crystal data and structure refinement for Eu_2(**Pt-L**)$_2$(OTf)$_6$.

Identification code	Eu_2(**Pt-L**)$_2$(OTf)$_6$	
Empirical formula	C114 H142 Eu2 F18 N18 O30 Pt2 S6	
Formula weight	3472.91	
Temperature	100(2) K	
Wavelength	0.71073 Å	
Crystal system	Triclinic	
Space group	P-1	
Unit cell dimensions	a = 14.8876(11) Å	a= 103.870(2) °.
	b = 16.7086(12) Å	b= 110.195(2) °.
	c = 18.0513(12) Å	g = 92.844(3) °.
Volume	4047.9(5) Å3	
Z	1	
Density (calculated)	1.425 Mg/m3	
Absorption coefficient	2.649 mm-1	
F(000)	1732	
Crystal size	0.11 x 0.10 x 0.10 mm3	
Theta range for data collection	2.256 to 25.196 °.	
Index ranges	-17<=h<=17, -20<=k<=19, -21<=l<=21	
Reflections collected	111533	
Independent reflections	14503 [R(int) = 0.0753]	
Completeness to theta = 25.196 °	99.7 %	
Absorption correction	None	
Refinement method	Full-matrix least-squares on F2	
Data / restraints / parameters	14503 / 0 / 863	
Goodness-of-fit on F2	1.045	
Final R indices [I>2sigma(I)]	R1 = 0.0398, wR2 = 0.0939	
R indices (all data)	R1 = 0.0610, wR2 = 0.1046	
Extinction coefficient	n/a	
Largest diff. peak and hole	1.811 and -1.001 e.Å-3	

Table S7. Crystal data and structure refinement for Lu_2(**Pt-L**)$_2$(DPEPO)$_2$(OTf)$_6$.

Identification code	Lu_2(**Pt-L**)$_2$(DPEPO)$_2$(OTf)$_6$	
Empirical formula	C178 H194 F6 Lu2 N16 O20 P4 Pt2 S2	
Formula weight	3919.60	
Temperature	298(2) K	
Wavelength	0.71073 Å	
Crystal system	Monoclinic	
Space group	$P2_1/n$	
Unit cell dimensions	a = 18.6809(11) Å	a= 90 °.
	b = 15.9420(10) Å	b= 92.432(2) °.
	c = 41.772(3) Å	g = 90 °.
Volume	12429.1(13) Å3	
Z	2	
Density (calculated)	1.047 Mg/m3	
Absorption coefficient	2.004 mm-1	
F(000)	3956	
Crystal size	0.12 x 0.10 x 0.08 mm3	
Theta range for data collection	2.198 to 30.568 °.	
Index ranges	-26<=h<=26, -22<=k<=22, -59<=l<=59	
Reflections collected	423376	
Independent reflections	38017 [R(int) = 0.0856]	
Completeness to theta = 25.242 °	99.9 %	
Absorption correction	None	
Refinement method	Full-matrix least-squares on F2	
Data / restraints / parameters	38017 / 1007 / 998	
Goodness-of-fit on F2	1.050	
Final R indices [I>2sigma(I)]	R1 = 0.0776, wR2 = 0.2185	
R indices (all data)	R1 = 0.1574, wR2 = 0.2697	
Extinction coefficient	n/a	
Largest diff. peak and hole	1.627 and -1.119 e.Å-3	

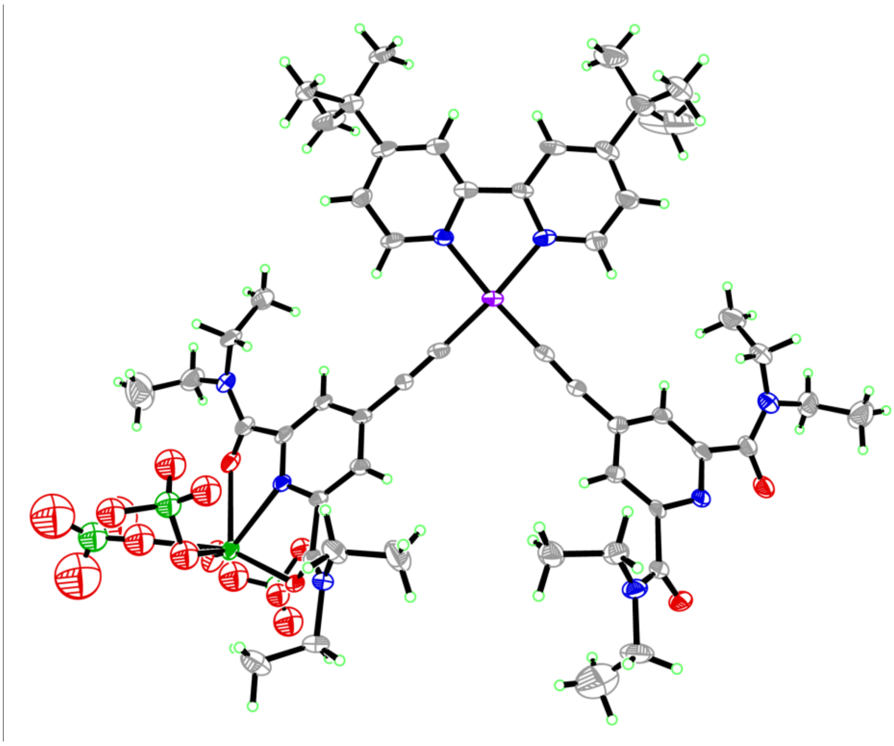

Figure S74. Ortep drawing of the asymmetric unit in the crystal structure of La$_2$(**Pt-L**)$_2$(ClO$_4$)$_6$ at 30% probability level.

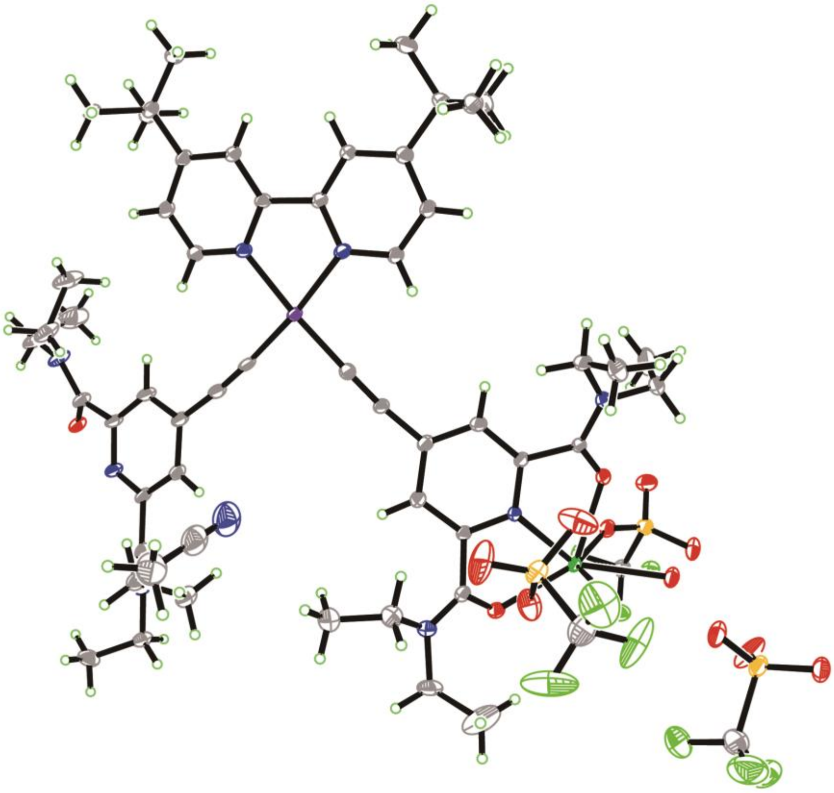

Figure S75. Ortep drawing of the asymmetric unit in the crystal structure of Eu$_2$(**Pt-L**)$_2$(OTf)$_6$ at 30% probability level.

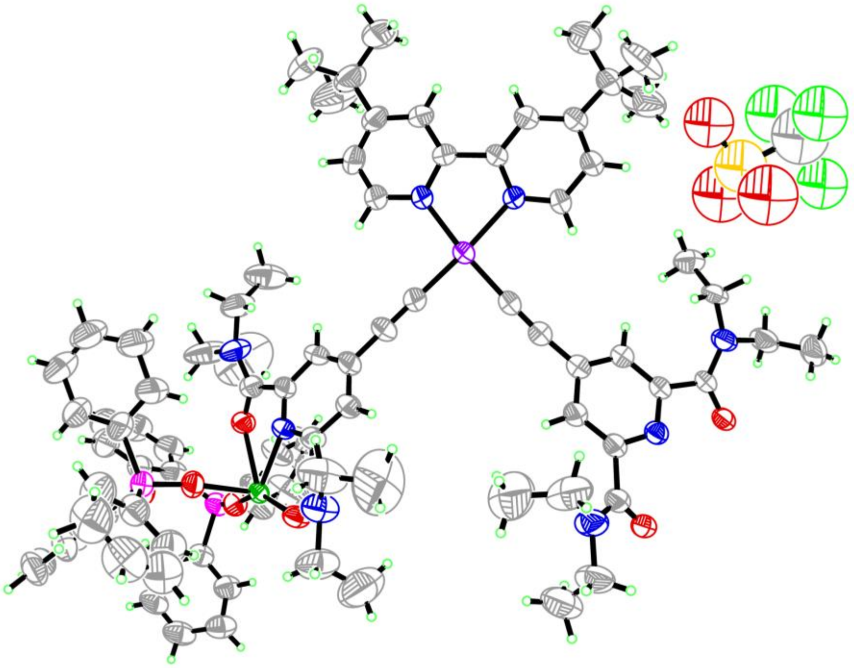

Figure S76. Ortep drawing of the asymmetric unit in the crystal structure of Lu_2(**Pt-L**)$_2$(DPEPO)$_2$(OTf)$_6$ at 30% probability level.

7. References

[1] a) G. Muller, B. Schmidt, J. Jiricek, G. Hopfgartner, J. P. Riehl, J.-C. G. Bünzli, C. Piguet, *Journal of the Chemical Society, Dalton Transactions* **2001**, 2655-2662; b) T. J. Egan, K. R. Koch, P. L. Swan, C. Clarkson, D. A. Van Schalkwyk, P. J. Smith, *J. Med. Chem.* **2004**, *47*, 2926-2934.

[2] S. I. Klink, G. A. Hebbink, L. Grave, P. G. B. Oude Alink, F. C. J. M. van Veggel, M. H. V. Werts, *The Journal of Physical Chemistry A* **2002**, *106*, 3681-3689.

[3] F. Xue, Y. Ma, L. Fu, R. Hao, G. Shao, M. Tang, J. Zhang, Y. Wang, *Physical chemistry chemical physics : PCCP* **2010**, *12*, 3195-3202.

[4] APEX III, Data collection software (version 2017.3)

[5] Sheldrick, G. M., *Acta Crystallogr. Sect. A*, **2008**, 64, 112.

[6] *Spek, A. L. J. Appl. Crystallogr.* **2003**, *36, 7–13.*